Transcriptional control mechanisms in the wall of the urinary bladder. Myocardin family coactivators and the transcriptomic impact of denervation.

Zhu, Baoyi

2018

Document Version:
Publisher's PDF, also known as Version of record

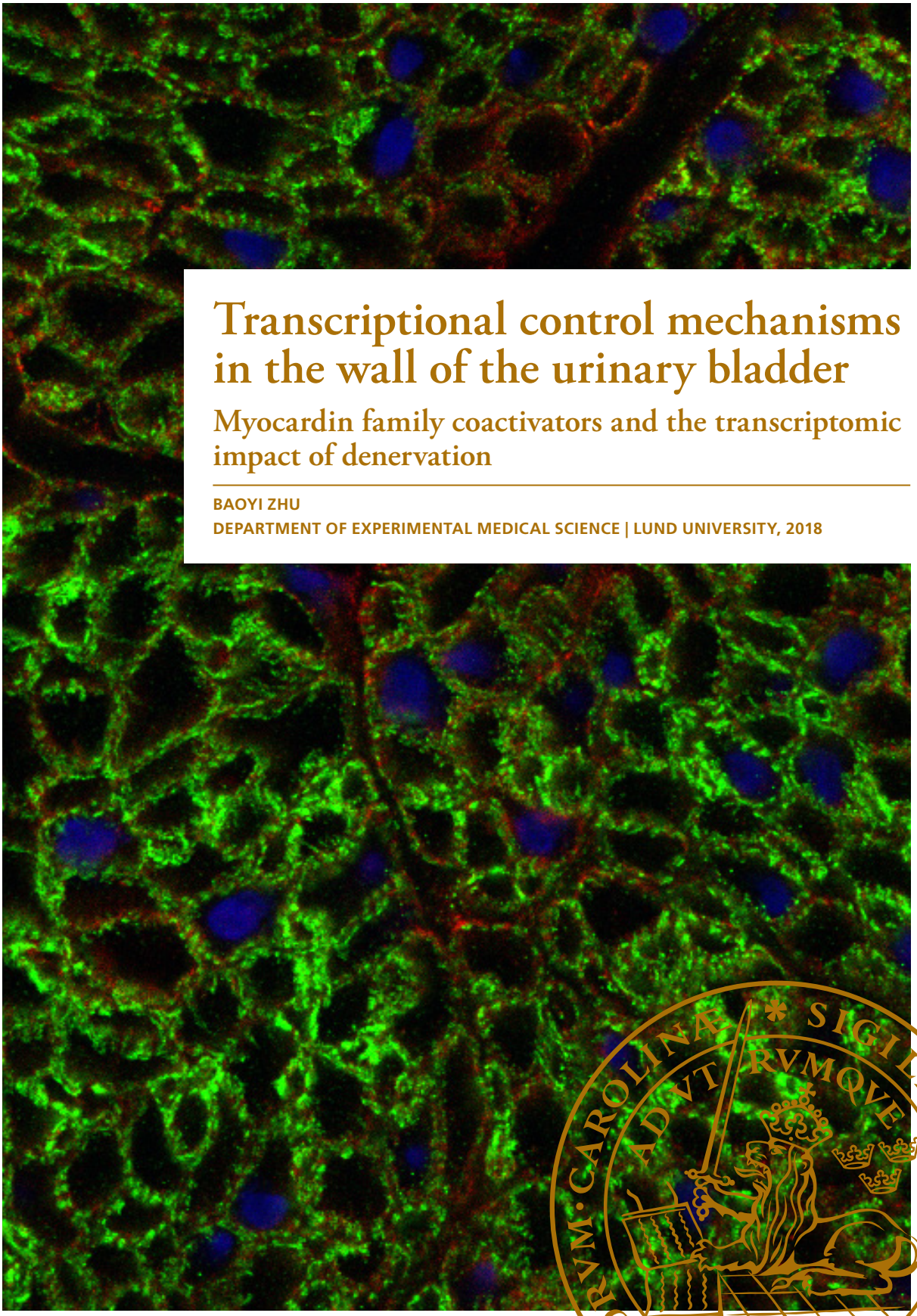

Transcriptional control mechanisms in the wall of the urinary bladder

Myocardin family coactivators and the transcriptomic impact of denervation

BAOYI ZHU
DEPARTMENT OF EXPERIMENTAL MEDICAL SCIENCE | LUND UNIVERSITY, 2018

Transcriptional control mechanisms in the wall of the urinary bladder

Myocardin family coactivators and the transcriptomic impact of denervation

Baoyi Zhu

LUND
UNIVERSITY

DOCTORAL DISSERTATION
By due permission of the Faculty of Medicine, Lund University, Sweden
To be defended in Segerfalksalen, BMC A10, Lund
September 20th, 2018, 09:00 a.m.

Faculty opponent
Professor Per Lindahl
Medical Biochemistry, Wallenberg Laboratory
University of Gothenburg

Organization
LUND UNIVERSITY
Faculty of Medicine
Department of Experimental Medical Science
Section of Cell and Tissue Biology
Author: Baoyi Zhu

Document name
DOCTORAL DISSERTATION

Date of issue
2018-09-20

Sponsoring organization

Title: Transcriptional control mechanisms in the wall of the urinary bladder
Subtitle: Myocardin family coactivators and the transcriptomic impact of denervation

Abstract

Urological problems can be caused by diseases that affect the bladder wall and its innervation. Contraction and relaxation of smooth muscle cells (SMCs) is essential for maintaining detrusor function and for emptying the bladder. It is well established that a family of regulatory proteins called Myocardin Related Transcription Factors (MRTFs) controls the property of SMCs. SMCs have a number of unique ultrastructural features, including caveolae in the membrane and “dense bodies” in the cytoplasm. An overarching aim of the work presented here was to investigate the regulatory mechanism of the key proteins in caveolae and dense bodies.

The generation of caveolae depends on caveolins and cavins. We found that most caveolae proteins are regulated by MRTFs via proximal promoter sequences. MRTFs thus likely represent major drivers of formation of caveolae in SMCs. We also found that Cavin3 (Prkcdbp) is preferentially expressed in SMCs compared to other cells. Knockout of *Cavin3* reduced the number of caveolae in the SMC membrane, but not elsewhere, and at the same time reduced Caveolin-1, Caveolin-3 and Cavin1. This suggests that Cavin3 contributes to the generation of caveolae in SMCs.

Dense bodies in smooth muscle may be regarded as equivalents of Z-discs in striated muscle. The protein Nexilin (*NEXN*) was previously identified as a Z-disc-localized protein that controls mechanical stability. We found that Nexilin (*NEXN*) is highly expressed in SMCs and regulated by MRTF- and YAP/TAZ-coactivators. Nexilin was moreover found to be a dense body-associated protein in SMCs that promotes actin polymerization, differentiation and motility.

Bladder wall remodelling in pathological situations is accompanied by reduced innervation. A second aim of this work was to define changes in gene expression after denervation. We show that numerous mRNAs and miRNAs are differentially expressed in the denervated bladder. Pathway analysis indicates that many of the differentially expressed genes are related to proliferation (60%). This is no surprise because the bladder weight increases 5-fold following denervation. Cthrc1 is upregulated at both the mRNA and protein levels, correlating with bladder weight, and overexpression and knockdown of this protein influences SMC proliferation *in vitro*.

Neural plasticity is influenced by neurotrophic factors released from the target organs. We addressed if the bladder may influence its own nerve supply by such a mechanism. We demonstrate that neurotrophic factors, including NGF, BDNF, and NT-3, are synthesized in the bladder wall, and promote outgrowth of neurites from the pelvic ganglia *in vitro*, presumably via Trk-receptors.

In conclusion, the studies summarized here provide understanding of the transcriptional control of key proteins and ultrastructural features of SMCs. They also unveil molecular mechanisms of bladder remodelling following denervation. Manipulation of some of the genes identified here represents promising strategies for recovering bladder function in disease.

Key words: Detrusor, Myocardin family coactivators, Caveolae, Nexilin, Denervation, Cthrc1, Pelvic ganglion

Classification system and/or index terms (if any)

Supplementary bibliographical information | Language

ISSN and key title: 1652-8220, Lund University, Faculty of Medicine Doctoral Dissertation Series 2018:104 | ISBN: 978-91-7619-672-4

Recipient’s notes | Number of pages | Price

Security classification

Signature  Date 2018-07-11

Transcriptional control mechanisms in the wall of the urinary bladder

Myocardin family coactivators and the transcriptomic impact of denervation

Baoyi Zhu

LUND
UNIVERSITY

Transkriptionella kontrollmekanismer i urinblåsans vägg

Myokardin-lika koaktivatorer och genaktivering vid denervation

朱宝益

LUNDS
UNIVERSITET

Cover images:
Immunofluorescence staining of YAP and CAV1 in human bladder

ISSN 1652-8220
ISBN 978-91-7619-672-4
Lund University, Faculty of Medicine Doctoral Dissertation Series 2018:104

Printed in Sweden by Media-Tryck, Lund University
Lund 2018

责任，团队，仁爱，奉献

宝剑锋从磨砺出
梅花香自苦寒来

Table of Contents

List of Papers

This thesis is based on the following articles, referred to in the text by their Roman numerals

I. **Zhu B**, Rippe C, Thi Hien T, Zeng J, Albinsson S, Stenkula KG, Uvelius B, Swärd K. Similar regulatory mechanisms of caveolins and cavins by myocardin family coactivators in arterial and bladder smooth muscle. PLoS One. 2017 May 25;12(5):e0176759.

II. **Zhu B**, Swärd K, Ekman M, Uvelius B, Rippe C. Cavin-3 (PRKCDBP) deficiency reduces the density of caveolae in smooth muscle. Cell Tissue Res. 2017 Jun;368(3):591-602.

III. **Zhu B**, Rippe C, Holmberg J, Zeng S, Perisic L, Albinsson S, Hedin U, Uvelius B, Swärd K. Nexilin/*NEXN* controls actin polymerization in smooth muscle and is regulated by myocardin family coactivators and YAP. Scientific Reports (in revision).

IV. Ekman M, **Zhu B**, Swärd K, Uvelius B. Neurite outgrowth in cultured mouse pelvic ganglia – Effects of neurotrophins and bladder tissue. Auton Neurosci. 2017 Jul;205:41-49.

V. **Zhu B**, Ekman M, Svensson D, Lindvall J, Nilsson BO, Uvelius B, Swärd K. Array profiling reveals contribution of Cthrc1 to growth of the denervated rat urinary bladder. Am J Physiol Renal Physiol. 2018 Jan 10. Doi: 10.1152/ajprenal.00499.2017.

Paper I, II, IV, and V are reproduced with permissions from the publishers.

Paper not Included

Rippe C, **Zhu B**, Krawczyk KK, Bavel EV, Albinsson S, Sjölund J, et al. Hypertension reduces soluble guanylyl cyclase expression in the mouse aorta via the Notch signaling pathway. Sci Rep. 2017;7(1):1334.

Abstract

Urological problems can be caused by diseases that affect the bladder wall and its innervation. Contraction and relaxation of smooth muscle cells (SMCs) is essential for maintaining detrusor function and for emptying the bladder. It is well established that a family of regulatory proteins called Myocardin Related Transcription Factors (MRTFs) controls the property of SMCs. SMCs have a number of unique ultrastructural features, including caveolae in the membrane and "dense bodies" in the cytoplasm. An overarching aim of the work presented here was to investigate the regulatory mechanism of the key proteins in caveolae and dense bodies.

The generation of caveolae depends on caveolins and cavins. We found that most caveolae proteins are regulated by MRTFs via proximal promoter sequences. MRTFs thus likely represent major drivers of formation of caveolae in SMCs. We also found that Cavin3 (Prkcdbp) is preferentially expressed in SMCs compared to other cells. Knockout of Cavin3 reduced the number of caveolae in the SMC membrane, but not elsewhere, and at the same time reduced Caveolin-1, Caveolin-3 and Cavin1. This suggests that Cavin3 contributes to the generation of caveolae in SMCs.

Dense bodies in smooth muscle may be regarded as equivalents of Z-discs in striated muscle. The protein Nexilin (*NEXN*) was previously identified as a Z-disc-localized protein that controls mechanical stability. We found that Nexilin (*NEXN*) is highly expressed in SMCs and regulated by MRTF- and YAP/TAZ-coactivators. Nexilin was moreover found to be a dense body-associated protein in SMCs that promotes actin polymerization, differentiation and motility.

Bladder wall remodelling in pathological situations is accompanied by reduced innervation. A second aim of this work was to define changes in gene expression after denervation. We show that numerous mRNAs and miRNAs are differentially expressed in the denervated bladder. Pathway analysis indicates that many of the differentially expressed genes are related to proliferation (60%). This is no surprise because the bladder weight increases 5-fold following denervation. Cthrc1 is upregulated at both the mRNA and protein levels, correlating with bladder weight, and overexpression and knockdown of this protein influences SMC proliferation *in vitro*.

Neural plasticity is influenced by neurotrophic factors released from the target organs. We addressed if the bladder may influence its own nerve supply by such a mechanism. We demonstrate that neurotrophic factors, including NGF, BDNF, and NT-3, are synthesized in the bladder wall, and promote outgrowth of neurites from the pelvic ganglia *in vitro*, presumably via Trk-receptors.

In conclusion, the studies summarized here provide understanding of the transcriptional control of key proteins and ultrastructural features of SMCs. They also unveil molecular mechanisms of bladder remodelling following denervation.

Manipulation of some of the genes identified here represents promising strategies for recovering bladder function in disease.

1. Introduction

The urinary tract consists of the kidneys, the ureters, the bladder, and the urethra. The urine passes through the ureters to the bladder where it is stored. Stored urine is expelled at socially acceptable times during micturition where the bladder muscle contracts and the sphincters in the urethra relax. This coordination is achieved by the central nervous system. Continence in children typically lags behind speech development, testifying to the complexity of the neural basis of micturition.

1.1. Micturition and bladder histology

Viewed by many as a simple storage reservoir, the bladder is in reality much more. The wall of the urinary bladder has three principal layers. The mucosa consists of an epithelial layer called the urothelium, and the cells that are in direct contact with urine are called umbrella cells. Underneath the urothelium is a layer of loose connective tissue and below that is the detrusor smooth muscle cell (SMC) layer. All of these layers contain nerve endings; sensory nerves dominate the epithelial/subepithelial compartment and function as filling receptors [1, 2]. Motor nerves are mainly cholinergic and dominate in the detrusor layer (Fig. 1) [3]. From their varicosities the neurotransmitter acetylcholine is released. Sensory nerves sense bladder filling and signal this to the pontine micturition center [4]. This center coordinates detrusor contraction with relaxation of the urethral sphincters. The preganglionic parasympathetic neurons destined for the bladder arise from the intermediolateral column of the sacral spinal cord (S2-S4), leave via the ventral roots, and make synapses in the pelvic ganglia or intramural ganglia. These ganglia then radiate postganglionic neurons to the pelvic organs including the bladder SMCs [3]. Detrusor contraction involves the neuronal release of mainly acetylcholine and ATP. These neurotransmitters bind to muscarinic and purinergic receptors on the SMCs [5, 6], causing contraction and bladder emptying.

On the surface of the SMC plasma membrane there are 50-100 nm bulb-like structures called caveolae (highlighted by arrowheads in Fig. 1). Caveolae are localized between electron-dense membrane regions called dense bands (dba, Fig. 1). Previous work has indicated that M_3 receptors are preferentially localized in

caveolae [7]. These receptors thus seem to be ideally localized to respond to neurotransmitters released from nearby neural varicosities (Fig. 1).

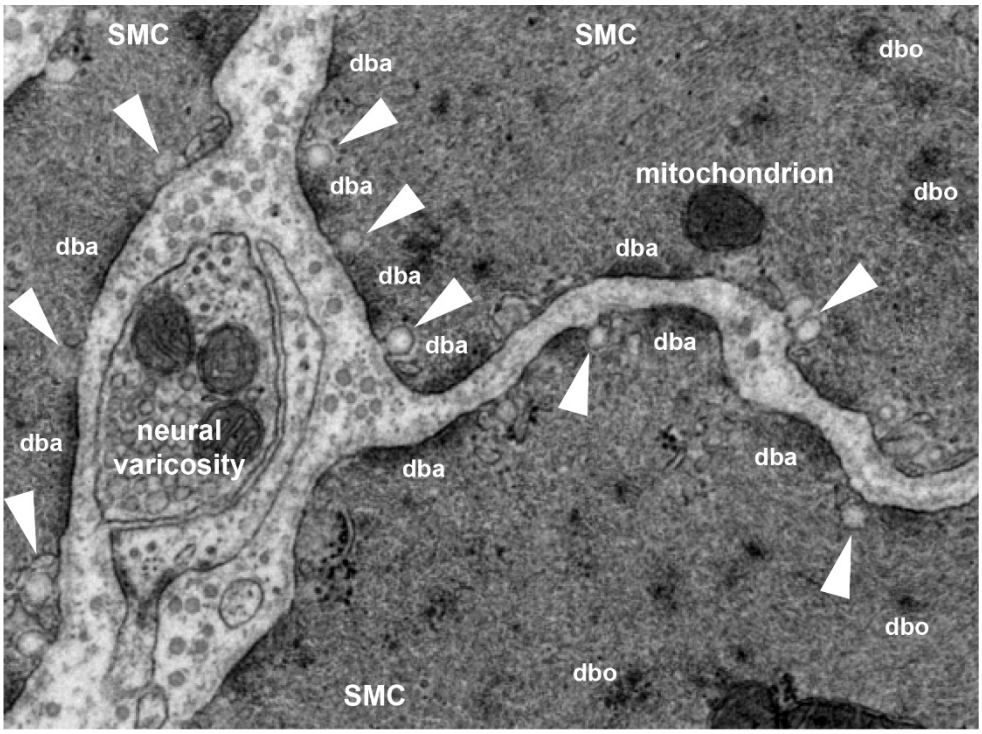

Figure 1. Electron micrograph of rat detrusor SMCs. Rat bladder SMCs were imaged using conventional electron microscopy to highlight cardinal morphological features of this cell type. Electron-dense (dark) areas at the membrane (dba: dense band) and in the cytoplasm (dbo: dense body) are abundant. Arrowheads point to caveolae which localize to dense band-free stretches of the cell membrane. In the centre-left is a neural varicosity. Its right side is wrapped in a Schwann-cell, whereas its left sider is open towards a SMC. Mitochondira whith well-preserved cristae are also visible. The gray spots in the matrix between the varicosity and the three SMCs are cross-sectioned collagen fibrils.

1.2. Contraction and relaxation of SMCs

Activation of bladder SMCs by acetylcholine and ATP is a multistep process. P2X1 receptors are ligand gated ion channels that contribute directly to membrane depolarization and Ca^{2+} influx [8]. M_3 receptors on the other hand are G_{q11}-coupled receptors [5], and stimulate generation of second messengers (IP_3, diacylglycerol) to cause release of Ca^{2+} from intracellular stores and membrane depolarization via as yet incompletely defined mechanisms. Both L- and T-type channels contribute to

depolarization-induced Ca^{2+} influx, and blockers of Ca^{2+} channels accordingly antagonize muscarinic contraction [9]. Like in other smooth muscles, activation of the contractile apparatus involves binding of calcium to calmodulin, phosphorylation of the myosin regulatory light chains by myosin light chain kinase (MYLK), and cross-bridge cycling [10, 11].

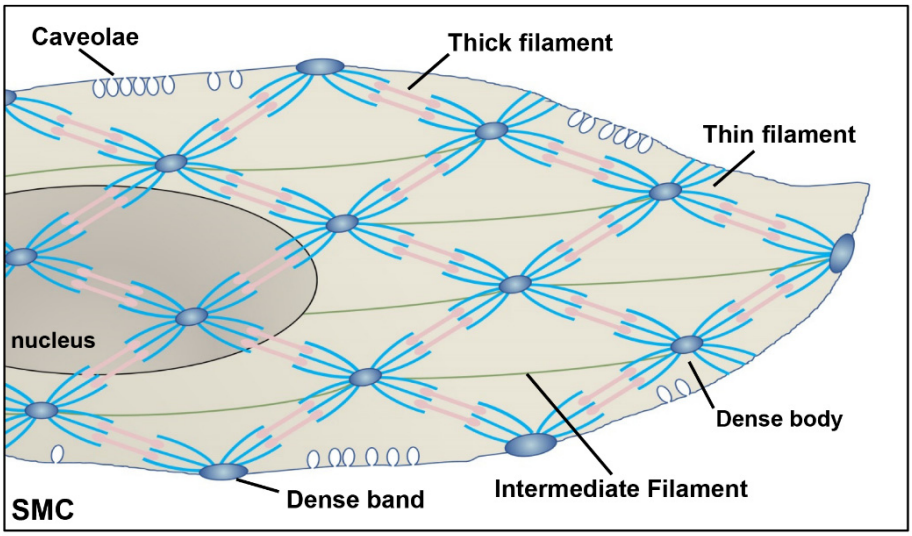

Figure 2. Schematic representation of dense bodies, dense bands, and caveolae in SMCs. Similar to striated muscle, there are attachment sites for thin filaments (actin, primarily *ACTA2*, light blue) in the cytoplasm and at the membrane. These structures are commonly called dense bodies (cytoplasm) and dense bands (plasma membrane). The thick filaments consist of myosin (*MYH11*) and the contractile unit between two dense bodies is the equivalent of a sarcomere in skeletal muscle. Caveolae which are small membrane-attached vesicles are located between dense bands. Some studies claim that intermediate filaments (green) connect dense bodies.

The contractile apparatus in bladder SMCs is built by smooth muscle α-actin (*ACTA2*) and myosin (*MYH11*), and mechanical interaction between these proteins is activated by phosphorylation of the myosin motor [12]. In striated muscle, myofilaments are organized in sarcomeres spanning between Z-discs in a highly periodic fashion. Myofilaments in the spindle-shaped SMCs are not organized in sarcomeres. Instead, the fibres transverse the cell in different directions between the so called dense bodies. Dense bodies are scattered throughout the cytoplasm (dbo, Fig. 1). As indicated above, similar structures are also seen at the cell membrane and are called dense bands (dba, Fig. 1). Dense bodies and dense bands contain α-actinin, but the detailed composition remains to be established. Dense bodies are connected to each other via intermediate filaments [13]. The overall organization of an SMC is schematically depicted in Figure 2.

A central mediator of SMC relaxation is the myosin phosphatase which is a trimeric enzyme consisting of a catalytic subunit (PP-1C, 37kDa), a myosin-binding subunit (130-kDa subunit), and a small subunit of unknown function (20-kDa subunit) [14]. The myosin phosphatase removes a phosphate group from myosin and thereby inhibits smooth muscle contraction. It is inhibited by the sequential activation of trimeric and monomeric G proteins (e.g. $G_{12/13}$→RhoA) and two kinases known as Rho-associated protein kinases or ROCKs (ROCK1 and ROCK2) [15].

1.3. Transcriptional mechanisms and lineage determinants of SMCs

The characteristic ultrastructural features (e.g. caveolae, dense bodies) and gene expression pattern (e.g. *ACTA2*, *MYH11*) that define SMCs are governed by cell-specific transcriptional control mechanisms. SMC differentiation is controlled by myocardin family coactivators (MRTFs, Myocardin Related Transcription Factors). These proteins include myocardin (*MYOCD*), MRTF-A (*MKL1*) and MRTF-B (*MKL2*) [16, 17]. A more distant relative is MAMSTR, but its expression level in SMCs is low [16, 18, 19].

In the healthy bladder, SMCs are normally present in a highly differentiated state, required for the cell's contractile function. In certain conditions, bladder SMCs modulate their phenotype to one that is adapted for growth and matrix synthesis rather than for contraction. This occurs in e.g. bladder outlet obstruction (BOO) [20] and in bladder cryoinjury [21]. MRTFs act by associating with the Serum Response Factor (SRF) [17, 22], which binds to so called CArG-boxes in the promotors of genes that define the contractile phenotype. Ternary Complex Factors (TCFs), critical effectors of Mitogen Activated Protein Kinases (MAPKs), bind to the same site on SRF as the MRTFs, but target another gene battery associated with proliferation. Thus, MAPK activation and resultant TCF phosphorylation will displace MRTFs from SRF and drive SMCs towards a more synthetic and proliferative phenotype with loss of contractile differentiation [23, 24].

The target genes of the MRTF/SRF complex are generally referred to as SMC differentiation markers, and they include smooth muscle myosin heavy chain (*MYH11*), smooth muscle α–actin (*ACTA2*), calponin (*CNN1*) and SM22α (*TAGLN*) [22, 25]. All of these proteins are integral components of the contractile filaments. Ultrastructural features of SMCs beyond the myofilaments are also regulated. Genes responsible for formation of caveolae, for example, were shown in one study to be targeted by the MRTFs [26], but the generality of this regulation remains to be established. The TCFs, which are antagonists of the MRTFs, drive expression of

genes important for growth, including the proto-oncogene c-Fos [23]. c-Fos promotes growth and is overexpressed in several cancers.

A striking illustration of the essential role of MRTFs in the bladder is the Megabladder mouse (*mgb*$^{-/-}$). This strain was created by mistake, and it was found to develop obstructive nephropathy with absurd bladder distension in utero. It was subsequently demonstrated that this results from defective bladder SMC differentiation, and genetic studies indicated disruption of a myocardin enhancer on chromosome 11 [27-30]. Inducible and SMC-specific deletion of myocardin also causes aneurysm-like distension of the bladder, but several other organs, including arteries, are similarly affected [31]. In the Megabladder mouse, it is only the bladder that is affected, suggesting a bladder-specific role of this particular myocardin enhancer.

1.4. Molecular constituents of caveolae and Cavin3

As illustrated in Figures 1 and 2, caveolae are abundant plasma membrane structures of bladder SMCs. These omega-shaped vesicles are also present at high densities in skeletal muscle cells, endothelial cells, and in adipocytes [32]. They are absent in many other cell types, including neurons and most epithelial cells. It has been proposed that caveolae play roles in cell signalling due to their ability to concentrate signalling molecules and to act as signalling platforms for receptors [33, 34]. The formation of caveolae depends on at least two families of unrelated proteins referred to as caveolins (Caveolin-1, -2, and -3) and cavins (Cavin1 to Cavin4) [35-39]. Caveolins are integral membrane proteins as illustrated in Figure 3A, and they have tissue-specific expression patterns. Caveolin-1 (*CAV1*) and Caveolin-2 (*CAV2*) are expressed in SMCs and endothelial cells while Caveolin-3 (*CAV3*) is largely restricted to skeletal muscle [35]. In keeping with this overall assertion, RNA-Seq shows that *CAV1* and *CAV2* are highly expressed in the human bladder, while the expression level of *CAV3* and *CAVIN4* is much lower (Fig. 3B).

Cavins are relatively recently discovered caveolae-associated proteins that form a trimeric complex in the cytosol which then associates with the cytoplasmic surface of caveolae (schematically depicted in 3A). It is likely that this association provides a stabilizing coat for caveolae [34]. It has been reported that the trimeric cavin-complex can be composed either of three Cavin1 molecules or of two Cavin1 molecules and one Cavin2 or one Cavin3 molecule [40, 41] (Fig. 3A). According to the mRNA expression levels of cavins in human bladder (Fig. 3B), it is likely that Cavin1/Cavin1/Cavin2 and Cavin1/Cavin1/Cavin3 complexes are almost equally abundant.

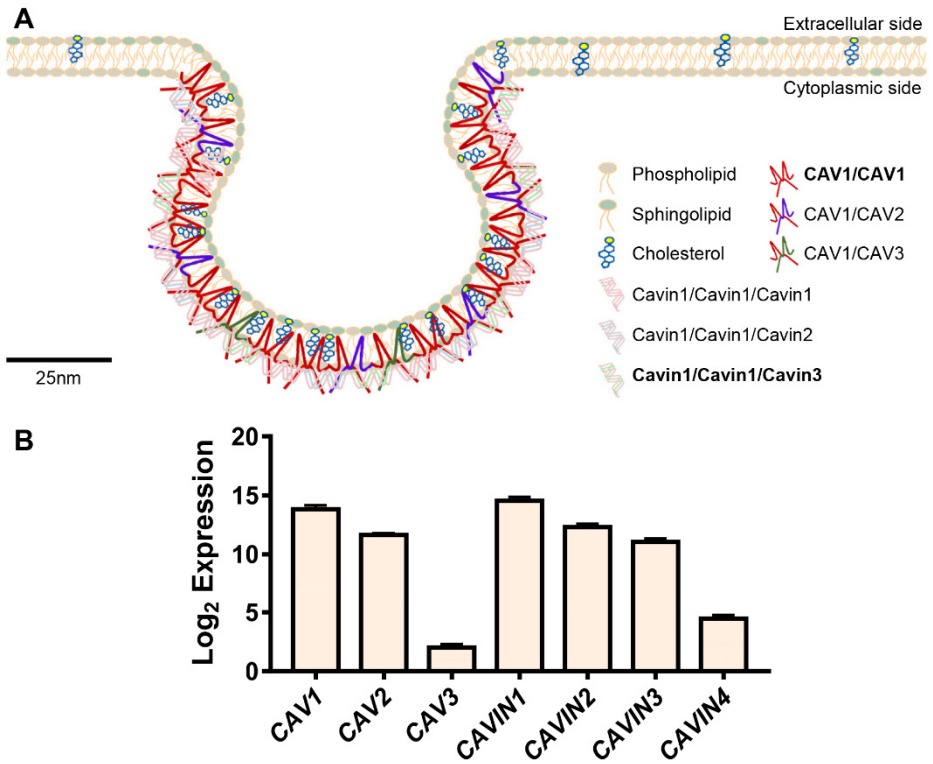

Figure 3. Molecular constituents of caveolae. Caveolae are enriched in certain lipids, including cholesterol and sphingolipids, as well as proteins from the caveolin and cavin families (A). Caveolins (CAV1, CAV2 and CAV3) are integral membrane proteins and essential components of caveolae. All caveolins have a hairpin domain embedded in the membrane. Both the amino terminus and the carboxyl terminus of caveolins are facing the cytoplasm. Caveolins form large complexes with up to 140 molecules. Cavins form trimers that associate with the cytoplasmic surface of caveolae. The trimers can be composed either of three Cavin1 molecules or of two Cavin1 molecules with one Cavin2 or one Cavin3 molecule. In this thesis I present data showing that Cavin3 contributes to formation of caveolae in mouse bladder SMCs. Based on mRNA expression levels (B, from the GTExPortal, n=11), it seems plausible that Cavin1/Cavin1/Cavin2 and Cavin1/Cavin1/Cavin3 complexes are equally abundant in human bladder SMCs. CAV3 and Cavin4 are less likely to contribute meaningfully to caveolae in human bladder SMCs because the levels of these are low.

Deficiency of *Cavin1* results in the complete absence of caveolae in SMCs, and breakdown of all caveolin proteins as wells as of Cavin3 [42]. Loss of *Cavin1* moreover results in impaired bladder contractility and detrusor hypertrophy [42], which is similar to knockout of *Caveolin-1* [43, 44]. So far, the role of Cavin2, Cavin3 and Cavin4 in bladder SMCs remains poorly explored, but a recent study demonstrated that deficiency of *Cavin2* resulted in loss of endothelial caveolae in some tissues. Loss of *Cavin3* on the other hand had no effect on endothelial or fibroblast caveolae [45]. These *in vivo* studies on Cavin3 contrast with *in vitro* work showing that Cavin3 is critical for formation of caveolae in a human fibroblasts cell line [46]. Thus, even if Cavin3 can contribute to formation of caveolae *in vitro*, its role in formation of caveolae *in vivo* remains to be established.

1.5. Molecular constituents of dense bodies and dense bands

As we know, striated muscle is referred to as "striated" for the simple reason that myofibrils appear to have light and dark segments in the microscope. The distance between dark lines (Z-lines or discs) defines a sarcomere. This is the basic contractile unit that shortens on activation [47, 48]. There are no Z-discs in smooth muscle, but dense bodies in the cytoplasm and dense bands in the plasma membrane [49] are equivalent structures (illustrated in Figure 1 and Figure 2). The thin filaments (actin) are anchored to cytoplasmic dense bodies, and fastened to the plasma membrane through the dense bands [50]. Thick filaments (myosin) connect thin filaments from two neighbouring dense bodies. There are also intermediate filaments connecting dense bodies. Dense bodies contain α-actinin [51], as do Z-discs in striated muscle [52].

Besides α-actinin and actin, dense bands contain vinculin, which plays a role in anchoring the cells via integrins to the extracellular matrix. Vinculin-containing dense bands and caveolae regions alternate with each other in a non-overlapping manner [53] (see also Figure 1 and Figure 2). However, this bipartite organization of the plasma membrane is lost when SMCs are isolated from tissue [54]. Dense bands also contain tensins, which bind to actin filaments and interact with the cytoplasmic tail of β-integrins [55, 56]. Due to their role in matrix adherence via integrins, dense bands are sometimes referred to as adherence junctions, and, in cell lines, the equivalent structures are referred to as focal adhesions. Proteomic level understanding of the composition of focal adhesions is emerging, and it has been estimated that the core “adhesome” consists of around 60 proteins (e.g. [57]). However, given the unique spatial organization of these structures in SMCs (i.e. dense bands), and the high mechanical demand on muscle in general, it is very likely

that dense bands in SMCs contain proteins that are not represented in the core "adhesome" [57].

1.6. Bladder denervation

As described above for rodents, the majority of the parasympathetic motor nerves reaching the urinary bladder come from the pelvic ganglia. These nerves play an important role in micturition. In this thesis, the term bladder denervation is used to describe experimental destruction of the pelvic ganglia using freezing. Partial denervation of the bladder is however common in patients with bladder overactivity caused by BOO due to benign prostatic hyperplasia [58, 59]. Bladder denervation may also occur after trauma and surgery [59, 60], and in diabetes [61]. Diabetic cystopathy is a common chronic complication of diabetes mellitus resulting from diabetic neuropathy. Denervation results in decreased bladder sensation, increased bladder capacity, development of residual urine, as well as overactive bladder (OAB) symptoms. Denervation moreover results in bladder hypertrophy as well as changes in intrinsic muscle activity, mechanical properties, and morphology [61-65].

1.7. Medical strategies to achieve re-innervation

Given the key role of neurons for bladder emptying it is no surprise that salvage or renewal of these cells represents an important goal of regenerative medicine. Contemporary strategies for neural regeneration include use of neurotrophic factors [66], scaffolds that provide guidance for sprouting neurons [67] and stem cells [68]. It is obvious that there is no easy fix, and there are many obstacles. For stem cell-based therapies, neurons have to be generated in sufficient numbers and at the right location. It has moreover become apparent that an obstacle for neural regeneration is scar formation [69]. Neural plasticity is influenced by the neurotrophic factors released from the target organs [70]. There are six neurotrophins included in the neurotrophic factor family: nerve growth factor (NGF), brain derived neurotrophic factor (BDNF), neurotrophin 3 (NT-3), neurotrophin 4/5 (NT-4/5), glial-derived neurotrophic factor (GDNF), and ciliary neurotrophic factor (CNTF) [71]. Neurotrophic factors are expressed in rodent bladder tissue, and the expression levels vary during postnatal development [72-75].

Many pathological states cause OAB symptoms, and these symptoms include urgency and increased micturition frequency. This suggests abnormal activity of

bladder sensory afferents due to neuroplastic changes. Accordingly, in pathologies associated with OAB symptoms, the expression of neurotrophic factors is changed in the bladder wall [76, 77]. It is also known that bladder neurotrophin levels change in spinal cord injury and cyclophosphamide-induced cystitis [78]. To devise strategies for re-innervation of the bladder it is reasonable to first define the intrinsic response of the bladder to loss of its nerve supply. Some of the mechanisms that promote re-innervation should arguably be activated in this situation, and if they can be defined and enhanced, a clinically meaningful neural recovery may be accomplished.

1.8. Transcriptomic analyses

Both bladder denervation and BOO can induce bladder hypertrophy. BOO can moreover cause progressive denervation. Bladder hypertrophy induced by BOO may therefore be due in part to denervation as such. Identification of common and unique gene expression signatures in these conditions may thus represent one way to unravel common and unique therapeutic targets.

There are numerous modern high throughput methods to measure gene expression. These include microarray technology, which can be done for both mRNAs and micro-RNAs (miRNAs), and RNA-Seq, which is more comprehensive. Microarray technology builds on the detection of multiple targets (RNAs or miRNAs) using nucleic acid probes that are deposited in small spots on a solid surface. Hybridization of the target with the spotted probes is done under stringent conditions, and the hybridization is detected and quantified to obtain relative expression levels. Because the experiment examines changes of multiple targets, the statistical methods have to be adapted. Most analysis tools use algorithms that address such concerns. One of them is the Significance Analysis of Microarrays (SAM) [79].

In a prior study from our group, the focus was on experimental BOO [80]. Many of the changes in those arrays were confirmed and shown to play roles in bladder hypertrophy, altered contractility, and adaptation to altered demand in subsequent studies [81-84]. Similar studies were also made using bladder samples from human patients with different urodynamically defined states of BOO [85]. However, gene expression surveys following bladder denervation have not been made.

1.9. Gene correlation analyses

Bioinformatics is a field combining large biological datasets with computer science, mathematics and statistics to obtain an understanding at a deeper level of biological or medical relationships. Gene Co-expression Networks (GCNs) and Gene Regulatory Networks (GRNs) are examples of terms in this discipline which are helpful for understanding the function of genes as wells as their regulation [86, 87].

Bioinformatics can be done using existing expression datasets generated using e.g. microarray or RNA-Seq technology. The GTEx Portal (www.gtexportal.org) is one such resource, characterizing human transcriptomes for a wide variety of human tissues. The original aim of this database was to study the relationship between genetic variation and gene expression [88], but we have used this dataset to define novel smooth muscle-enriched genes and to correlate different mRNAs with each other. Publications using this database are accumulating (www.gtexportal.org/home/publicationPage). For instance, a recent publication regarding tissue-specific gene expression was based on the GTEx project [89].

Theoretically, co-expression or correlation of two gene products can be due to regulation by the same transcription factor. They can also correlate because one gene is downstream of the other gene, but correlations may also arise due to chance. Intervention studies are required to distinguish between these possibilities. The use of bioinformatics to identify SMC-specific genes is not novel [90], but the quality of existing datasets increases, and these datasets become increasingly comprehensive with time.

In prior work from our group, data from GTEx was used for examining the correlations between transcription factors and target genes [26, 91]. Briefly, data from across-samples was normalized using the trimmed mean of M-values (TMM) normalization method [92], and correlations were analysed with the non-parametric Spearman method [93]. The same basic strategy was used here, but with some variation detailed in the respective papers.

2. Aims of Thesis

2.1. Subproject I: Transcriptional control of constituents of caveolae

Caveolae are important organelles for SMCs in the urinary bladder. The generation of caveolae depends on caveolins and cavins. Prior work demonstrated that myocardin family coactivators (MRTF-A, MYOCD) can increase transcription of caveolins and cavins in vascular smooth muscle. **The aim of this study was to investigate the transcriptional control of caveolins and cavins by myocardin family coactivators in rat and human bladder SMCs.**

2.2. Subproject II: *Cavin3* knockout

The expression of caveolins and cavins varies in a tissue-specific manner. Deficiency of *Caveolin-1* or *Cavin1* results in the complete absence of caveolae in bladder SMCs. Deficiency of *Cavin2* results in loss of endothelial caveolae in some tissues. Loss of *Cavin3* on the other hand has no effect on endothelial or fibroblast caveolae, but reduces the density of caveolae in a human fibroblasts cell line. **The aim of this study was to characterize the functional and morphological effects of *Cavin3* knockout using bladder and vascular SMCs.**

2.3. Subproject III: Regulation of Nexilin by actin-controlled coactivators

Nexilin (*NEXN*) is expressed in striated muscle, localizing to Z-discs, where it influences mechanical stability. We noted that Nexilin (*NEXN*) is also highly expressed in SMCs, and showed that *NEXN* correlates with MRTFs (*MYOCD, MKL1, MKL2*) and YAP/TAZ (*YAP1 and WWTR1*), representing two families of mechano-responsive coactivators. **The aim of this study was to test if Nexilin**

(*NEXN*) is regulated by the MRTF- and the YAP/TAZ-coactivator families, and to examine if Nexilin (*NEXN*) affects actin polymerization and SMC motility.

2.4. Subproject IV: Sprouting from the pelvic ganglia

Regeneration of the nerves arising from the pelvic ganglia is an attractive strategy for therapy of denervation-associated bladder instability. Neurotrophic factors, including nerve growth factor (NGF) and brain derived neurotrophic factor (BDNF), target different neurotrophin receptors (TrkA, TrkB and TrkC), that may have different roles in survival and growth of autonomic neurons. **The aim of this study was to investigate the expression of neurotrophic factors in bladder tissue, and to study the effect of bladder tissue on the sprouting from rat pelvic ganglia *in vitro*.**

2.5. Subproject V: Transcriptional impact of bladder denervation

Both bladder denervation and bladder outlet obstruction (BOO) are prevalent urological conditions causing bladder hypertrophy and hyperplasia. Partial denervation has been reported in the obstructed bladder, suggesting that denervation may contribute to growth caused by BOO. **The aim of this study was to define shared and unique transcriptomic signatures in BOO and total denervation, respectively.**

3. Materials and Methods

This section describes the main methods and techniques used. I have tried to give a comprehensive description, because techniques lay the foundation of scientific quality. Further details may be found in the respective papers (Appendices I-V).

3.1. Ethics

Ethical applications for the animal experiments were submitted to the Swedish Board of Agriculture (www.jordbruksverket.se), and protocols were approved by the Malmö/Lund Ethical Committee (for approval numbers see the respective papers). Interventions and care were in accordance with national guidelines and the European Parliament Directive 2010/63/EU. The experiments using animals comply with the ARRIVE guidelines (Animal Research: Reporting *In Vivo* Experiments) and were designed with "no alternative to *in vivo* experiments", "the minimum use of animals" and "the minimal suffering", in accordance with "The Three Rs". For example, we did not sacrifice animals only for isolating primary cells, but obtained tissues for cell isolation from animals sacrificed for the use of other organs. In Paper V (bladder denervation project), female rats were used to allow for comparison with data from bladder outlet obstruction (BOO), also in consideration of reducing animal use. Animals were euthanized by gradually increasing the atmospheric carbon dioxide concentration, which is considered to elicit a minimum amount of pain and fear.

Human detrusor muscle was retrieved from bladders removed surgically to save patients from cancer. Written informed consent was obtained, and the experiments were approved by the Regional Ethical Review Board at Lund University (https://www.epn.se, approval no. 2008–4). Procedures conformed to the Declaration of Helsinki. Primary bladder smooth muscle cells (SMCs) from humans were used for two reasons. One was that data from human cells are more relevant for understanding human physiology and disease. The other was that such use minimizes animal suffering.

3.2. Cell culture

Human bladder smooth muscle cells (HBSMCs) were isolated from detrusor muscle strips prepared by microdissection. Cells from four individuals, one female and three males with a median age of 71 were used unless specified. Rat bladder SMCs were isolated from female Sprague-Dawley rats (approximately 200 g). Cells were grown in DMEM/Ham's F12 (1:1) supplemented with glutamine, fetal bovine serum (FBS) and antibiotics (50 units/ml penicillin, 50μg/ml streptomycin). Although isolation of primary smooth muscle is a mature technology, great care was taken to isolate pure smooth muscle. Also, cells were isolated as soon as the fresh tissues were harvested. Cells were identified as SMCs by morphology and gene expression of smooth muscle markers. Human coronary artery SMCs (HCASMCs) were from Gibco. They were cultured in Medium 231 with 5% Smooth Muscle Growth Supplement (SMGS) and antibiotics (50 units/ml penicillin, 50μg/ml streptomycin). All cells were cultured in a water-jacketed cell incubator (37℃, 5% CO_2 in air), and passaged using trypsin at confluence. Experiments were done using cells in passages 3 to 8.

3.3. Gene overexpression and silencing using recombinant adenoviruses

Virus transduction is often used as a tool in basic research and is actively studied for its potential in gene therapy [94, 95]. Virus transduction is rather safe because the transferred genetic sequences do not encode viral proteins critical for generation of new viruses, and hence these infections do not cause cellular damage typically seen with viruses [96, 97]. The recombinant adenoviruses used in my thesis, including those for overexpression of wildtype genes and short hairpin RNAs (shRNAs), were obtained from Vector Biolabs. The virus vector was the human adenovirus type-5. The entire viral genome of human adenovirus type-5 is linear double-stranded DNA of approximately 36 kB. Two phases of adenovirus transcription, so called early and late phases, occur before and after replication. The early-transcribed DNA regions are E1 to E4 [94, 98-101]. The recombinant adenoviruses used in my thesis had the E1/E3 region deleted. Deletion of E1 ensures replication deficiency, precluding infectivity. Deletion of E3 region allows the vector to accommodate larger recombinant genes. Recombinant adenoviruses can infect 100% of cells, including dividing, non-dividing, and primary cells. Our experience is that they are somewhat more effective with human cells than with rodent cells. Adenoviruses can code for proteins without integrating into the host

cell genome, and do not inactivate genes or activate oncogenes [95, 97]. Once the adenoviruses get inside the cells, they translocate to the nuclear pore complex, and release their DNA into the nucleus. Thereafter transcription begins [95, 97].

ShRNA is an artificial RNA molecule with a tight hairpin turn, which can be used for silencing gene expression. The mechanism is called RNA interference (RNAi). The expression of shRNA requires an expression vector [102, 103]. As described above, recombinant adenoviruses were used as vectors for shRNA in my project. After transcription, shRNAs exit the nucleus, are cleaved by the endonuclease Dicer in the cytoplasm, and the resulting short interfering RNA (siRNA) oligonucleotides enter the RNA-induced silencing complex (RISC). This results in cleavage of complementary mRNAs [104, 105]. The same can be achieved using chemically synthesized siRNAs, but in this case, some means of cell entry is needed.

In my experiments, recombinant adenoviruses were applied to the cells at different concentrations (normally 100-300 MOI (Multiplicity of Infection)) by addition to the cell-culture medium and incubation for 24 h. Upon application, cells are infected by the adenoviruses, leading to expression of the gene of interest. The appropriate amount of viruses used for infecting cells is very important, since insufficient virus titers will lead to suboptimal infection. Too much virus on the other hand may cause cytotoxicity or other effects. In my experience, human SMCs maintain their morphology after transduction with empty recombinant adenoviruses (Ad-CMV-null or Ad-U6-null) at concentrations up to 600 MOI. However, 300 MOI of virus containing shRNA against *Cthrc1* is toxic to human bladder SMCs, and 500 MOI of virus containing shRNA against *NEXN* is toxic to human coronary artery SMCs, but much less toxic to human bladder SMCs. Thus, cytotoxicity of recombinant adenoviruses depends on the genetic material transferred and on cell type used.

The classical adenovirus receptor is called Coxsackie and Adenovirus Receptor (CAR). Adenovirus type-5 engages CAR as its primary attachment receptor to the cells [106, 107]. However, human SMCs are CAR deficient, but substantially expresses the species B receptor CD46 [108]. The concentration of adenovirus used for human SMCs were relatively high in my experiments as it was found to be required. This could be because infection via CAR is more effective than through CD46. A recent study also showed that there are some molecules, such as heparan sulfate and sialic acid, which can also mediate adenovirus infection [109, 110], but it is not known whether adenoviruses can infect human SMCs through these molecules.

The effect of viral overexpression was confirmed by RT-qPCR and western blotting, respectively. Adenoviruses usually allow high expression of the recombinant protein; however, it should be kept in mind that this does not mean that every cell is infected. Also, cells will lose the adenovirus through cell division. For example, in Paper III (Nexilin project), I used a scratch assay to detect the cell

mobility in the cell-free area, and typical moving cells were selected to measure the speed of cell movement. A limitation of this experiment was that I did not confirm that the selected cells were 100% virus-containing.

3.4. Gene silencing with siRNAs

SiRNA is a class of double-stranded RNA molecules that are 20-25 nucleotides long and operating within the RNAi mechanism, preventing translation [111]. SiRNA is a useful tool for modulating gene expression that has also generated interest in RNA interference-based therapy [112]. The use of synthetic siRNAs for therapy hinges on effective delivery into cells. Following siRNA entry, it binds to other proteins to form the RISC, and the siRNA becomes single stranded. This single stranded species binds to a complementary mRNA (target mRNA) and directs mRNA cleavage [111].

In my experiments, siRNAs were purchased from Ambion Thermo Scientific, allowing for transient suppression of target gene expression. SiRNA transfection was done using Oligofectamine transfection reagent (Invitrogen) in Opti-MEM medium (Gibco), eliminating degrading factors in cell culture medium and FBS (i.e. RNases). SiRNA transfection was done according to the manufacturer's instructions, and the final siRNA concentration was 50 nM. The cells were harvested or treated as indicated 72 hours after transfection. The silencing effect for each siRNA was confirmed by RT-qPCR. All targeted genes were reduced by more than 50% after silencing compared to the negative control. The Oligofectamine transfection regent has a capacity for siRNAs up to 200nM, which allows transfection of three siRNAs (against *SRF*, *YAP1* and *WWTR1*, respectively) at 50nM each, giving reductions of *SRF*, *YAP1* and *WWTR1* by 64.9±3.4%, 65.6±4.5%, and 58.3±3.9%, respectively.

3.5. MTT assay

Cell proliferation was assessed using the MTT (3-(4,5-dimethylthiazol-2-yl)-2,5-diphenyltetrazolium bromide, Thiazolyl Blue Tetrazolium Blue) assay. This may be the most common tetrazolium-based assay for assessment of cell viability or cell proliferation *in vitro*. MTT powder was purchased from Sigma, and dissolved in Phosphate Buffered Saline (PBS) at 5 mg/ml to produce a yellowish stock solution, which is stable at 4 ºC for 1 week. When water-soluble MTT is taken up by viable cells, it is reduced [113]. Reduction of MTT generates a dark blue, water-insoluble

formazan salt, and the amount of this salt is proportional to the number of living cells. In our experiments, cells were seeded in 96-well plates and treated as indicated. After treatment, the culture medium was replaced by serum-free medium for 2 h. This medium was then replaced with serum-free medium containing MTT (0.5 mg/ml) followed by incubation for 1-2 h. The medium was gently removed, and the cell-associated formazan was dissolved in 100 µl of dimethyl sulfoxide (DMSO). The absorbance of the blue solution was measured at 540 nm in a Multiscan GO Microplate Spectrophotometer (Thermo Scientific). The incubation time with MTT depends on the experimental conditions and the amount of cells. I usually stoped the incubation when the dark blue precipitate was clearly visible. In my MTT experiments, I starved the cells for 2 h before MTT incubation to avoid any acute and confounding effects of serum as such. When changing medium, great care was taken to avoid aspiration of cells or precipitate and I was meticoulously adding equal volumes of medium and DMSO. I also took great care to to seed the cells at similar densities in each well.

3.6. RNA isolation

Cultured SMCs were rinsed twice with ice-cold PBS and lysed in Qiazol (Qiagen). Cells were lysed by pippeting up and down gently several times, followed by transfer to a 1.5 ml tube. To reduce RNA degradation, samples were kept on ice during the whole procedure. Total RNA was obtained using the Qiagen miRNeasy mini kit (Qiagen) manually, or using the QIAcube workstation (Qiagen) according to the manufacturer's protocol. Genomic DNA can interfere with qPCR quantification. DNase digestion was thus performed during RNA purification by using RNase-Free DNase Set (Qiagen). A Nanodrop spectrophotometer (Thermo Scientific) was used to check absorbance at 260 and 280 nm for determination of sample concentration and purity. The A260/A280 ratio should be close to 2.0 for pure RNA, and for RT-qPCR experiments, ratios between 1.9 and 2.1 were considered acceptable. In paper V (bladder denervation project), the quality (integrity) of RNA used for microarrays was also determined by the 28S to 18S rRNA ratio (RIN, RNA integrity number) using capillary gel electrophoresis. This was done at the core facility used.

It is more challenging to isolate RNA from bladder tissue than from cells as RNA degrades more easily in tissue. Thus, it is important to freeze the tissue in liquid nitrogen immediately after dissection. A pre-chilled French press was also used to grind (smash) tissue hard-frozen in liquid nitrogen to a powder. After that, the tissue was transferred to a 2 ml tube, and a metal bead was added together with Qiazol lysis reagent. The 2 ml tube was then put into a pre-chilled TissueLyser LT Adapter

(Qiagen) and complete tissue disruption was achieved using the TissueLyser LT machine (Qiagen). Such thorough tissue homogenization is important for maximal RNA yields.

3.7. RT-qPCR

Reverse Transcription - quantitative Polymerase Chain Reaction (RT-qPCR) is a technique used in molecular biology to detect RNA expression. It includes two steps, reverse transcription (RT) and quantitative polymerase chain reaction (qPCR) [114]. In the step of RT, complementary DNA (cDNA) was transcripted from RNA templates, while in the step of qPCR, amplification of DNA was quantitatively measured using fluorescent dyes [115, 116]. Quantitative real-time PCR is one kind of qPCR, which utilizes fluorescent DNA labeling techniques, such as SYBR Green or TaqMan Probes [117-119]. In my experiments, the expression of mRNAs was detected using one-step RT-qPCR reactions in the StepOnePlus qPCR cycler (Applied Biosystems). This means that the RT step and the qPCR step happen in a single tube. In each PCR tube of a 96-well plate, a 10 µl reaction system was prepared using the Quantifast SYBR Green RT-PCR kit (Qiagen) and the Quantitect primer assays kit (Qiagen) for individual target genes. Primer sequences have been validated, but Qiagen considers them to be commercially sensitive and thus keeps them secret. After the reaction system was prepared, RT step was started (50 ºC, 10 min). This was followed by a PCR activation step (95 ºC, 5 min), which activates HotStarTaq DNA Polymerase and also ends reverse transcription and denatures template cDNA. 2-step cycling (Denaturation, 95℃, 10 s; Annealing and Extension 60 ℃, 30 s) was then performed for 40 cycles. SYBR Green binds all double-stranded DNA molecules, emitting a fluorescent signal on binding. This fluorescent signal was detected at the extension step of the 2-step cycling. When the fluorescence crosses a predefined threshold, the number of reaction cycles is presented as the Ct (cycle threshold) value. Finally, melting curve analysis of the PCR product was performed to verify specificity. Fold changes of gene expression were calculated using the 2(-Delta Delta C(T)) method ($2^{-\Delta\Delta Ct}$ method) [116].

RT-qPCR amplifies the target genes at the same time as the reference genes, which can be used to normalize the mRNA level of each sample. This allows comparison of the target gene expression level across different samples. The matter of choosing different reference genes is important and can affect the results. Indeed, it is recommended to use more than one reference gene [120]. In our experiments, 18S ribosomal RNA (18S) was used as a reference gene throughout. Stability of 18S versus other housekeeping genes, for example, GAPDH and β-actin, was routinely

confirmed. Also, the Ct values of 18S between different samples did not vary much in individual experiments.

qPCR detection is very sensitive because the DNA is amplified several orders of magnitude. Thus, variability is common. It is very important to use equal volumes of RNA as template for each reference gene and target gene, and duplicates for each gene in one sample is recommended. In one experiment, I usually have more than one sample for each treatment, usually duplicate samples for 6-group experiments and triplicate samples for 4-group experiments. No Template Controls (NTC) are also important to identify whether there is reagent contamination or primer dimer formation.

3.8. Western blotting

In western blotting proteins are separated by electrophoresis and transferred to a membrane. They are then detected by antibodies referred to as primary and secondary antibodies [121]. In my experiments, cultured SMCs were rinsed twice with ice-cold PBS and then transferred to Laemmli buffer (60 mM Tris-Hcl, pH 6.8, 10% glycerol, 2% SDS) containing protease inhibitor cocktail (Sigma-Aldrich) and Halt™ phosphatase inhibitors (Thermo Fisher Scientific) for lysis. For preparing tissue samples, animal bladder tissue stored at -80 ºC was crushed into powder using a French press precooled in liquid nitrogen. The tissue powder was transferred to a 2 ml tube and Laemmli sample buffer was added together with a metal bead. The 2 ml tube was next put into a pre-chilled TissueLyser LT Adapter (Qiagen) and tissue disruption was performed on TissueLyser LT machine (Qiagen) as described above. Samples were kept on ice for 20 min, and then sonicated for 10 s. This was followed by heating to 100 ºC for 5-10 min, and centrifugation for 20 min at 14000 rpm. Supernatants were collected in new tubes and the protein concentration was measured using a detergent-compatible protein assay kit from Bio-Rad. The absorbance of the samples was measured at 750 nm in a Multiscan GO Microplate Spectrophotometer (Thermo Scientific). To prepare the loading samples, the protein concentration of the lysates was adjusted to 1 µg/µl, after adding bromophenol blue (0.01%) and β-mercaptoethanol (5%). 20µl of the lysates (i.e. ~20µg protein) was then loaded in the wells of Bio-Rad TGX Criterion gels (Any KD or 4-15%), and proteins were separated using Bio-Rad Tris/Glycine/SDS electrophoresis buffer at 200-250V. Electrophoresis-separated proteins were transferred to a precut nitrocellulose membrane (pore size 0.2 µm) with the Trans-Blot Turbo aggregate (Bio-Rad). All membranes were blocked using 1x Tris Buffered Saline (TBS) with 1% Casein (Bio-Rad) for 2 h and incubated with primary antibodies at 4 ºC overnight or up to 48 h. The primary antibodies used are summarized in Table 1.

Membranes were washed five times in TBS-T and then incubated with HRP-conjugated secondary anti-mouse or anti-rabbit antibodies (Cell Signaling Technology). Immunoreactive bands were visualized using SuperSignal West Femto reagents (Thermo Fisher Scientific). Chemiluminescence was imaged using the LI-COR Odyssey Fc instrument (LI-COR Biosciences) and images were analyzed using Image Studio software. The signal of the protein of interest was normalized first to the loading control (HSP90, GAPDH or β-Actin). The resultant values for all groups, including the controls, were then normalized to the mean of the control samples, giving variation around 1 for the controls.

Although protein samples are more stable than RNA samples, loading samples should be stored at -80 ºC. Large volumes of lysates should be aliquoted to avoid multiple freeze thaw cycles. Protein determination is important for calculation of loading volumes. Although protein expression levels are normalized to reference proteins such as HSP90, it is important to load equal amounts of protein in each well. β-mercaptoetahnol, which is used to cleave disulphide bonds and destabilize the secondary and tertiary structure, causing unfolding of the protein, should be added after protein quantification. This is because it is volatile and can interfere with protein concentration determinations [122, 123].

Needless to say, great care is required at every step for high quality western blot results. An important and often neglected aspect of the technique is antibody validation. Antibody validation is the direct demonstration that the antibody detects the intended protein. The golden standard for antibody validation is knockout or knockdown of the protein to be detected, but overexpression is also acceptable. In Figure 7E of this thesis, validation of the Cavin3 antibody is illustrated. Many, but not all, of the antibodies I have used have been validated by me (c.f. Figure 12B for another example), or by others. Using little cited antibodies for the first time, it is necessary to incubate full membranes to see how many bands there are, and to determine their molecular weights. It is also important to note if there are strong unspecific bands that interfere with detection of a week but specific band (i.e. having the expected molecular weight and showing sensitivity to knockout, knockdown or overexpression). The presence of multiple bands does not necessarily imply poor specificity. In Paper V (bladder denervation project), the antibody against Cthrc1 from MMCRI (Maine Medical Center Research Institute) yielded at least two bands between 37 and 20 kDa. According to evidence in the literature, Cthrc1 is an N-glycosylated and secreted protein. An additional modification may occur when Cthrc1 is secreted, and multimers may also form [124]. The different Cthrc1 bands thus likely reflect the presence and absence of such modifications. Indeed, when I overexpressed or knocked Cthrc1 down, the 37/20 kDa bands became stronger and weaker, respectively, providing hard-core evidence of specificity.

Table 1. Primary antibodies used for immunoblotting

No.	Targets	Antibodies	Source
1	Actin	Anti-pan actin: rabbit polyclonal, #AAN01	Cytoskeleton Inc.
2	BDNF	BDNF antibody, ab108383	Abcam
3	Calponin	Calponin [EP798Y], ab46794	Abcam
4	Caveolin1	Caveolin-1 (D46G3) mAb, #3267	Cell Signaling Technology
5	Caveolin2	Clone 65/Caveolin 2 (RUO), 610685	BD Transduction Lab.
6	Caveolin3	Clone 26/Caveolin 3 (RUO), 610421	BD Transduction Lab.
7	Cavin1	PTRF antibody, ab48824	Abcam
8	Cavin2	SDPR antibody, ab113876	Abcam
9	Cavin3	PRKCDBP antibody, 16250-1-AP	Proteintech
10	CD68	CD68 antibody KP1, MCA5709	Bio-Rad
11	Cthrc1	monoclonal Cthrc1, Vli55	MMCRI
12	DKK3	Anti-Dkk3 antibody [EPR15611], ab186409	Abcam
13	FLOT2	Flotillin-2 (C42A3) Rabbit mAb, #3436	Cell Signaling Technology
14	GAPDH	GAPDH clone 6C5, MAB374	Merck Millipore
15	Gelsolin	Gelsolin (D9W8Y) Rabbit mAb, #12953	Cell Signaling Technology
16	GM130	GM130 Antibody (EP892Y), NB110-57012	Novus Biologicals
17	GUCY1A3	GUCY1A3 Antibody (3G6B2), MA5-17086	Thermo Fisher Scientific
18	GUCY1B3	Gucy1b3 antibody, 19011-1-AP	Proteintech
19	HSP90	Clone 68/Hsp90 (RUO), 610418	BD Transduction Lab.
20	MEP50/WDR77	MEP50 (D56B8) Rabbit mAb, #2018	Cell Signaling Technology
21	MRTF-A	MKL1/MRTF-A, #14760	Cell Signaling Technology
22	MYH11	Smooth muscle Myosin heavy chain 11, ab53219	Abcam
23	MYLK	Anti-Myosin Light Chain Kinase antibody, M7905	Sigma-Aldrich
24	MYPT/MYPT1	MYPT1 Antibody, #2634	Cell Signaling Technology
25	Nexilin	monoclonal Nexilin [NX38], ab213628	Abcam
26	NGF	Anti-NGF antibody [EP1320Y], ab52918	Abcam
27	NT-3	Anti-Neurotrophin 3 antibody, ab65804	Abcam
28	Osteopontin	Anti-Osteopontin antibody, ab91665	Abcam
29	p27KIP1	p27 Kip1 (D37H1) Rabbit mAb, #3688	Cell Signaling Technology
30	PDI	PDI (C81H6) Rabbit mAb, #3501	Cell Signaling Technology
31	PERK	PERK (C33E10) Rabbit mAb, #3192	Cell Signaling Technology
32	p-Erk	Phospho-Erk1/2(Thr202/Tyr204), #9101	Cell Signaling Technology
33	Pleiotrophin	Anti-Pleiotrophin antibody [EPR3041], ab79411	Abcam
34	PLOD2	PLOD2-Specific Antibody, 21214-1-AP	Proteintech
35	PRC1	PRC1 Antibody, #3639	Cell Signaling Technology
36	p-STAT3(S727)	Phospho-Stat3 (Ser727), #9134	Cell Signaling Technology
37	p-STAT3(Y705)	Phospho-Stat3 (Tyr705) (D3A7), #9145	Cell Signaling Technology
38	p-YAP	Phospho-YAP (Ser127) Antibody, #4911	Cell Signaling Technology
39	SM22	SM22 alpha antibody, ab14106	Abcam
40	STAT3	Stat3 (124H6) Mouse mAb, #9139	Cell Signaling Technology
41	t-Erk	Erk1/2 Antibody, #9102	Cell Signaling Technology
42	Trk A	Anti-TrkA antibody [EP1058Y], ab76291	Abcam
43	Trk B	Anti-TrkB antibody, ab51190	Abcam
44	Trk C	TrkC (C44H5) Rabbit mAb #3376	Cell Signaling Technology
45	YAP	YAP Antibody, #4912	Cell Signaling Technology
46	β-Actin	β-Actin clone AC-15, A5441	Sigma-Aldrich

Another challenge in western blotting is stripping and re-probing, which is a time-efficient method for determining multiple protein targets within a single gel run [125]. I used Restore™ PLUS western blot stripping buffer (Thermo Fisher) for this. In such cases it is necessary to check the efficiency of the stripping by re-exposing the membrane with ECL reagents. If the stripping buffer has failed to remove all antibody from the membrane, the signal from the ineffectively stripped antibody may interfere with subsequent detection(s). Also, I never striped the membrane more than twice since stripping always causes loss of epitopes [125].

Last but not least, when we talk about gene expression, it should be appreciated that mRNA levels are not always consistent with protein levels. That is, one cannot use PCR alone and skip western blotting. Discrepancies at mRNA and protein levels arise due to post-transcriptional regulation, including microRNA-mediated regulation [126, 127], but protein synthesis and degradation rates are also important. Long half-lives of caveolin proteins turned out to be a reason for different results at the mRNA and protein levels in one of my studies (c.f. Figure 4F through H below).

3.9. Immunohistochemistry

Immunohistochemistry (IHC) is a method for demonstrating the presence and location of proteins in tissue sections. Although less sensitive than western blotting, it allows for observation of the protein its natural context. In my expreiments, bladder detrusor strips, small mesenteric arteries and caudal arteries were isolated, fixed in 4% paraformaldehyde (PFA), and embedded in paraffin. 5 µm sections were cut and mounted on slides. The slides were deparaffinized and rehydrated with xylene, ethanol and cold tap water. After antigen retrieval with 0.1% trypsin (Sigma) for 20 min (37 ºC), the sections were treated with 4% H_2O_2 in methanol for 20 minutes at room temperature to inhibit endogenous peroxidase activity. After blocking with 3% bovine serum albumin (BSA, Sigma) for 1-2 h, sections were incubated overnight (4 ºC) with primary antibody (e.g. anti-Cavin3, Proteintech, 16250-1-AP, 1:200) dissolved in PBS containing 3% BSA. Sections were rinsed in PBS with 0.025% Triton X-100 for 5 min three times, followed by incubation with secondary antibody conjugated with HRP (horseradish peroxidase, Cell Signaling) at a dilution of 1:200. DAB solution (Dako) was added to activate the chromogenic reaction and maintained until brownish color was observable. Slides were then rinsed gently with distilled water. Nuclei were stained with hematoxylin (Histolab) [128]. Slides were dehydrated and mounted, and micrographs were captured with an Olympus DP72 microscope and Olympus CellSens Dimension software.

Signal amplification via indirect chromogenic detection, such as that in immunohistochemistry, increases signal strength. Thus, immunohistochemistry has

greater sensitivity than immunofluorescence. A drawback is that subcellular resolution may be poorer because color pigments are not anchored like the antibodies themselves and may diffuse away from the enzyme-linked secondaries. For Cavin3 we used both immunohistochemistry and immunofluorescence, and in this case, both detection methods supported membrane-association of the antigen (compare figures 6H, bottom right, and 7B).

3.10. Immunofluorescence

Immunofluorescence (IF) is a a specific example of immunohistochemistry. Different fluorescent dyes not only allow simultaneous staining of different tragets, but also allows for co-localization studies. Thus, immunofluorescence was used for the expriment where I double stained Nexilin and Caveolin-1. Fresh human detrusor muscle strips were dissected from human bladders. Healthy tissue far from the urothelial carcinoma was used. Strips were embedded in O.C.T. COMPOUND (VWR, 361603E) and frozen at -80 ºC (liquid N_2). 10 µm cross-sections were cut and mounted on slides stored at -80 ºC. For staining, the slides were rewarmed to room temperature for 15 min and washed with PBS three times, then blocked with 3% BSA for 1-2 hours at room temperature. The sections were incubated with the Nexilin primary antibody (1:200, Abcam, ab213628) and CAV1 primary antibody (1:400, Cell Signaling Technology, #3267) diluted in PBS containing 3% BSA at 4 ºC overnight. After washing with PBS three times, the slides were incubated with Goat anti-Mouse IgG Alexa Fluor Plus 488 (Invitrogen, A32723) and donkey anti-rabbit Alexa Fluor® 647 (Invitrogen, A31573) (1 hour each, 1:200) diluted in PBS with 3% BSA. Nuclei were counterstained with DAPI (0.1–1 µg/mL, Invitrogen, D1306) for 3-5 min. After washing the slides were mounted with Fluorescence Mounting Medium (Dako, S3023). Images were captured using an Olympus DP72 microscope equipped with a digital camera using the software Olympus CellSens Dimension. The fluorescence intensity of CAV1, NEXN and YAP1 was also determined by a laser scanning confocal microscope (LSM5, PASCAL, Carl Zeiss AG). For Cavin3 staining in small mesenteric and caudal arteries, sections were prepared and incubated with primary antibody as described above in 3.9. This was followed by incubation with secondary antibody with specificity for rabbit coupled to Cy2 (Jackson, West Grove, PA, USA).

For double staining of two antigens some critical issues have to be considered. First, when staining different antigens in the same section, it is important to use primary antibodies from different species (for example, mouse antibody against one antigen and rabbit antibody against another antigen). An alternative is to use directly fluorescence-conjugated primary antibodies. The signal from directly conjugated

primaries is typically weaker. Thus, it is advisable to target the most highly expressed antigen using the direct-conjugated primary. Some people also argue that it is better to choose secondary antibodies from the same species, and that the best choice for blocking is the serum from the same species as the secondary. Moreover, fluorophores should be chosen to have narrow emission spectra with good separation to avoid spectral overlap.

3.11. Pelvic ganglia co-culture set-up

Culture of pelvic ganglia was developed here for studying neurite outgrowth. Compared to *in vivo* models, this *in vitro* model offers a well-defined environment that can be easily manipulated and analysed. In my experiments, the pelvic ganglia and pieces of urinary bladder and diaphragm were dissected from female NMRI mice (weighing 20-25 g). Tissues were mounted with Matrigel® (Collaborative research Inc.) and cultured in 35-mm plastic culture dishes containing 2 ml RPMI 1640 medium (Sigma-Aldrich). The same medium was maintained in the culture dishes throughout the experiment. One piece of pelvic ganglion was attached to center of each culture dish, and 6 pieces (approximal 1 mm^3) of urinary bladder or diaphragm tissue were attached 3 mm from the ganglion in a circle (c.f. Figure 11A beolw). Tissue cultures were kept in an incubator at 37 ºC with a humidified atmosphere of 5% CO_2 in air. The culture dishes were taken out from the incubator for quantification once per day for five days. The longest sprouting neurites were identified and their lengths were measured using a light microscope (Olympus SZ61). Measurements were made on live-images using a calibrated scale bar in the eyepiece of the microscope. 10 different neurites per ganglion were identified and measured at each time point. The neurite outgrowth from the ganglia was imaged on day 5 using an Olympus AX70TRF microscope.

There are many different media that can be used for pelvic-ganglion culture, including DMEM-HAM/F12 (1:1) and RPMI 1640 medium [129-132]. Different growth supplements can also be used [130, 133]. Since the aim of my experiment was to detect the effect of bladder tissue on the pelvic ganglia, specified nerve growth supplements were avoided.

Neurite outgrowth occurred in all directions, but certain sites in the ganglion appeared to act as preferential starting points. To evaluate the growth of neurites, the ten longest neurites for each pelvic ganglion were measured and the average of the lengths was calculated [131]. In the co-culture system, the ganglia and the neurites grew on a planar surface (two dimensions) and many neurites grew across each other. How this affects the growth is not known. Three-dimensional (3D)

culture, which is commonly used in stem cell research, may perhaps offer an advantage to the 2D model used by us [130].

3.12. Transmission electron microscopy

Transmission electron microscopy (TEM), sometimes also known as conventional electron microscopy, is a microscopy technique in which the image is formed by a beam of electrons passing through a specimen and focusing onto an imaging device. TEM allows a significantly higher resolution than light microscopy due to the smaller wavelength of electrons. In my experiments, small mesenteric arteries from wild type and Cavin3 knockout mice were fixed by immersion in 2.5% glutaraldehyde in 0.1 M Sodium Cacodylate buffer (pH 7.4). Urinary bladders were dissected from perfusion-fixed mice. The mice were anaesthetized using 4% isoflurane and the thoracic cavity was opened for access to the heart. A catheter was inserted into the aorta through an incision in the left ventricle, and an outlet was made in the right atrium. After washing with PBS, fixative was infused and the bladder was isolated. Small mesenteric arteries and pieces of the bladders were post-fixed in 1% osmium tetroxide for 2 hours, stained with uranyl acetate, dehydrated and embedded in Araldite. Sections were stained with toluidine blue to choose areas for TEM. Sections with 50-70 nm thickness were collected on metal grids and stained with electron dense stain (uranyl acetate) before imaging in the TEM. Images were taken at 60K magnification in a JEOL JEM 1230 microscope (Jeol, Tokyo, Japan). Caveolae were identified as vesicles that resided within 100 nm from the cell membrane and were quantified using ImageJ (NIH, Bethesda, MD, USA). Caveolae are prominent structures in the cell membrane, and can be recognized relatively easily by their characteristics, including their size (50-100nm), their Ω-shape and the presence of a neck. One challenge when quantifying things using TEM is to acquire images randomly. This is particularly hard for rare structures. Caveolae are relatively abundant however, and for image acquisition we try to follow the cell membrane of cross-sectioned cells until we reach the starting point, assuring good coverage.

3.13. Immuno-electron microscopy

TEM is an useful tool to investigate the intricate structures of the cell. However, subcellular localization of a wide range of specific proteins can not be identified. Immunoelectron microscopy, which uses gold labeling on sections, is a powerful

technique for mapping the distribution of proteins in an intact biological systems [134]. In my experiments, fresh human bladder strips were fixed in 1.5% paraformaldehyde (PFA) and 0.5% glutaraldehyde in 0.1M PBS, and were dehydrated in ethanol and infiltrated with Lowicryl HM20. The specimens were subsequently polymerized using UV light, and 50 nm sections were cut in a Leica Ultrotom UC7 and mounted on pioloform-coated gold grids (Maxtaform H5). Sections were blocked with 1% BSA in PBS and then incubated with Nexilin primary antibody (1:80-1:200, Abcam, ab213628) in a damp chamber at 4 ºC. Following washing in PBS, the sections were incubated with 10 nm gold nanoparticle-conjugated secondary antibody (anti rabbit). Following further washing in PBS, sections were contrasted in 4% uranylacetate at 40 ºC. Images were taken in a FEI Tecnai 120kv Biotwin electron microscope.

3.14. Bladder denervation surgery

Sprague-Dawley rats (female, 200-250g) were chosen for bladder denervation using a cryo-ablation method, by which reliable bladder denervation in the female rat has been produced previously [65]. The rats were anesthetized by intramuscular administration of Ketalar (100 mg/kg, Parke-Davis) and xylazin (15 mg/kg, Bayer AG). The lower abdomen was opened, and the ganglionic area was dissected free from connective tissue bilaterally. The ganglionic areas were then frozen using a liquid nitrogen filled probe. The ureter and the urethra were well protected. After thawing, the freezing step was repeated. The abdominal cavity was closed. The rats could not void voluntarily after the operation, and their bladders were emptied twice per day by manual abdominal compression. Rats used as controls were exposed to all the procedures, including dissection of connective tissue from the ganglionic areas, but no cryo-ablation was made. 10 days after surgery, rats were sacrificed, and the bladders were dissected out, cleaned and emptied. Bladder weights were determined. 12 control bladders and 19 denervated bladders were included in the experiments. Protein homogenates from obstructed rat bladders were from recent work [82].

The samples size (6 sham-operated and 6 denervated bladders) was based on a discussion with the Swegene Centre for Integrative Biology at LU (SCIBLU) Affymetrix unit. Statistical power was considered, but ethical and economic considerations also played a role.

Complete bladder denervation requires complete destruction of the pelvic ganglia. We used a liquid nitrogen filled probe to freeze the ganglionic areas. If the temperature or the duration of cryo-ablation is insufficient, or if there is some anatomical variation, this might result in incomplete denervation. In Paper V, the

second denervated rat bladder (Den2) had a lower weight than other denervated bladders, and also had an mRNA expression profile that more closely resembled that of sham-operated controls. We believe that this was a result of incomplete denervation. This sample was included in the statistical analysis, because there were no formal grounds for exclusion.

3.15. Actin polymerization assay

Actin exists in two forms: monomeric or globular (G-actin), and filamentous (F-actin). F-actin is a two-helical polymer of G-actin molecules that associates with numerous actin-binding proteins to form the thin filaments of differentiated smooth muscle [135]. The filamentous form of actin is the major component of the actin cytoskeleton [136]. Historically, the thin filaments of SMCs were considered to be relatively stable and similar to those in striated muscle cells. However, more and more studies have shown that smooth muscle thin filaments are dynamic, and that remodelling of the actin cytoskeleton regulates smooth muscle function [135, 137]. Since F-actin forms from G-actin, both can be recognized by the same antibody. F-actin and G-actin can thus not be distinguished by western blotting under denaturing conditions. I therefore used a sedimentation method to separate F-actin from G-actin. Briefly, after treatment of human bladder or coronary artery SMCs, cells were washed twice with ice-cold PBS and lysed in 100 µl actin-stabilizing lysis buffer (0.1 M PIPES (pH 6.9), 30% glycerol, 5% DMSO, 1 mM $MgSO_4$, 1mM EGTA, 1% Triton-X100, 1mM ATP, and protease inhibitor cocktail (Sigma-Aldrich, P8340)). Lysates were transferred to 1.5 ml Eppendorf tubes and centrifuged for 75 min at 20,000 G (4 ºC). This pellets the F-actin at the bottom of the tube and the G-actin remains in the supernatant. All supernatants were then transferred to new tubes. Pellets remaining in the original tubes were dissolved in 60µl actin depolymerizing buffer (0.1 M PIPES (pH 6.9), 1 mM $MgSO_4$, 10 mM $CaCl_2$ and 5 µM cytochalasin D) by sonication. SDS-PAGE loading samples were then prepared from the supernatants (G-actin) and dissolved pellets (G-actin derived from F-actin, thus measuring F-actin) by mixing with Laemli sample buffer (×2) containing bromophenol blue (0.02%) and β-mercaptoethanol (10%). SDS-PAGE and western blotting was done as described above using a pan-actin antibody (Cytoskeleton Inc, #AAN01) and a secondary anti-rabbit antibody (Cell Signaling Technology). The densitometric signal of G-actin and F-actin was determinated in Image Studio, and the F/G-actin ratio for each treatment was calculated by dividing the signal for the F-actin by the signal for the G-actin.

During the procedure, the G-actin and F-actin need to be separated by centrifugation following cell homogenization with actin-stabilizing lysis buffer.

After this separation samples were loaded into neighbouring wells of the gel. To get accurate results, I found that it was important to homogenise the cells using equal volume of actin-stabilizing lysis buffer, to harvest all the G-actin supernatant of each sample, to dissolve the F-actin pellet completely using an equal volume of actin depolymerizing buffer, and to load equal volumes of G-actin loading samples (and F-actin loading samples). It is also important to centrifuge the cell lysates at a high speed (e.g. 20,000 G) to harvest all the F-actin.

The pan-actin antibody that I used recognizes all isoforms of actin, including alpha-actin, beta-actin and gamma-actin. All actins contribute to F-actin, but the assay does not distinguish between isoforms. This leaves open the possibility that *NEXN* knockdown only affects polymerization of a certain subtype of actin.

3.16. Cell migration

A scratch assay was used to measure cell migration over a cell-free area in the cell monolayer using a real-time cell imaging system (HoloMonitor M4, Phase Holographic Imaging, Lund Sweden) [138]. Human bladder SMCs were seeded in 6-well plates (Sarstedt, 83.3920.005). 24h after seeding, cells were transduced with virus encoding shRNA against *NEXN* (300MOI) or empty adenoviral vector (null), respectively. 24h after viral transduction, the virus-incubation media were exchanged for fresh media with 10% FBS to establish cell confluence. 12h before the assay started, FBS was removed from the medium to inhibit cell proliferation. A scratch was made in the middle of the well using a Gelloader Pipette Tip (Sarstedt), and the wound was imaged every 20-40 min. This allowed monitoring of cell motility, cell divisions, and cell confluence in the wounded area for the duration of the experiment (22h). Data was acquired using the HoloMonitor and later analyzed using the Hstudio M4 software system.

HoloMonitor M4 is a phase holographic imaging system. By using a holographic imaging technique, the cells can be captured in a three-dimensional image directly in the cell culture plate inside the incubator, and at regular time intervals with no labelling [139]. Cellular behaviour, such as cell mobility, can continuously be visualized and quantified over time by analysing real-time images [140].

The wound healing assay (scratch assay) that I used is an *in vitro* technique for detecting collective cell migration [141-146]. Although it has been described as a straightforward assay [147], the technique has also been criticized because it is difficult to reproduce among researchers. The manual creation of a scratch of uniform size for example is a challenge [148].

In the area of a scratch, two principal types of cell migration can actually be identified: single cell migration and collective cell migration [147]. Collective cell

migration can be measured as the reduction of gap size (width) of the wound, which can be measured by traditional imaging techniques, such as manually imaging by light microscopy. Traditional imaging techniques, which usually rely on long time intervals, may not capture single cell migration. In my experiment, using a real-time holographic imaging system and high image capture rates (1 image per 20-40 min), single cell migration was readily observed and quantified. During the experiment, I noticed that the edges of the cells was not straight, which complicates measurements of gap size. I also noticed that some cells migrated into the wound quickly, and then migrated away. Such behaviour may be due to heterogeneous speeds of migration and different directions of cell migration. To bypass such problems, I measured the cell confluence (cell-covered area/initial gap area) and calculated the real-time relative cell confluence (individual time-point cell confluence / initial cell confluence) rather than gap width. The small fluctuations in the relative cell confluence (Fig. 10C) arise when cells migrate into and out of the scratch. I also tracked migrating cells and calculated the speed of the movement.

3.17. Statistics

Statistical calculations were performed in GraphPad Prism 7. Summarized data is presented in graphs as means ± S.E.M. In animal experiments, each animal represents one biological replicate (n=1). In cell experiments, each well represents one replicate, but we always aimed for three independent confirmations on different occasions. Single comparisons between two groups were made using a two-tailed student's t-test. Multiple comparisons were made using one-way ANOVA (analysis of variance) followed by Bonferroni's post-hoc test. Cell confluence was tested using RMANOVA (Repeated measures ANOVA). Single correlations were tested using the Spearman method whereas multiple correlations were tested using Pearson in Excel. The mRNA expression data from microarray experiment was Log_2-transformed before statistical testing. $P<0.05$ was considered significant. *, ** and *** means $P<0.05$, $P<0.01$ and $P<0.001$, respectively.

There are of course a number of situations where my statistical choices can be disputed. In figure 6 (*Cavin3* knockout project), for example, when I compared the number of caveolae in the membrane between wild-type and *Cavin3* knockout mice, three mice per genotype were used. This is a small sample size, but the analysis was based on many images per animal (e.g. 17-31 60k images per animal for small mesenteric arteries), giving very precise quantification. The result of a parametric test was presented in that paper, and this relies on normally distributed data, but with so little data, one cannot determine with certainty that this criterion is fulfilled. However, the differences were significant independently of the test used. The

density of caveolae is >1/μm, and the total length of membrane analysed was about 1000 μm, meaning that the analysis includes roughly 1000 individual organelles. The density of caveolae therefore varied little between the three mice in each group, thus yielding solid P-values.

Another example is figure 12 (bladder denervation project), where I used the MTT assay to detect the effect of Cthrc1 on cell proliferation. Since I defined each culture well as one biological replicate, and each independent experiment included 3 to 4 wells per group, this gives a large n value, which gave a highly significant result ($P<0.001$) for both overexpression and knockdown. In reality, the effect of Cthrc1 knockdown in cell culture was rather modest at low FBS concentrations (albeit significant).

4. Results and Discussion

4.1. **Part I:** MRTF targeted genes and studies of their function

4.1.1. Subproject I: MRTFs drive transcription of caveolins and cavins

i. Gain-of-function experiments support regulation of caveolins and cavins by MRTFs

Prior work demonstrated that caveolins and cavins are increased following viral overexpression of MRTFs in human coronary artery SMCs. Overexpression of myocardin moreover increased the density of caveolae [26]. This suggested that MRTFs may be responsible for formation of a key morphological membrane feature of SMCs, namely caveolae. Many aspects of this biological control mechanism remained unknown however. This included the generality of the effect (i.e. is it also seen in visceral/urogenital SMCs and in other species?), and the genetic regions involved (promoters vs. distal enhancers). There was also concerns that the loss-of-function experiments performed earlier [26], involving small molecule inhibitors and not including specific molecular interventions such as silencing or knockout, were insuffficient. This study was initiated to address these important questions and concerns. For me personally, it also provided an introduction to SMC research.

I could show that viral overexpression of MRTF-A/*MKL1* and MYOCD/*MYOCD* in rat bladder SMCs increased caveolins and cavins at both the mRNA and the protein levels. Small molecule inhibitors of MRTF/SRF signaling moreover reduced *CAV1* and *CAVIN1* in both human and rat bladder SMCs, similar to what had previously been reported for human arterial SMCs. Using promoter-reporter assays I was then able to show that MRTF-A/*MKL1* and MRTF-B/*MKL2* regulate caveolins and cavins via proximal promoter sequences throughout. I also found that GATA6, known to repress many SMC-specific and MRTF-regulated genes [149], reduces caveolins but not cavins.

It can be argued that overexpression of human transcription factors in rodent cells is meaningless, but there are many examples of important discoveries made in this way in the literature [150, 151]. In my experiments I overexpressed human MRTF-

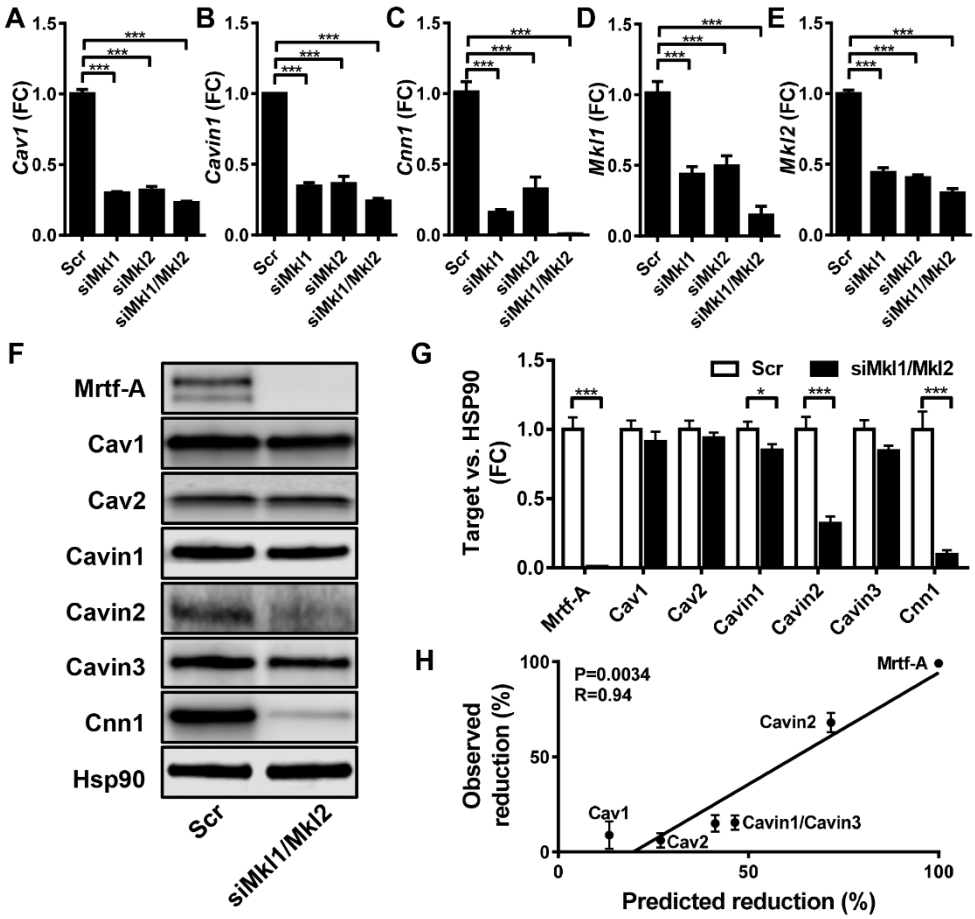

Figure 4. Silencing of *Mkl1* (Mrtf-A) and *Mkl2* (Mrtf-B) reduces *Cav1* and *Cavin1*. Mouse SMCs were transfected with scrambled (negative control) siRNA (Scr) or with siRNA (20 nM) against *Mkl1*, *Mkl2* or a combination of both for 96 hours. The mRNA level of *Cav1*, *Cavin1* and *Cnn1* (a smooth muscle marker) were reduced by silencing as shown using RT-qPCR (A-C). The degree of knockdown of *Mkl1* and *Mkl2* is shown in panels D and E (n=3~6). Protein levels were assessed by western blotting and are shown in panels F and G (n=12). Mtrf-A expression was reduced as expected, but among the caveolins and cavins, only Cavin1 and Cavin2 were reduced. I speculated that this might be due to a slow protein turnover rate for remaining caveolae proteins. To address this, I calculated the expected reduction of caveolae proteins at 96h from mRNA levels, previously determined protein half-lives, and assuming exponential decay. When plotted against the observed reduction, these numbers correlated tightly (Spearman method) (H), arguing that many caveolae proteins are so stable that reductions at the protein level are not be expected with transient silencing approaches.

A/*MKL1* in rat and human bladder SMCs using an adenoviral vector containing an effective promoter from the cytomegalovirus (CMV) [152]. *Cav1* and *Cavin1* were upregulated to the same extent in rat and human bladder SMCs. One may argue that *Mkl1* from rat would not have done the same, but given the sequence conservation of rat and human *Mkl1*, this seems improbable. Species-specific transcription has been intensely debated in recent years [153, 154]. Some maintain that that homologous tissues and genetic sequence are responsible for directing transcriptional programs, and that differences in epigenetic machinery, cellular environment, and transcription factors are less important [154-159]. Having shown that MRTFs affect caveolins and cavins in both human and rat cells, I subscribe to this view.

ii. Knockdown of Mkl1 and Mkl2 downregulates caveolins and cavins at the mRNA level

A key aim in paper I was to achieve silencing of MRTFs in SMCs to study if this reduces caveolins and cavins. For this I used mouse aortic SMCs cultured *in vitro* and transfected them with siRNAs against *MKL1* (Mrtf-A), *MKL2* (Mrtf-B), or both. Scrambled negative control siRNA was used as control. 96 h after transfection, *Cav1* (*Caveolin1*) and *Cavin1* mRNAs were reduced by more than 60% (Fig. 4A, B). This was similar to the prototypical SMC marker *Cnn1* (Fig. 4C). The effect was marginally greater with combined silencing of *Mkl1* and *Mkl2*. Reduction of *Mkl1* and *Mkl2* was also confirmed by RT-qPCR (Fig. 4D, E). *Mkl1* was reduced by the *Mkl2* siRNA and *vice versa*, indicating cross-reactivity of the siRNAs (Fig. 4D, E).

iii. Slow degradation maintains the protein level of caveolins after silencing of Mkl1 and Mkl2

Our next step was to analyze the protein levels of caveolins and cavins after silencing of *Mkl1* (Mrtf-A) and *Mkl2* (Mrtf-B). Mrtf-A was convincingly reduced at 96 h after siRNA transfection (Fig. 4F, top blot). The protein levels of Cavin1 and Cavin2 were also reduced, but Cav1, Cav2 and Cavin3 levels were unaffected (Fig. 4F and summarized data in G). We reasoned that protein stability in the setting of our experiment might be due to slow protein turnover rates. To address this hypothesis, we made a computational prediction of the protein levels at 96h (post knockdown) assuming exponential protein decay. Protein half-lives were obtained from a recent comprehensive study in mouse fibroblasts [160]. Strikingly, when the predicted reduction was compared with the observed reduction, a highly significant correlation was evident (Spearman correlation analysis, Fig. 4H). This supported our speculation that caveolins are so stable at the protein level that a reduction is very hard to detect using transient silencing approaches. This should be a lesson for all nasty reviewers “out there” that indirect silencing of long-lived structural

proteins may indeed be very difficult; a lack of effect at 96h (4 days) is a rule (four out of six) rather than an exception, and much longer periods of silencing are typically needed.

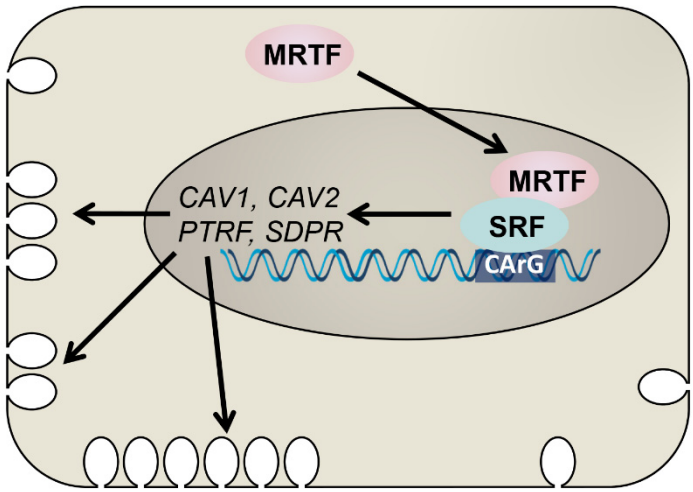

Figure 5 Myocardin family coactivators (MRTFs) drive formation of caveolae by promoting the transcription of caveolins and cavins in SMCs. In this study, I demonstrate that MRTFs act via the proximal promoters of caveolins and cavins to cause gene activation. MRTF members (MRTF-A, MRTF-B, and MYOCD) bind to the transcription factor serum response factor (SRF) and act as coactivators. The SRF-binding DNA motif is called a CArG box, and this motif is present in some but not all caveolin and cavin promoters. Based on this, and previous work, I propose that myocardin family coactivators represent important, if not major, drivers of caveolae-formation in SMCs.

From the work presented in this paper we concluded that caveolins and cavins are very likely to be controlled by MRTFs in SMCs from both blood vessels and the bladder and in several species. This regulation involves proximal promoter sequences. This basic concept is schematically illustrated in Figure 5. Given that MRTFs are actin sensitive and mechanoresponsive coactivators, it follows that the density of caveolae may respond to changes in cell tension and actin polymerization.

4.1.2. Subproject II: Morphological and functional consequences of *Cavin3* (*Prkcdbp*) deficiency

i. The density of caveolae in SMC membrane is reduced by Cavin3 deficiency

One of the cavins is Cavin3. It is likely that dependence on Cavin3 for generation of caveolae is tissue-specific [45, 46]. To understand the role of Cavin3 in generation of caveolae in endothelial cells and SMCs we used a global knockout approach. After mouse breeding and genotyping, electron microscopy (Fig. 6A through F) was used to determine the membrane density of caveolae (highlighted in pink color in Fig. 6) in tissues from wildtype and *Cavin3* knockout mice. The density of caveolae (i.e. number of caveolae per micrometer membrane) in endothelial cells was well maintained after *Cavin3* knockout, whereas the density of caveolae in small mesenteric artery SMCs was reduced by 39%. A 46% reduction of the density of caveolae was seen in bladder SMCs (see summarized data in Fig. 6G). We reasoned that the differential dependence on Cavin3 for formation of caveolae in different cell types may be due to differential expression of Cavin3. In keeping with this hypothesis, we found that Cavin3 was expressed specifically in medial SMCs in arteries, with much lower expression in endothelial and adventitial cells (Fig. 6H). It has been reported that cavins (Cavin1, Cavin2 and Cavin3) form a trimeric complex in the cytosol which then associates with the cytoplasmic surface of caveolae [34]. This trimeric complex can be composed either of three Cavin1 molecules or of two Cavin1 molecules and one Cavin2 or one Cavin3 molecule [40, 41]. Our morphological observations suggest that Cavin3 contributes to the cavin complex in SMCs, but not in endothelial cells, and that this is due to a low expression level in the latter cells.

ii. Downregulation of Cav1, Cav3 and Cavin1 following knockout of Cavin3

Cavin3 knockout reduced caveolae in bladder SMCs similar to arterial SMCs. Cavin3 expression and location in the bladder was examined using immunohistochemistry. This demonstrated that Cavin3 localizes to SMC membranes (Fig. 7A, B). *Cavin3* deficiency eliminated Cavin3 staining from this location (Fig. 7D), but some staining remained in the mucosa (Fig. 7C, left convoluted surface).

We also examined the expression of Caveolin-1 (Cav1), Caveolin-3 (Cav3) and Cavin1 (Ptrf) using western blotting in both arteries and the bladder. In the bladder, all of the latter proteins were reduced in *Cavin3* knockout mice (Fig. 7E, F). In arteries, Cavin1 and Cav1 were reduced. Total extracellular signal-regulated kinase (t-Erk) and phosphorylated Erk (p-Erk) were also measured, and phosphorylation of

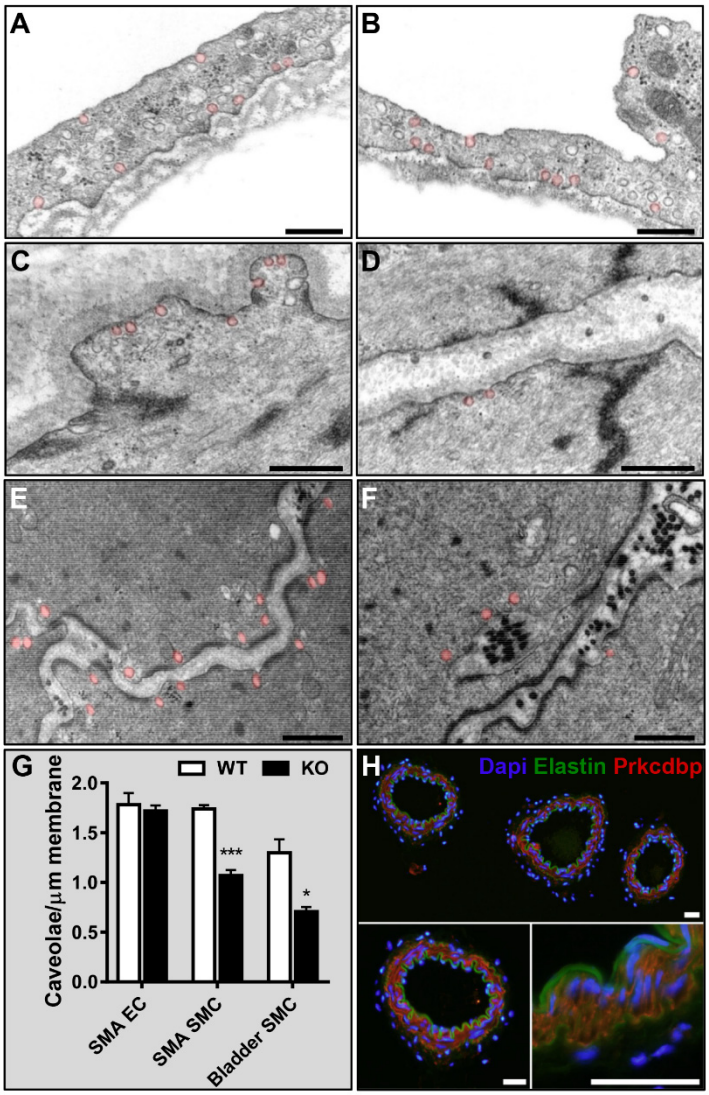

Figure 6. Reduced density of caveolae in SMCs, but not in endothelial cells, in *Cavin3* knockout mice. Panels A through F show electron micrographs of wild type (WT) and *Cavin3* knockout (KO) mouse tissues (WT: A, C, E; KO: B, D, F). A and B show small mesenteric artery endothelial cells (SMA EC) whereas C and D show SMCs. E and F show bladder SMCs. Caveolae are highlighted using half-transparent pink. Black bars represent 500 nm. G: number of caeolae per µm plasma membrane in the respective cell types (n=3). In panel H, Cavin3 (Prkcdbp, red) was stained in small mesenteric and caudal arteries from mice using immunofluorescence. Nuclei were stained with DAPI (blue), and elastic laminae were visualized using autofluorescence (green). Cavin3 staining was seen in medial SMCs but not elsewhere as shown in the images at higher magnification. White bars represent 35 µm.

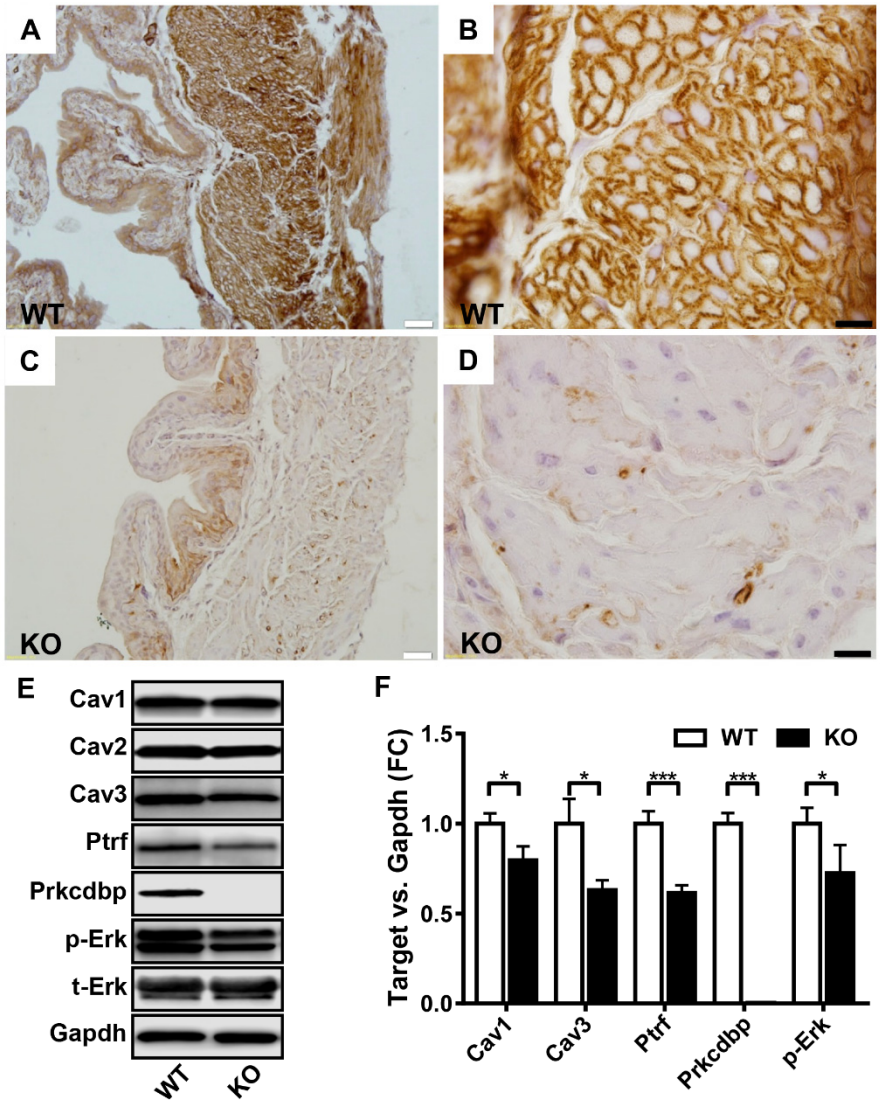

Figure 7. Cavin3 (Prkcdbp) is expressed in detrusor myocytes and knockout leads to a reduction of Cav1, Cav3 and Cavin1. Expression of Cavin3 in bladder SMCs from wild type (WT) and *Cavin3* knockout (KO) mice was determined by immunohistochemistry (A-D, n=3, white bars 20 μm, black bars 50 μm). Cavin3 (brown) mostly localized to SMC plasma membranes as shown in the high magnification cross sections (B). Cavin3 staining was largely absent in KO bladder SMCs (C, D). Caveolae proteins as well as p-Erk and t-Erk were assessed by western blotting (E, F, n=13). The expression of Cav1, Cav3 and Cavin1 (Ptrf) was reduced by *Cavin3* KO. Phosphorylation of Erk was also reduced.

Erk was found to be slightly reduced in *Cavin3* knockout bladders (Fig. 7E, F). A recent study found that Cavin3 controls the balance between ERK and Akt signaling in fibroblasts, and loss of *Cavin3* promotes Akt signaling through suppression of EGR1 and PTEN [46]. However, increased phosphorylation of Akt was not detected in our experiment (not shown). Perhaps, compensatory mechanisms are at play in bladder tissue *in vivo*.

iii. Functional effects of Cavin3 knockout in small arteries and the bladder

We conducted an extensive search for functional consequences of *Cavin3* deletion using myography. In small mesenteric arteries, cirazoline (α_1-receptor agonist) responses were unchanged, and muscarinic relaxation was identical. Intriguingly however, relaxation after inhibition of nitric oxide (NO) synthesis was reduced in knockout vessels. This suggested a greater dependence on NO for relaxation. In keeping with this hypothesis, we also observed increased relaxation by sodium nitroprusside, which releases NO, and by Bay 41-2272, which directly activates the soluble guanylyl cyclase (sGC). The α1 subunit of sGC (GUCY1A3) was moreover increased at the protein level. The molecular basis of these effects remains speculative at present, but based on our recent work showing that sGC expression is controlled by JAG1-NOTCH signaling in the vascular wall [91], one may speculate that this juxtacrine signaling mechanism works better with flat cell membranes as compared to vesicle-rich cell membranes (Fig. 8). In keeping with the rather modest changes of arterial function, we also noted that blood pressure was unchanged in *Cavin3* knockout mice.

Bladder contractility appeared to be unaffected in the knockout mice. It should be noted however, that the long protocols used in these experiments precluded normalization of force to cross-sectional area (which entails weighing and measuring the lengths of the strips, a cumbersome procedure at the end of a long experiment). This leaves the possibility that there is a slight change of bladder contractility that went unnoticed.

In view of evidence in the literature suggesting that caveolae may be mechanoprotective organelles [161, 162], we also set out to examine the response of the bladder to outlet obstruction. This intervention increases residual urine and stretches bladder SMCs, causing mechano-induced hypertrophic SMC growth [163]. Contrary to expectation, the ≈40% reduction of SMC caveolae in the knockout was not associated with altered overall growth of the obstructed urinary bladder. Induction of an unfolded protein response marker (PDI), and repression of SMC markers (MYH11, CNN1, Cavin1) was similar. STAT3 was also similarly activated in wildtype and knockout mice, despite previous reports that STAT3 associates with caveolae [164]. The only difference observed was a slightly reduced induction of the Golgi protein GM130, but the functional relevance of this change remains unknown.

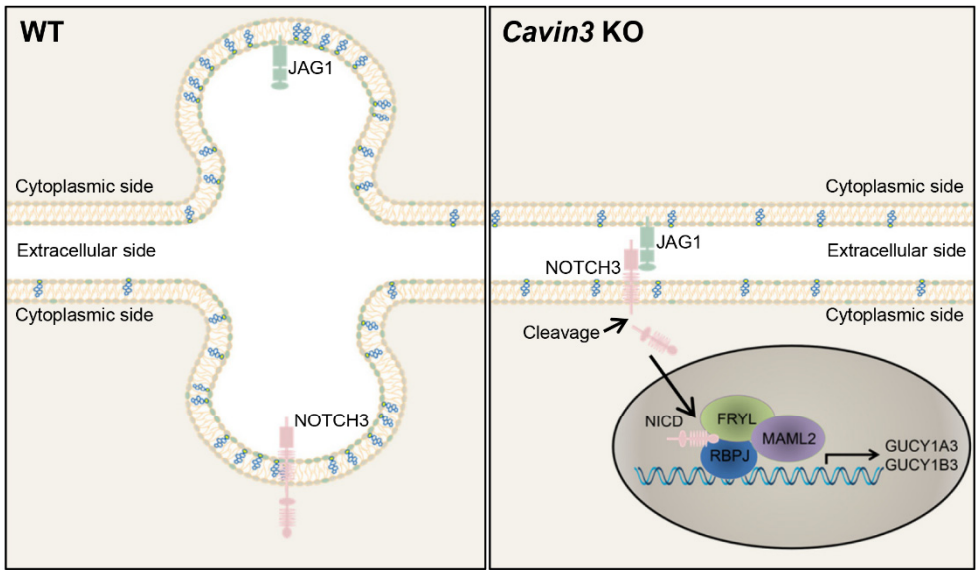

Figure 8. Speculative explanation for increased expression of soluble guanylyl cyclase in *Cavin3* knockout mice. JAG1-NOTCH3 is a ligand receptor pair that controls nuclear gene transcription. Key target genes include GUCY1A3 and GUCY1B3 which are subunits of the soluble guanylyl cyclase (sGC) (see "Papers not included"). In wild type (WT) vascular SMCs, a fraction of JAG1 ligands and NOTCH3 receptors may hide in caveolae. In *Cavin3* knockout (KO) SMCs, membranes are flatter, and hence the ligand and its receptor, both of which are membrane-attached, may be more closely apposed allowing for an interaction. When the ligand JAG1 binds to the NOTCH receptor, its intracellular domain (NICD) is cleaved and translocated into the nucleus, where it drives expression of sGC.

On the basis of these findings we concluded that Cavin3 contributes to formation of caveolae in SMCs, but that loss of *Cavin3* has very modest functional consequences. Cavin3 does not appear to be critical for survival, for blood pressure regulation, or for mechanically induced signaling and growth.

4.1.3. Subproject III: Nexilin is regulated by MRTFs and YAP, and affects actin polymerization and SMC motility

i. Nexilin localizes to dense bodies and dense bands

Bioinformatics at the mRNA (GTEx) and protein levels (Human Protein Atlas) raised our interest in the protein Nexilin. Nexilin is encoded by the *NEXN* gene, and is localized at Z-discs in striated muscle cells where it contributes to mechanical stability [165]. Localization and function of Nexilin in differentiated SMCs had not been studied. We noted that Nexilin staining was prominent in SMCs and that the *NEXN* mRNA correlated closely with mRNAs of SMC markers (e.g. *MYH11*). We therefore examined the expression and localization of Nexilin in the human detrusor using immunofluorescence staining. Staining for Nexilin revealed localization at the membrane and in the cytoplasm of SMCs (Fig. 9A, green). Non-continuous Caveolin-1 (CAV1, Fig. 9A, red) staining was seen at the cell membrane, consistent with the two-domain membrane organization typically seen in SMCs (see Introduction and Figure 1, 2). Double staining for Nexilin and CAV1 indicated little overlap in the membrane, and no overlap in the cytoplasm (Fig. 9A, yellow in overlay).

Nexilin distribution in human bladder SMCs was further studied using confocal microscopy. This showed that the green puncta of Nexilin distribute in the cytoplasm and at the cell membrane (Fig. 9B). Fluorescence intensity along a membrane profile (white contour in Fig. 9B) showed non-overlapping CAV1 and Nexilin staining (Fig. 9C), indicating that the proteins occupy different membrane domains. This strongly suggested that Nexilin localizes to dense bands in the membrane, and possibly to dense bodies in the cytoplasm.

To directly address whether Nexilin associates with dense bands and dense bodies we used immuno-electron microscopy and a gold particle-conjugated secondary antibody. Gold particles appear as black spheres with diameters of 10 nm in these micrographs (see white arrowheads in Fig. 9D). Two or more gold particles were often found at dense bands and at dense bodies (Fig. 9D). Solitary gold particles occasionally appeared in the cytoplasm, in nuclei and in mitochondria, whereas clusters of two or more particles at these locations were rarely, if ever, observed. This further supports the view that Nexilin localizes to dense bodies and dense bands.

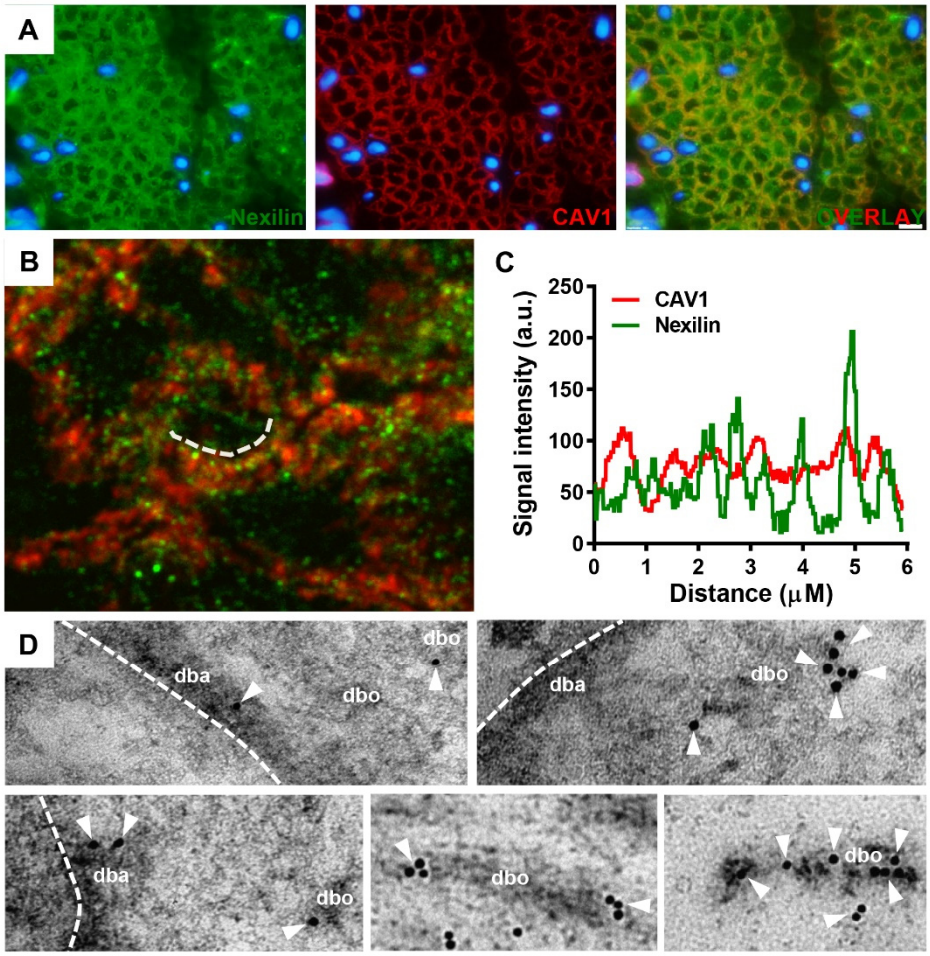

Figure 9: Nexilin/*NEXN* is expressed in SMCs and localizes to dense bodies and dense bands. Nexilin (green) and CAV1 (red) in cross-sectioned human urinary bladder SMCs were labeled by dual immunofluorescence staining and imaged using conventional fluorescence microscopy (A, white scale bar: 10 μm). In panel B, Nexilin and CAV1 were imaged using confocal microscopy, showing punctate distribution of Nexilin (green) in the cytoplasm and at the membrane that overlaps poorly with CAV1 (red) staining. The fluorescence intensity along a membrane profile (white contour in panel B) showed that Nexilin and CAV1 antibodies stain non-overlapping membrane domains (B). Immuno-electron microscopy using the same Nexilin antibody but a gold-conjugated (10 nm) secondary antibody is shown in panel D. Gold particles appear as black spheres with diameters of 10 nm. Examples of dense bodies (dbo) and dense bands (dba) are shown, and white arrowheads highlight gold particles. Note that the milder fixation needed for preservation of immune epitopes reduces contrast compared to conventional EM (Figure 1) making it more difficult to distinguish e.g. caveolae.

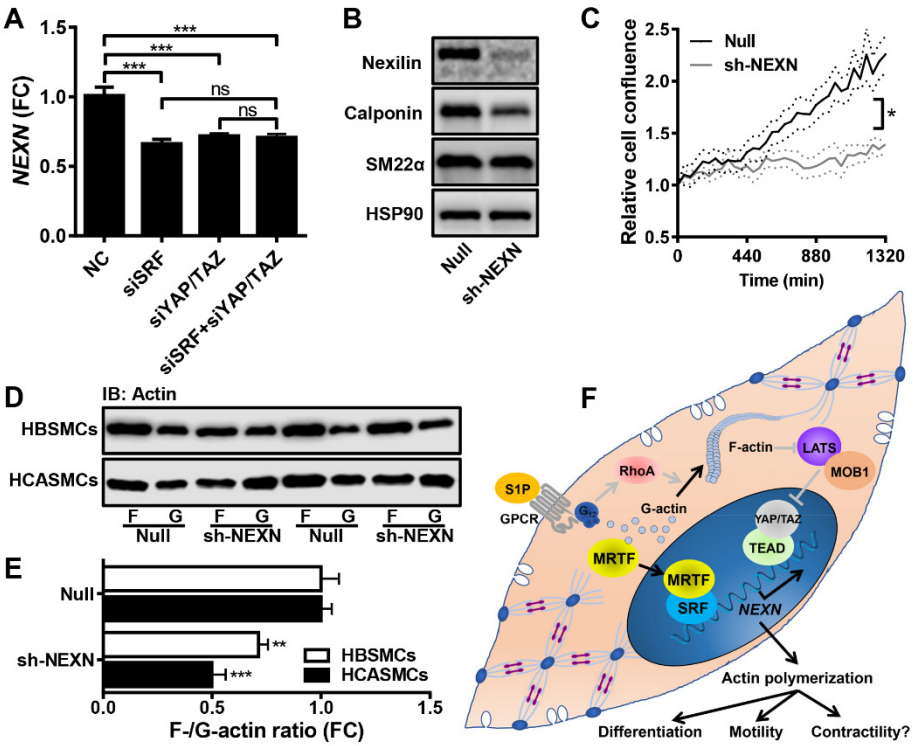

Figure 10. Nexilin/*NEXN* expression is controlled by myocardin family coactivators and by YAP, and silencing of *NEXN* reduces SMC marker expression and actin polymerization. Human bladder SMCs (HBSMCs) were transfected with siRNAs against *SRF* (siSRF), or *YAP1* and *WWTR1* (siYAP/TAZ). A combination of the three siRNAs was also tried. Silencing of SRF and of YAP/TAZ reduced the *NEXN* mRNA level, but no additive effect of combined silencing was apparent (A, n=6). This results is consistent with overexpression of YAP1 and of MRTFs, both of which increased *NEXN* levels (not depicted). In panels B-E, *NEXN* was silenced using a short hairpin adenoviral construct (sh-NEXN, 300MOI). Empty adenoviral vector (null) served as control. *NEXN* silencing reduced SMC differentiation markers (Calponin and SM22α) (B, n=12), cell migration (C, n=9~10), and filamentous relative to monomeric actin levels (D, E). Filamentous (F-) and globular (G-) actin was determined by a sedimentation assay followed by western blotting using a pan-actin antibody. Both HBSMCs (n=12) and coronary artery SMCs (HCASMCs, n=6) were studied. Panel F summarizes the results of the paper in graphic form. Nexilin, encoded by the gene *NEXN*, is regulated by changes in actin polymerization via MRTFs and YAP/TAZ. Nexilin, which localizes to dense bands and dense bodies, affects the F/G-actin ratio and SMC marker expression as well as cell migration.

ii. Nexilin/NEXN expression is controlled by MRTFs and by YAP

We reasoned that the high expression of Nexilin/*NEXN* in smooth muscle may be governed by smooth muscle-specific transcriptional control mechanisms involving the MRTFs. To approach this possibility, we correlated *NEXN* with all other RNAs in the tissues with highest expression levels. This revealed correlations with MRTFs, but also suggested that another group of transcriptional coactivators, YAP/TAZ (*YAP1/WWTR1*), correlate even better with *NEXN*. MRTFs and YAP/TAZ share the property that they are controlled by the ratio of filamentous (F-) to globular (G-) actin [17, 166, 167]. Both coactivator families are moreover considered to be mechanoresponsive.

I found that activation of YAP using Sphingosine-1-phosphate (S1P) or overexpression increased *NEXN* in both human coronary artery and bladder SMCs. Overexpression of MRTFs had the same effect. To probe the role of MRTFs and YAP/TAZ in *NEXN* regulation more specifically, siRNAs targeting *SRF* (siSRF), *YAP1* and *WWTR1* (siYAP/TAZ) were used for gene silencing. Dual knockdown of *YAP1* and *WWTR1* was done to avoid compensatory induction of TAZ*/WWTR1*. The siRNA against *SRF* reduced the *NEXN* mRNA by 34% and the combination of siRNAs against *YAP1* and *WWTR1* downregulated *NEXN* mRNA by 28% (Fig. 10A). No additive effect of combined knockdown of *SRF*, *YAP1* and *WWTR1* was evident. Taken together, these findings indicated that Nexilin/*NEXN* expression is controlled by MRTF/SRF signaling and by YAP/TAZ, i.e. two coactivator families regulated by actin dynamics. Accordingly, the *NEXN* mRNA and protein levels were highly sensitive to Latrunculin B which causes depolymerization of actin.

iii. Silencing of NEXN reduces SMC markers and actin polymerization

To investigate the function of Nexilin/*NEXN* in SMCs, an shRNA adenoviral construct against *NEXN* was used for knockdown. The protein level of Nexilin, as well as typical SMC markers (Calponin and SM22α) was determined using western blotting, showing that *NEXN* silencing reduced SMC markers (Fig. 10B). Motility of human bladder SMCs was analyzed using a scratch assay. Cells were monitored using a real-time imaging system. The cell density in a cell-free area caused by scraping was reduced following silencing of *NEXN* (Fig. 10C). No mitoses were evident in the recordings, arguing that *NEXN* knockdown decreased cell migration rather than cell proliferation. Filamentous relative to monomeric actin levels were measured using a sedimentation assay followed by western blotting. The ratio of filamentous (F-) to globular (G-) actin was reduced in both bladder and coronary artery SMCs (Fig. 10D and summarized data in E).

These findings, taken together, indicated that Nexilin is a muscle-enriched protein controlled by two families of actin-regulated coactivators: the MRTFs and

YAP/TAZ. Nexilin localizes to dense bodies and dense bands in SMCs, and it influences actin dynamics, cell motility and SMC differentiation (graphically summarized in Fig. 10F). It is moreover likely that the impact of Nexilin on SMC differentiation depends on its ability to affect the F-/G-actin ratio and thus indirectly MRTF activity. In the first part of my thesis I have thus identified and validated novel MRTF targets and deciphered their function.

4.2. **Part II:** Interaction between bladder nerves and their target cells

4.2.1. Subproject IV: Co-culture of the pelvic ganglion with bladder tissue increases neurite outgrowth

i. The co-culture model and stimulation of neurite outgrowth by bladder

The bladder is controlled by parasympathetic and sympathetic neurons which in the rat mainly come from the pelvic ganglion. These neurons play an important role in normal bladder function. Bladder denervation is a consequence of many diseases, such as bladder outlet obstruction (BOO) and diabetes. Rescue and regeneration of neurons and their connections to the bladder represents an important goal. It has been reported that neural plasticity is influenced by neurotrophic factors released from the nerve-targeted organs [70]. Thus, to define strategies for re-innervation of the bladder, it is reasonable to explore if bladder tissue has an effect on outgrowth of neurites from the pelvic ganglion. We devised an *in vitro* method to test this possibility. This was done by co-culturing of the pelvic ganglion with bladder tissue pieces (Fig. 11A). The length of the neurite outgrowth from pelvic ganglion was measured daily (Fig. 11B), showing that co-culture with bladder tissue increased neurite outgrowth, whereas no effect was observed following co-culture with diaphragm compared to no-tissue control. Swelling and neurite bulbs, recognized as signs of neurite degeneration, could be seen in the growing neurites from the ganglion cultured with diaphragm (Fig. 11F), but were less apparent when bladder tissue was present (Fig. 11E).

ii. The bladder contains BDNF and NT-3

Since no ganglion cells are present in the bladder segments used for the co-culture, we can rule out that effects were due to neurotrophic factors released from ganglion cells. The number of tissue pieces, the size of tissue pieces, and the distance between the tissue pieces, were similar for bladder and diaphragm, arguing that neurotrophic factors were differently produced by bladder and diaphragm.

We addressed the possibility that bladder and diaphragm produce different neurotrophins using western blotting. It was found that bladder contained more active BDNF and NT-3 than did diaphragm. The diaphragm, on the other hand, contained more NGF. Accordingly, outgrowth of VIP-positive (cholinergic) neurites appeared to be more enhanced by BDNF/NT-3 than by NGF. The opposite was true for TH-positive neurites.

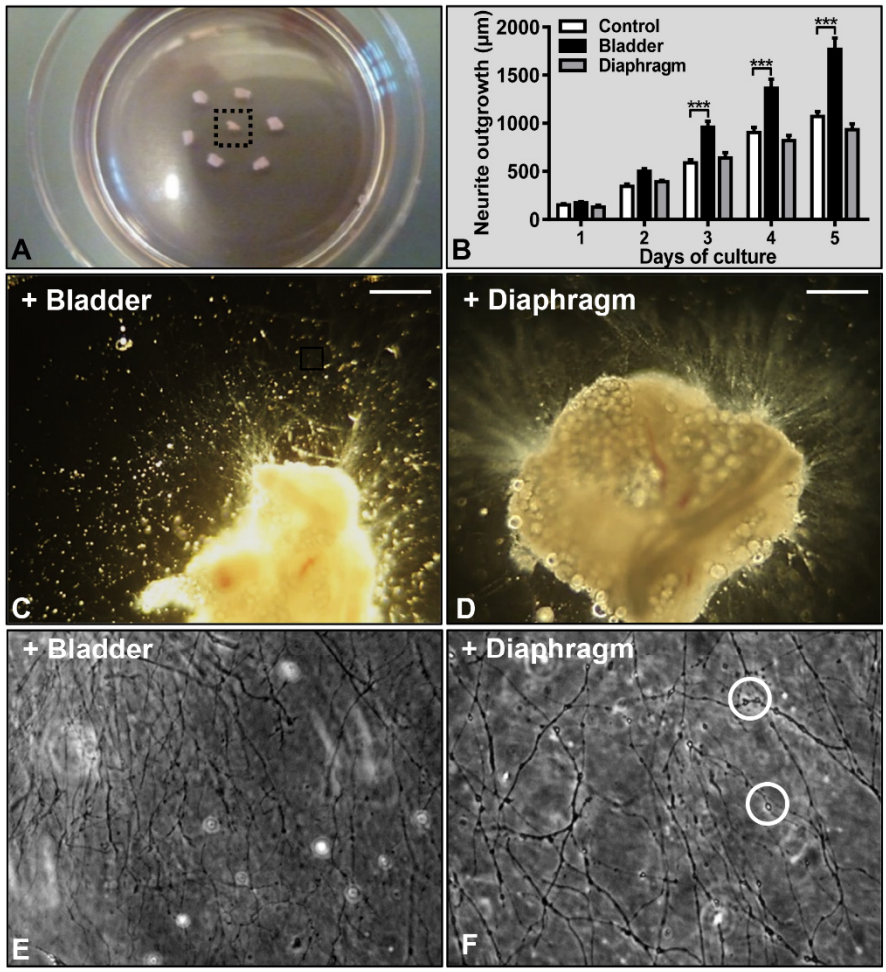

Figure 11. Co-culture of the pelvic ganglion with tissue pieces from the urinary bladder increases neurite outgrowth. One piece of mouse pelvic ganglion (A, black frame) was co-cultured with 6 pieces of urinary bladder (approximately 1 mm^3 each) attached 3 mm from the ganglion in a circle. Co-culture with diaphragm was done in a similar fashion. The longest neurites (average length of the ten longest neurites for one pelvic ganglion) were measured daily over 5 days and the result was summarized in panel B (n=7~12). Neurite outgrowth increased in the presence of bladder tissue but not with diaphragm. The outgrowth from the ganglia in the presence of bladder tissue (C) and diaphragm tissue (D) was imaged on day 5 using an Olympus AX70TRF microscope (white scale bars represent 200 µm). Signs of degeneration (swelling and neurite bulbs) could be found in the growing neurites from the ganglion cultured with diaphragm tissue (F, white circles), but were less apparent after culture with bladder tissue (E).

We thus concluded that the bladder tissue produces neurotrophic factors that influence outgrowth of neurites from the pelvic ganglion. For regeneration of the motor nerve supply to the bladder via neurotrophins, BDNF and NT-3 should thus be prioritized over NGF.

4.2.2. Subproject V: Cthrc1 is increased by bladder denervation and promotes SMC proliferation

i. Cthrc1 is upregulated in denervated and obstructed bladders

Bladder denervation and BOO are prevalent urological conditions. Both conditions lead to bladder growth. BOO in itself also causes partial denervation, suggesting that the conditions are intertwined and could share molecular mechanisms that may be targeted for diagnosis and therapy. This hypothesis was addressed using a rat denervation model and microarray analyses for mRNAs and microRNAs. Comparison was then made with array data for the obstructed bladder generated in a previous study [80]. Common differentially expressed genes in the two conditions were identified. We also defined a smaller, shared, gene expression module using more stringent cut-offs for significance (Q=0, by SAM analysis) and fold change (FC<0.5 or >3). This smaller signature contains many genes studied previously in obstruction, including e.g. Thbs4 [82]. One of the highly upregulated genes in this smaller signature was Cthrc1 (collagen triple helix repeat containing 1) which had not been studied previously in any of these urological conditions.

I demonstrated using western blotting that Cthrc1 increases preferentially in denervation (Fig. 12A, Den vs. Ctrl D), with a smaller change in obstruction (Obs vs. Ctrl O). The change at the protein level was consistent with the change at the mRNA level. β-actin was used as loading control since it is reasonably stable in both models (based on array data and a comparison of loading controls). In the western blots for Cthrc1, at least two bands were observed. It has been reported that Cthrc1 is an N-glycosylated secreted protein. An additional modification depending on N-glycosylation occurs when Cthrc1 is secreted and multimers may also form [124]. The different Cthrc1 bands thus likely reflect the presence and absence of such modifications. Immunoreactive bands increased following overexpression of *CTHRC1* in human bladder SMCs using an adenovirus, and they were reduced following knockdown of *CTHRC1* using an shRNA (Fig. 10B). This indicates that the antibody is specific.

ii. TGF-β1 and miR-30d-5p converge on Cthrc1 causing its induction

We also considered the molecular basis of Cthrc1 induction. Early work indicated that TGF-β is capable of inducing Cthrc1 [168] and we noted that several TGF-β isoforms were increased in the arrays. We could also show that stimulation of human

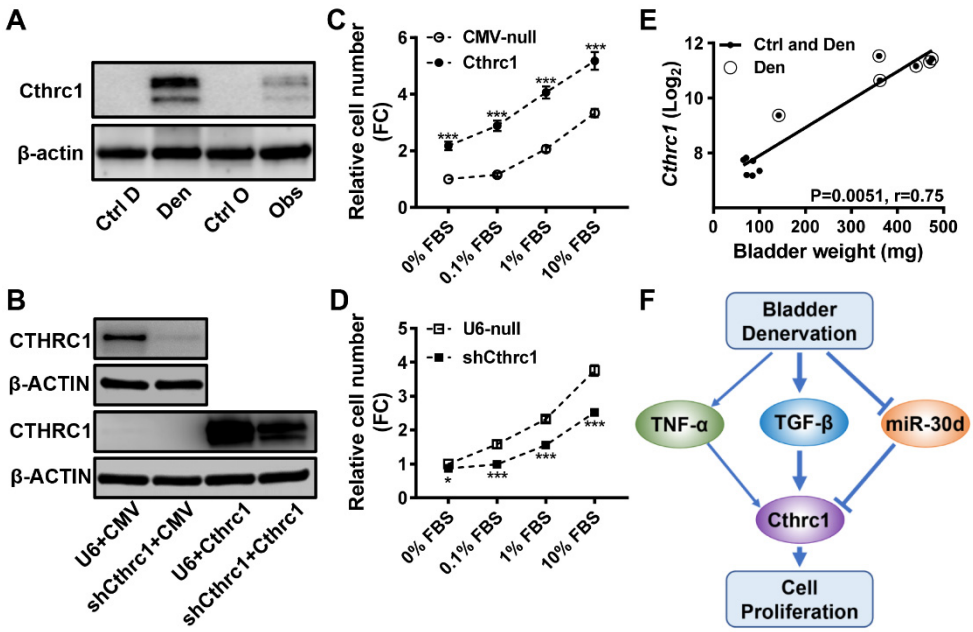

Figure 12. Cthrc1 is upregulated in denervated and obstructed bladders, and manipulation of Cthrc1 levels influences proliferation of human bladder SMCs. Bladders from control (Ctrl D and Ctrl O), denervated (Den), and obstructed (Obs) rats were quickly frozen in liquid nitrogen after dissection and weighing. Cthrc1 was then determined by western blotting (A, n=6). Panel B shows western blots for Cthrc1 after silencing with shRNA (shCthrc1) and overexpression (Cthrc1), respectively (n=3). The effect of silencing was difficult to appreciate when run side by side with overexpression samples. The same silencing samples were therefore loaded in isolation on separated gels and the resulting blots are shown on top. Panels C and D show relative cell numbers at different concentrations of Fetal Bovine Serum (FBS) after overexpression (Cthrc1, 200MOI, n=20) and knockdown (shCthrc1, 100MOI, n=14), of Cthrc1, respectively. Panel E shows correlation between bladder wet weight and the *Cthrc1* mRNA level following denervation. Panel F shows a graphical summary of the results of the study. Bladder denervation leads to induction of TGFβ and repression of miR-30d. These contribute to raising the Cthrc1 level. Cthrc1 finally promotes bladder growth.

bladder SMCs with TGF-β1 increased *CTHRC1*. Work had further demonstrated that CTHRC1 is a target of the miR-30 family of miRNAs and we noted a robust reduction of miR-30d-5p in the arrays. Accordingly, inhibition of this miRNA increased CTHRC1.

iii. CTHRC1 influences proliferation of human bladder SMCs

Bladder denervation induces bladder growth and hyperplasia of detrusor SMCs [64, 169]. We therefore aimed to test the hypothesis that Cthrc1 contributes in this regard, possibly as a co-receptor for Wnt [124]. We first tested if CTHRC1 affects the proliferation of bladder SMCs. An MTT assay was made following manipulation of CTHRC1 expression. It was found that overexpression of *CTHRC1* increased cell proliferation over a range of different serum concentrations (Fig. 10C), whereas knockdown of *CTHRC1* had the opposite effect (Fig. 10D).

iv. Expression of Cthrc1 correlates with the bladder weights of rats

The weights of the isolated bladders were measured on termination of the denervation experiment and before freezing. A 5.6-fold increase of mean wet weight was observed in denervated bladders compared to controls. I correlated the individual bladder weights with the Cthrc1 level derived from the microarrays (Spearman rank-order method). I found that, in keeping with a role in bladder growth, Cthrc1 correlated significantly with the individual bladder weights (Fig. 10E). This further supports the view that Cthrc1 may contribute to growth of the denervated rat bladder.

In all, this study identified an expression signature shared between bladder denervation and obstruction. A member of this gene signature is Cthrc1, a co-receptor for Wnt in the planar cell polarity (PCP) pathway. Cthrc1 plays a role for growth of bladder SMCs and its level correlates with bladder weight. A cartoon showing involvement of Cthrc1 in bladder growth following denervation is shown in Figure 10F. A similar role of Cthcr1 in the urothelium cannot be ruled out.

5. General Conclusions

Paper I.

The work in this paper shows that myocardin family coactivators control many of the genes responsible for generation of caveolae in rat and human bladder SMCs. It is further demonstrated that promoter reporters, containing approximately 1000 nucleotides from the proximal promoters of caveolins and cavins, are driven by MRTF-A and MRTF-B. Silencing of *Mkl1* (Mrtf-A) and of *Mkl2* (Mrtf-B) via RNA interference reduces expression of *Caveolin*-1 and *Cavin1*. The mRNA levels of these caveolae proteins are also reduced by MRTF/SRF inhibitors. Thus, Myocardin family coactivators regulate most caveolins and cavins via proximal promoter sequences and represent important, perhaps major, drivers of caveolae formation in SMCs.

Paper II.

This study shows that *Cavin3* (Prkcdbp) is preferentially expressed in the smooth muscle layer of arteries and the bladder. Knockout of *Cavin3* (Prkcdbp) reduces (by 40-50%), but does not eliminate, caveolae in SMC membrane. An associated reduction of Caveolin-1, Caveolin-3 and Cavin1 is seen in the bladder, suggesting that caveolae complexes consist of Cav1/Cav3 and Cavin1/Cavin3 (mouse). *Cavin3* ablation slightly enhances NO-dependent vascular relaxation, but has no effect on contractility or mechanically stimulated growth of the bladder wall. *Cavin3* (Prkcdbp) therefore contributes to the generation of caveolae in smooth muscle, but its deficiency has modest effects on contractility and growth.

Paper III.

This paper provides novel knowledge on Nexilin*/NEXN* in SMCs. Nexilin*/NEXN* is highly expressed in smooth muscle and localizes to dense bands and dense bodies. Nexilin expression is regulated by actin dynamics via myocardin family coactivators and YAP/TAZ through sequences in its proximal promoter. Knockdown of *NEXN* reduces the F-/G-actin ratio and cell motility, most likely via effects on dense body attachment sites for actin. Knockdown of *NEXN* also reduces SMC markers. This is to be expected from its effect on actin dynamics. In all, Nexilin is a dense body/dense band-associated protein in SMCs. It promotes actin

polymerization, amplifies SMC differentiation, and is regulated by myocardin family coactivators and YAP/TAZ.

Paper IV.

This *in vitro* study shows that neurotrophic factors, including NGF, BDNF, and NT-3, are synthesized in the bladder and control outgrowth of VIP-positive (cholinergic) and TH-positive (adrenergic) neurites from the pelvic ganglia *in vitro*, presumably via Trk-receptors.

Paper V.

Here I show that numerous mRNAs and miRNAs are differentially expressed in the urinary bladder after denervation. Pathway analysis indicates that many of the differentially expressed genes are related to proliferation (60%), which is consistent with a 5.6-fold increase in bladder weight. Cthrc1 is upregulated at both the mRNA and protein levels, and correlates with bladder weight. Overexpression and knockdown of this gene product moreover influences SMC proliferation *in vitro*. Cthrc1 is induced by TGF-β1 stimulation and by miR-30d-5p inhibition. In conclusion, a transcriptomic signature of bladder denervation is identified, and a role of Cthrc1 in bladder growth is defined.

6. Future Perspectives

Functional problems with urine storage, including the lower urinary tract syndrome (LUTS), are major stigmas for patients, and represent a surprisingly large economic burdens on society. Despite this, research efforts in functional urology are minimal, especially considering the extent of the clinical problem. Bladder function depends on the main tissues in the bladder, the extracellular matrix, bladder innervation, and central nervous control. Most of these domains of bladder structure and function have been touched upon in the present thesis, and novel insights have been gained. Progress is therefore slowly made towards understanding of this large, complicated, and mysterious system.

In my view, pharmaceutical intervention and gene therapy may be paths toward functional recovery of the bladder. To get there, it is however necessary to understand the genetic regulatory mechanisms that govern contractility and proliferation of bladder SMCs. This may likewise be helpful for regenerative medicine, such as when we try to guide neurons or stem cells for re-innervation. In my thesis, great effort has been spent to decipher the regulatory mechanisms of caveolae and their composition. I have also identified Nexilin as an SMC-enriched protein important for the contractile phenotype of bladder SMCs. Cthrc1, a molecule involved in bladder growth, has also been investigated. In the long run, such regulatory mechanisms may be targeted for clinical benefit.

Research technique is a very important aspect of science. It can be said, without exaggeration, that new results are obtained when novel techniques with greater precision or reach than old ones are applied. This does not imply disavowal of prior work, instead, it is inheritance. Here, I isolated RNA from denervated bladders and measured their levels using microarrays. This provided a preliminary glimpse into the vast molecular underpinnings of bladder growth following denervation, but much is still unknown. One of those unknowns is in which cells expression changes occur. Therefore, a logical continuation of this work would be to apply single cell transcriptomics.

In one of the studies presented here I used a global knockout approach to study the *in vivo* role of Cavin3. In case of complex phenotypes, it can be argued that a smooth muscle-specific and inducible knockout is preferable for exploration of SMC gene function *in vivo*. In the close future, we will generate such knockouts for *NEXN*. This will allow us to study the function of this protein in arteries and the

bladder *in vivo*, with minimal compensation and confounding effects from lack in other cell types (such as cardiomyocytes).

As we know, bladder denervation occurs for many reasons, such as in trauma, diabetes, and bladder outlet obstruction (BOO). This in turn causes functional bladder disturbances. Here I have used a rat model to study the response to denervation. It should be noted that denervation has mechanical consequences due to the accumulation of urine in a bladder that cannot be emptied. This in turn elevates the intravesical pressure, and this is likely an important confounding factor. Thus, a model of bladder denervation that bypasses this problem, such as denervation with continuous catheterization to avoid distension, may be necessary to isolate changes occurring as a result of denervation from those occurring due to distension.

In this thesis, the bladder tissue used for co-culture with the pelvic ganglion was from normal bladders. Consequently, the established model does not address questions relating to how the pelvic ganglion is affected by pathological bladder tissue. Moreover, the bladder extracellular matrix has been shown to orchestrate cellular behaviour [170], and this important aspect that is lacking from the sprouting study.

Human tissue samples from denervated and obstructed bladder are scarce because patients with localized urothelial carcinomas who need partial or total cystectomy usually don't undergo urodynamic testing. On the other hand, patients with BOO or bladder denervation usually don't need surgery. Volunteers and financial support may allow for collection of human bladder samples together with integrated urodynamic results. This would be of great relevance for further research in the discipline of functional urology. Thus, many shortcomings in the field may be addressed in future work, making the future of functional urology bright. This will however require support and prioritization.

7. Popular Summary

The urinary bladder is an organ for storage and expulsion of urine. The bladder wall needs to relax when urine is stored, and it needs to contract when we pee. Normal micturition (a fancy word for peeing) requires normal bladder function, which may be lost when there is problem in the bladder wall or the nerves controlling the bladder. It is common that people are bothered by unusually frequent urges to urinate, but there may also be problems getting started. Such problems are very common in aging males with prostate enlargement. Growth of the prostate, the gland that surrounds the urethra in men, can encroach on the outflow and cause subsequent changes in the bladder wall, such as hypertrophy of bladder smooth muscle, and a reduced density of nerve endings. Many other diseases similarly cause functional bladder problems accompanied by bladder wall remodelling. In diabetes and trauma, for example, the nerves that control the bladder are sometimes damaged (a situation called denervation), and this may, in severe cases, require insertion of a catheter to empty the bladder (catheterization).

Functional bladder problems have not always been taken seriously. This may be because it is a non-fatal disease, and not as fearful as stroke or cancer. However, such problems may significantly reduce the quality of life, and affect work output. Recovery is moreover poor and recurrence is common. If these arguments are not enough to convince you that the bladder is worthy of study, I recommend delving into health economics. Costs caused by functional problems in the lower urinary tract are, in fact, staggering.

Since bladder smooth muscle cells are responsible for the contraction of bladder wall, understanding the regulation of these cells is of great importance. The first part of my thesis deals with this particular issue.

Caveolae are omega-formed small pits in the cell membrane of smooth muscle cells. Caveolae play a role in signal transduction, and many neurotransmitter receptors are located in caveolae. The generation of caveolae depends on several proteins, and includes the so called caveolins (Cav1, Cav2, Cav3) and cavins (Cavin1 to Cavin4). Prior work demonstrated that knockout of *Cavin1* or *Cav1* in mice impairs the contractility of the bladder, and causes hypertrophy. In my first project, I used techniques for gene manipulation to demonstrate that a particular family of transcription factors (myocardin family coactivators) regulates the expression of caveolae proteins. In my second project, I used gene knockout

techniques to demonstrate that loss of Cavin3 protein leads to a reduction of caveolae in both arterial and bladder smooth muscle. These discoveries may be helpful for developing strategies to recover smooth muscle function pharmacologically, as well as for regenerative medicine.

In the third project, I investigated the protein Nexilin. This protein is known to be expressed in striated muscles, so named because of the repeating dark and bright lines seen in microscopy. Those dark lines, which separate the sarcomeres, are called Z-discs and this is where Nexilin is localized. More recently, another study found that *NEXN* gene variants associate with coronary artery disease. Using imaging, I found that Nexilin is present in dense bodies in smooth muscle. Dense bodies are functional equivalents of the Z-discs in cardiac muscle. I also found that Nexilin is regulated by myocardin family coactivators, as well as by YAP. The latter is a coactivator in a signaling pathway called Hippo. I finally demonstrated that Nexilin promotes actin polymerization and amplifies differentiation of smooth muscle cells.

Activation of the bladder wall is controlled by the nerves that enter via the pelvic ganglia. In the second part of my thesis I addressed questions relating to the nerve supply of the bladder.

In the fourth project, we establish an *in vitro* co-culture system for the pelvic ganglia together with urinary bladder tissue. We find that sprouting (outgrowth) of nerve endings is promoted in the presence of bladder tissue. This argues that the bladder releases some factor to attract nerves. We also found that bladder tissue, devoid of neurons, can indeed produce such factors. These included the neurotrophic factors BDNF and NT-3. Our findings do not necessarily imply that injection of neurotrophic factors into the bladder could recover its innervation, because some of them are already there, but a model system was established that opens up for testing new ideas for promoting neural recovery.

In the fifth project, a bladder denervation model was used to chart gene expression changes following denervation. Bladder denervation involves the damaging of the nerves controlling the bladder, and we used a bilateral freezing method. We then investigated the transcriptomic response of the bladder wall to denervation using high throughput technology. We identified an expression signature that is shared with bladder outlet obstruction. We also studied one gene, *Cthrc1*, which may play a role in the growth of bladder, in further depth. To the best of our knowledge, this is the first gene activity survey of the urinary bladder after denervation. The differentially expressed mRNAs offer a lot of clues for bladder remodelling which may allow us to develop strategies for recovery of bladder function.

In summary, I have identified and examined numerous molecular mechanisms responsible for bladder wall remodelling. These may be useful for developing strategies to recover bladder function in disease.

8. Acknowledgements

I close my eyes and try to look into the future, imagining what my memories of Sweden will be like. I listen to songs that have accompanied me over the last 18 years, trying to recall every detail. Fluorescence-stained smooth muscle cells appear before me, like stars shining in the dark and limitless universe, but also important insights, the work and the lunches, are vivid. I would like to think that my memories of Sweden will be fond ones and here I would like to express my deepest gratitude to all of those that helped and supported me during my PhD. If a name cannot be found in the list, it can be found in my memory.

First and foremost, to my life-coach, **Karl Swärd**, my main supervisor, for your guidance and support throughout my PhD and my life in Sweden. What I learnt is much more than how to do research. I know from you what is real happiness in life, and that science and dedication is eternal as truth instead of money and power. I learnt the publication process and why not to focus on impact factors, which are mere instruments of lazy reviewers. I will always remember that a paper is not what you should fight for, but it is the reward when you have worked hard enough. I have also come to share your view that family and children are more important in life than the outcome of an experiment or the verdict of a journal. I have embarked on a career, as every student does during PhD, but also shaped my soul at the same time, just because you were there.

Bengt Uvelius, I would like to put your name together with Karl's, however, you can only overlap with him in my heart, as it is impossible to tell which is more important between caveolae and dense bands, or between Snus and beer. Knowledge and history are your specialty areas, easily told by the vast number of books standing in your room and your bike running to and from the hospital. I have also been inspired by your tales of fishing expeditions. Your enthusiasm for science never gets old, and you were never afraid of war. I hope reading will always fill me warmth when I turn old, as it does to you.

Haibo Zhou, Chonghe Jiang, I am grateful to you for believing in me enough to support me as a PhD student in Sweden. I will never know how I was selected, since during my two years at the hospital all I did was working as a doctor. Also, I will never forget how professor Jiang works as a doctor, taking care of out-patients in the morning, doing surgery and working in the lab in the afternoon, visiting the

patients after surgery in the evening. The best way of repaying is by moving on, and I will.

Catarina Rippe and **Mari Ekman**, for sharing your knowledge and skills in the lab during my PhD, especially for caring about me every time I needed help or support. Even if there are many differences between countries and societies, I hope I will understand life in the same way that you do.

Bengt-Olof Nilsson, a respectable gentleman, talks softly, walks quietly, seems non-existent in the lab, but yet takes care of everything, such as closing all the doors and turning off all the lights (but leaving one on for me). Every "God morgon" and "Adjö" from you is heart-warming. Many thanks for your kind support and help during my PhD and in my projects.

Sebastian Albinsson, as modest as the coffee you make every morning. When I asked you a question, you said you don't know exactly. But after a while, I got an answer in detail by e-mail and sometimes even with a reference. You never give a promise, but everything you try will turn out to be the best. Thank you so much for helping me with equipment, chemicals, techniques, experimental design, data analysis, and also for contributing to my projects.

Jianwen Zeng, thank you so much for your insightful discussions about the project when I met with difficulties. You always supported me as a senior colleague, but also as a brother, sharing experiences from life, carrying me through difficult barriers. I also fondly remember the delicious sausages sent from my hometown.

Mario Grossi, **Siv Svensson**, for all the help around the lab, the kitchen. I always deeply feel that you are helping everyone around kindly. I respect and admire that sentiment. Especially thanks to Mario, for your "best experience for experiments", for spending a lot of time with me when I felt lonely, and for the orecchiette, tiramisu and focaccia. Finally, there is still a mission that I don't know how to complete, how shall I deliver a hug from Mario to Siv?

Daniel Svensson, for your great help with my project and my experiments. For your homemade beer, your delicious cooking, and for helping me with moving house. I think we should go deep into the forest to look for mushrooms again.

Johan Holmberg, many many thanks for your nice sections and beautiful staining, for the techniques that you showed me, for the antibody Karl ordered which will come in the weekend, one day.

Azra Alajbegovic, **Katarzyna Krawczyk**, for your kind help with the lab work and for the experience of being simultaneous PhDs going through the motions with presentations, experiments and everything else.

Katarzyna Kawka, for your kind help with plasmids and ordering things. The lab has become my second home and I can think of no better caretaker.

Björn Hansson, for you great help with the F-/G-actin assay, the method, the reagents and the centrifuge. Thanks also to you spontaneous and decisive supervisor **Karin Stenkula** for collaboration and for finding the way in the Cavin2 antibody jungle.

Thi Hien Tran, many thanks for your help with the RNA interference experiments in my first paper.

Anja Meissner, for many nice talks which opened up my mind, for helping me with S1P incubations, and for your homemade cookies.

Björn Olde, for your kind help with the luciferase promotor reporter assays.

Björn Morén, **Sebastian Wasserstrom**, for sharing your vast experience with immunofluorescence staining and using Confocal Microscopy.

Premkumar Siddhuraj, for helping me with stainings and for showing me Hoechst nuclear staining and a nice mounting method for immunofluorescence.

Selvi Celik, **Neha Pimpalwar**, for sharing the qPCR machine, and for inviting me to sample your delicious cakes.

Fatima Daoud, for your active contribution and curious discussion in our project, especially for enduring my strict ways with such a positive spirit, for company in the lab over the weekends, and for sharing with me your grandeur goal: to try everything that can be eaten in Sweden.

Marycarmen Arevalo, for sharing your experience about experimental animals.

Ping Li, **Shaohua Zeng**, **Yun Zhang**, for working hard together during day and night, for sharing experiences about working and travelling and life, for your delicious dumpling and steamed bun (*baozi*), for table tennis and many eating competitions.

All the other members, new and former, of the greater Vascular Physiology environment, **Per Hellstrand**, **Ina Nordström**, **Kristina E Andersson**, **Mardjaneh Karbalaei Sadegh**, **Alexandra Aidoukovitch**, **Emma Anders**, **Nicholas Don-Doncow**, **Sara Dahl**. It has been a great honor to work with such a group of skilled and helpful researchers.

Many thanks to all my colleagues and friends, current and former, at BMC D12, **Carl Magnus Clausson**, **Carlos Urey**, **Daisy Bornesund**, **Dingyuan Hu**, **Ernesto Gonzalez**, **Hamid Akbarshahi**, **Ihdina Dewi**, **Joanna Daszkiewicz-Nilsson**, **Jonas Erjefält**, **Katarzyna Said Hilmersson**, **Magdalena Barbachowska**, **Mandy Menzel**, **Maya Jälmby**, **Monika Bauden**, **Olof Gidlöf**, **Paulina Bryl-**

Gorecka, **Roland Andersson**, **Samuel Cerps**, **Sangeetha Ramu**, **Sofia Mogren**, for all the breakfasts and Christmas parties, for all the greetings and smiles which makes the work environment peaceful and comfortable.

Many thanks to all my collaborators and all others that offered help and collaboration, including **Ulf Hedin**, **Ljubica Perisic Matic**, **Peter Walter**, **Silke Nock**, for the creative thinking and the novel chemicals.

My family, you have my deepest gratitude for your full support and understanding!

I would also like to thank all my extended relatives and friends from outside of Lund, close and far, for making sure there is more in my life than research.

When living as a human, it is not always possible to do what you want to do. There is always a person that you respect, and you are willing to do as he expects, at the same time, there is always a person that you love, and you are willing to dedicate your whole life to her.

9. Abbreviations

Akt	Protein kinase B
Ang II	Angiotensin II
ANOVA	Analysis of variance
ATP	Adenosine triphosphate
BDNF	Brain-derived neurotrophic factor
BOO	Bladder outlet obstruction
BSA	Bovine serum albumin
CAV	Caveolin
Cch	Carbachol
CD68	Cluster of differentiation 68
cGMP	cyclic guanosine monophosphate
CNN1	Calponin 1
CNTF	Ciliary neurotrophic factor
Cthrc1	Collagen triple helix repeat containing 1
DAG	Diacylglycerol
DAPI	4',6-diamidino-2-phenylindole
DBA	Dense band
DBO	Dense body
DCP	Diabetic cystopathy
DKK3	Dickkopf WNT signaling pathway inhibitor 3
DMEM	Dulbecco's modified eagle's medium
DMSO	Dimethyl sulfoxide
EC	Endothelial cells
ECM	Extracellular matrix

EGR1	Early growth response protein 1
EGTA	Ethylene glycol-bis(β-aminoethyl ether)-N,N,N',N'-tetraacetic acid
EIF2AK3	Eukaryotic translation initiation factor 2 alpha kinase 3
EM	Electron microscopy
ER	Endoplasmic reticulum
ERK1/2	Extracellular signal–regulated kinase 1 and 2
FBS	Fetal bovine serum
FC	Fold change
FLOT2	Flotillin-2
GAPDH	Glyceraldehyde 3-phosphate dehydrogenase
GATA6	GATA binding protein 6
GCN	Gene co-expression network
GDNF	Glial-derived neurotrophic factor
GPCR	G protein–coupled receptor
GRN	Gene regulatory network
GSN	Gelsolin
GTEx	the Genotype-Tissue Expression project
HEPES	4-(2-hydroxyethyl)-1-piperazineethanesulfonic acid
HK	High potassium (K^+)
HRP	Horseradish peroxidase
Hsp90	Geat shock protein 90
IHC	immunohistochemistry
IP3	Inositol trisphosphate
ISX	Isoxazole
JAG1	Protein jagged-1
Jasp	jasplakinolide
KO	Knockout
Lat B	Latrunculin B
LUTS	Lower urinary tract symptoms

MAP	Mean arterial pressure
MAPK	Mitogen-activated protein kinase
MASTER	MEF2 activating motif and SAP domain containing transcriptional regulator
MEF2	Myocyte enhancer factor 2
MEP50	Methylosome protein 50
MKL1	Megakaryoblastic leukemia 1
MKL2	Myocardin-like protein 2
MOI	Multiplicity of Infection
MRTF	Myocardin Related Transcription Factor
MTT	3-(4,5-dimethylthiazol-2-yl)-2,5-diphenyltetrazolium bromide
MURC	Muscle-restricted coiled-coil protein
MW	Molecular weight
MYLK	Myosin light-chain kinase
MYOCD	Myocardin
MYPT	Myosin phosphatase targeting protein
NGF	Nerve growth factor
NMRI	Naval Medical Research Institute
NT-3	Neurotrophin 3
NT-4/5	Neurotrophin 4/5
OAB	Overactive bladder
OPN	Osteopontin
P2X1	Purinergic receptor P2X 1
PBS	Phosphate-buffered saline
PCP	Planar cell polarity
PCR	Polymerase chain reaction
PERK	Pancreatic eIF-2alpha kinase reticulum kinase
PFA	Paraformaldehyde
PIPES	Piperazine-N,N′-bis
PLOD2	Procollagen-lysine, 2-oxoglutarate 5-dioxygenase 2

PMC	Pontine micturition center
PRC1	Protein regulator of cytokinesis 1
PRKCDBP	Protein kinase C delta binding protein
PTEN	Phosphatase and tensin homolog
PTN	Pleiotrophin
PTRF	Polymerase I and transcript release factor
qPCR	Quantitative PCR
RhoA	Ras homolog gene family, member A
RISC	RNA-induced silencing complex
RMANOVA	Repeated measures ANOVA
RNAi	RNA interference
ROCK	Rho-associated protein kinase
RT	Reverse transcription
RT-qPCR	Reverse transcription quantitative polymerase chain reaction
S1P	Sphingosine-1-phosphate
SAM	Significance analysis of microarrays
SDPR	Serum deprivation-response protein
SDS	Sodium dodecyl sulfate
sGC	soluble guanylyl cyclase
shRNA	Short hairpin RNA
siRNA	Small interfering RNA
SMA	Small mesenteric arteries
SMC	Smooth muscle cell
SMGS	Smooth muscle growth supplement
SPP1	Secreted phosphoprotein 1 (Osteopontin)
SRF	Serum response factor
STAT3	Signal transducer and activator of transcription 3
TBS	Tris Buffered Saline
TCF	Ternary complex factor
TEM	Transmission electron microscopy

TGF-β1	Transforming growth factor beta 1
TH	Tyrosine hydroxylase
TMM	the Trimmed mean of M-values
TNFα	Tumor necrosis factor alpha
TRIS	Tris(hydroxymethyl)aminomethane
VIP	Vasoactive intestinal peptide
WDR77	WD repeat-containing protein 77

10. References

1. Cockayne DA, Hamilton SG, Zhu QM, Dunn PM, Zhong Y, Novakovic S, et al. Urinary bladder hyporeflexia and reduced pain-related behaviour in P2X3-deficient mice. Nature. 2000;407(6807):1011-5. Epub 2000/11/09. doi: 10.1038/35039519. PubMed PMID: 11069181.
2. Apostolidis A, Popat R, Yiangou Y, Cockayne D, Ford AP, Davis JB, et al. Decreased sensory receptors P2X3 and TRPV1 in suburothelial nerve fibers following intradetrusor injections of botulinum toxin for human detrusor overactivity. J Urol. 2005;174(3):977-82; discussion 82-3. Epub 2005/08/12. doi: 10.1097/01.ju.0000169481.42259.54. PubMed PMID: 16094018.
3. Brown TC, Bond CE, Hoover DB. Variable expression of GFP in different populations of peripheral cholinergic neurons of ChAT(BAC)-eGFP transgenic mice. Auton Neurosci. 2018;210:44-54. Epub 2017/12/31. doi: 10.1016/j.autneu.2017.12.005. PubMed PMID: 29288022; PubMed Central PMCID: PMCPMC5878110.
4. Yoshimura N, Kaiho Y, Miyazato M, Yunoki T, Tai C, Chancellor MB, et al. Therapeutic receptor targets for lower urinary tract dysfunction. Naunyn Schmiedebergs Arch Pharmacol. 2008;377(4-6):437-48. Epub 2007/11/24. doi: 10.1007/s00210-007-0209-z. PubMed PMID: 18034230.
5. Matsui M, Motomura D, Karasawa H, Fujikawa T, Jiang J, Komiya Y, et al. Multiple functional defects in peripheral autonomic organs in mice lacking muscarinic acetylcholine receptor gene for the M3 subtype. Proc Natl Acad Sci U S A. 2000;97(17):9579-84. Epub 2000/08/16. PubMed PMID: 10944224; PubMed Central PMCID: PMCPMC16907.
6. Burnstock G. Purinergic signalling. Br J Pharmacol. 2006;147 Suppl 1:S172-81. Epub 2006/01/13. doi: 10.1038/sj.bjp.0706429. PubMed PMID: 16402102; PubMed Central PMCID: PMCPMC1760723.
7. Ekman M, Rippe C, Sadegh MK, Dabestani S, Morgelin M, Uvelius B, et al. Association of muscarinic M(3) receptors and Kir6.1 with caveolae in human detrusor muscle. Eur J Pharmacol. 2012;683(1-3):238-45. Epub 2012/03/14. doi: 10.1016/j.ejphar.2012.02.039. PubMed PMID: 22410194.
8. Vial C, Evans RJ. P2X receptor expression in mouse urinary bladder and the requirement of P2X(1) receptors for functional P2X receptor responses in the mouse urinary bladder smooth muscle. Br J Pharmacol. 2000;131(7):1489-95. Epub 2000/11/23. doi: 10.1038/sj.bjp.0703720. PubMed PMID: 11090125; PubMed Central PMCID: PMCPMC1572476.

9. Schneider T, Fetscher C, Krege S, Michel MC. Signal transduction underlying carbachol-induced contraction of human urinary bladder. J Pharmacol Exp Ther. 2004;309(3):1148-53. Epub 2004/02/11. doi: 10.1124/jpet.103.063735. PubMed PMID: 14769832.
10. Somlyo AP, Somlyo AV. Signal transduction and regulation in smooth muscle. Nature. 1994;372(6503):231-6. Epub 1994/11/17. doi: 10.1038/372231a0. PubMed PMID: 7969467.
11. Morano I, Chai GX, Baltas LG, Lamounier-Zepter V, Lutsch G, Kott M, et al. Smooth-muscle contraction without smooth-muscle myosin. Nat Cell Biol. 2000;2(6):371-5. Epub 2000/06/15. doi: 10.1038/35014065. PubMed PMID: 10854329.
12. Kamm KE, Stull JT. The function of myosin and myosin light chain kinase phosphorylation in smooth muscle. Annu Rev Pharmacol Toxicol. 1985;25:593-620. Epub 1985/01/01. doi: 10.1146/annurev.pa.25.040185.003113. PubMed PMID: 2988424.
13. Small JV, Gimona M. The cytoskeleton of the vertebrate smooth muscle cell. Acta Physiol Scand. 1998;164(4):341-8. Epub 1999/01/15. doi: 10.1046/j.1365-201X.1998.00441.x. PubMed PMID: 9887957.
14. Shirazi A, Iizuka K, Fadden P, Mosse C, Somlyo AP, Somlyo AV, et al. Purification and characterization of the mammalian myosin light chain phosphatase holoenzyme. The differential effects of the holoenzyme and its subunits on smooth muscle. J Biol Chem. 1994;269(50):31598-606. Epub 1994/12/16. PubMed PMID: 7989330.
15. Kimura K, Ito M, Amano M, Chihara K, Fukata Y, Nakafuku M, et al. Regulation of myosin phosphatase by Rho and Rho-associated kinase (Rho-kinase). Science. 1996;273(5272):245-8. Epub 1996/07/12. PubMed PMID: 8662509.
16. Sward K, Stenkula KG, Rippe C, Alajbegovic A, Gomez MF, Albinsson S. Emerging roles of the myocardin family of proteins in lipid and glucose metabolism. J Physiol. 2016;594(17):4741-52. Epub 2016/04/10. doi: 10.1113/JP271913. PubMed PMID: 27060572; PubMed Central PMCID: PMCPMC5009794.
17. Olson EN, Nordheim A. Linking actin dynamics and gene transcription to drive cellular motile functions. Nat Rev Mol Cell Biol. 2010;11(5):353-65. Epub 2010/04/24. doi: 10.1038/nrm2890. PubMed PMID: 20414257; PubMed Central PMCID: PMCPMC3073350.
18. Creemers EE, Sutherland LB, Oh J, Barbosa AC, Olson EN. Coactivation of MEF2 by the SAP domain proteins myocardin and MASTR. Mol Cell. 2006;23(1):83-96. Epub 2006/07/05. doi: 10.1016/j.molcel.2006.05.026. PubMed PMID: 16818234.
19. Black BL, Olson EN. Transcriptional control of muscle development by myocyte enhancer factor-2 (MEF2) proteins. Annu Rev Cell Dev Biol. 1998;14:167-96. Epub 1999/01/19. doi: 10.1146/annurev.cellbio.14.1.167. PubMed PMID: 9891782.
20. Zderic SA, Chacko S. Alterations in the contractile phenotype of the bladder: lessons for understanding physiological and pathological remodelling of smooth muscle. J Cell Mol Med. 2012;16(2):203-17. Epub 2011/06/29. doi: 10.1111/j.1582-4934.2011.01368.x. PubMed PMID: 21707917; PubMed Central PMCID: PMCPMC3289974.

21. Faggian L, Pampinella F, Roelofs M, Paulon T, Franch R, Chiavegato A, et al. Phenotypic changes in the regenerating rabbit bladder muscle. Role of interstitial cells and innervation on smooth muscle cell differentiation. Histochem Cell Biol. 1998;109(1):25-39. Epub 1998/02/07. PubMed PMID: 9452953.

22. Miano JM. Myocardin in biology and disease. J Biomed Res. 2015;29(1):3-19. Epub 2015/03/10. doi: 10.7555/JBR.29.20140151. PubMed PMID: 25745471; PubMed Central PMCID: PMCPMC4342431.

23. Hill CS, Marais R, John S, Wynne J, Dalton S, Treisman R. Functional analysis of a growth factor-responsive transcription factor complex. Cell. 1993;73(2):395-406. Epub 1993/04/23. PubMed PMID: 8477450.

24. Wang Z, Wang DZ, Hockemeyer D, McAnally J, Nordheim A, Olson EN. Myocardin and ternary complex factors compete for SRF to control smooth muscle gene expression. Nature. 2004;428(6979):185-9. Epub 2004/03/12. doi: 10.1038/nature02382. PubMed PMID: 15014501.

25. Miano JM. Serum response factor: toggling between disparate programs of gene expression. J Mol Cell Cardiol. 2003;35(6):577-93. Epub 2003/06/06. PubMed PMID: 12788374.

26. Krawczyk KK, Yao Mattisson I, Ekman M, Oskolkov N, Grantinge R, Kotowska D, et al. Myocardin Family Members Drive Formation of Caveolae. PLoS One. 2015;10(8):e0133931. Epub 2015/08/06. doi: 10.1371/journal.pone.0133931. PubMed PMID: 26244347; PubMed Central PMCID: PMCPMC4526231.

27. Singh S, Robinson M, Nahi F, Coley B, Robinson ML, Bates CM, et al. Identification of a unique transgenic mouse line that develops megabladder, obstructive uropathy, and renal dysfunction. J Am Soc Nephrol. 2007;18(2):461-71. Epub 2007/01/05. doi: 10.1681/ASN.2006040405. PubMed PMID: 17202422.

28. Singh S, Robinson M, Ismail I, Saha M, Auer H, Kornacker K, et al. Transcriptional profiling of the megabladder mouse: a unique model of bladder dysmorphogenesis. Dev Dyn. 2008;237(1):170-86. Epub 2007/12/12. doi: 10.1002/dvdy.21391. PubMed PMID: 18069694.

29. McHugh KM. Megabladder mouse model of congenital obstructive nephropathy: genetic etiology and renal adaptation. Pediatr Nephrol. 2014;29(4):645-50. Epub 2013/11/28. doi: 10.1007/s00467-013-2658-6. PubMed PMID: 24276861; PubMed Central PMCID: PMCPMC3928515.

30. DeSouza KR, Saha M, Carpenter AR, Scott M, McHugh KM. Analysis of the Sonic Hedgehog signaling pathway in normal and abnormal bladder development. PLoS One. 2013;8(1):e53675. Epub 2013/01/12. doi: 10.1371/journal.pone.0053675. PubMed PMID: 23308271; PubMed Central PMCID: PMCPMC3538723.

31. Huang J, Wang T, Wright AC, Yang J, Zhou S, Li L, et al. Myocardin is required for maintenance of vascular and visceral smooth muscle homeostasis during postnatal development. Proc Natl Acad Sci U S A. 2015;112(14):4447-52. Epub 2015/03/26. doi: 10.1073/pnas.1420363112. PubMed PMID: 25805819; PubMed Central PMCID: PMCPMC4394251.

32. Hnasko R, Lisanti MP. The biology of caveolae: lessons from caveolin knockout mice and implications for human disease. Mol Interv. 2003;3(8):445-64. Epub 2004/03/03. doi: 10.1124/mi.3.8.445. PubMed PMID: 14993453.

33. Bastiani M, Parton RG. Caveolae at a glance. J Cell Sci. 2010;123(Pt 22):3831-6. Epub 2010/11/05. doi: 10.1242/jcs.070102. PubMed PMID: 21048159.

34. Parton RG, del Pozo MA. Caveolae as plasma membrane sensors, protectors and organizers. Nat Rev Mol Cell Biol. 2013;14(2):98-112. Epub 2013/01/24. doi: 10.1038/nrm3512. PubMed PMID: 23340574.

35. Tang Z, Scherer PE, Okamoto T, Song K, Chu C, Kohtz DS, et al. Molecular cloning of caveolin-3, a novel member of the caveolin gene family expressed predominantly in muscle. J Biol Chem. 1996;271(4):2255-61. Epub 1996/01/26. PubMed PMID: 8567687.

36. Hill MM, Bastiani M, Luetterforst R, Kirkham M, Kirkham A, Nixon SJ, et al. PTRF-Cavin, a conserved cytoplasmic protein required for caveola formation and function. Cell. 2008;132(1):113-24. Epub 2008/01/15. doi: 10.1016/j.cell.2007.11.042. PubMed PMID: 18191225; PubMed Central PMCID: PMCPMC2265257.

37. Vinten J, Johnsen AH, Roepstorff P, Harpoth J, Tranum-Jensen J. Identification of a major protein on the cytosolic face of caveolae. Biochim Biophys Acta. 2005;1717(1):34-40. Epub 2005/10/21. doi: 10.1016/j.bbamem.2005.09.013. PubMed PMID: 16236245.

38. Hansen CG, Bright NA, Howard G, Nichols BJ. SDPR induces membrane curvature and functions in the formation of caveolae. Nat Cell Biol. 2009;11(7):807-14. Epub 2009/06/16. doi: 10.1038/ncb1887. PubMed PMID: 19525939; PubMed Central PMCID: PMCPMC2712677.

39. Mohan J, Moren B, Larsson E, Holst MR, Lundmark R. Cavin3 interacts with cavin1 and caveolin1 to increase surface dynamics of caveolae. J Cell Sci. 2015;128(5):979-91. Epub 2015/01/16. doi: 10.1242/jcs.161463. PubMed PMID: 25588833.

40. Ludwig A, Howard G, Mendoza-Topaz C, Deerinck T, Mackey M, Sandin S, et al. Molecular composition and ultrastructure of the caveolar coat complex. PLoS Biol. 2013;11(8):e1001640. Epub 2013/09/10. doi: 10.1371/journal.pbio.1001640. PubMed PMID: 24013648; PubMed Central PMCID: PMCPMC3754886.

41. Kovtun O, Tillu VA, Jung W, Leneva N, Ariotti N, Chaudhary N, et al. Structural insights into the organization of the cavin membrane coat complex. Dev Cell. 2014;31(4):405-19. Epub 2014/12/03. doi: 10.1016/j.devcel.2014.10.002. PubMed PMID: 25453557.

42. Karbalaei MS, Rippe C, Albinsson S, Ekman M, Mansten A, Uvelius B, et al. Impaired contractility and detrusor hypertrophy in cavin-1-deficient mice. Eur J Pharmacol. 2012;689(1-3):179-85. Epub 2012/05/31. doi: 10.1016/j.ejphar.2012.05.023. PubMed PMID: 22643325.

43. Sadegh MK, Ekman M, Rippe C, Sundler F, Wierup N, Mori M, et al. Biomechanical properties and innervation of the female caveolin-1-deficient detrusor. Br J Pharmacol. 2011;162(5):1156-70. Epub 2010/11/26. doi:

10.1111/j.1476-5381.2010.01115.x. PubMed PMID: 21091642; PubMed Central PMCID: PMCPMC3051387.

44. Woodman SE, Cheung MW, Tarr M, North AC, Schubert W, Lagaud G, et al. Urogenital alterations in aged male caveolin-1 knockout mice. J Urol. 2004;171(2 Pt 1):950-7. Epub 2004/01/10. doi: 10.1097/01.ju.0000105102.72295.b8. PubMed PMID: 14713860.
45. Hansen CG, Shvets E, Howard G, Riento K, Nichols BJ. Deletion of cavin genes reveals tissue-specific mechanisms for morphogenesis of endothelial caveolae. Nat Commun. 2013;4:1831. Epub 2013/05/09. doi: 10.1038/ncomms2808. PubMed PMID: 23652019; PubMed Central PMCID: PMCPMC3674239.
46. Hernandez VJ, Weng J, Ly P, Pompey S, Dong H, Mishra L, et al. Cavin-3 dictates the balance between ERK and Akt signaling. Elife. 2013;2:e00905. Epub 2013/09/27. doi: 10.7554/eLife.00905. PubMed PMID: 24069528; PubMed Central PMCID: PMCPMC3780650.
47. Gregorio CC, Trombitas K, Centner T, Kolmerer B, Stier G, Kunke K, et al. The NH2 terminus of titin spans the Z-disc: its interaction with a novel 19-kD ligand (T-cap) is required for sarcomeric integrity. J Cell Biol. 1998;143(4):1013-27. Epub 1998/11/17. PubMed PMID: 9817758; PubMed Central PMCID: PMCPMC2132961.
48. Clark KA, McElhinny AS, Beckerle MC, Gregorio CC. Striated muscle cytoarchitecture: an intricate web of form and function. Annu Rev Cell Dev Biol. 2002;18:637-706. Epub 2002/07/27. doi: 10.1146/annurev.cellbio.18.012502.105840. PubMed PMID: 12142273.
49. Ashton FT, Somlyo AV, Somlyo AP. The contractile apparatus of vascular smooth muscle: intermediate high voltage stereo electron microscopy. J Mol Biol. 1975;98(1):17-29. Epub 1975/10/15. PubMed PMID: 1195377.
50. Bond M, Somlyo AV. Dense bodies and actin polarity in vertebrate smooth muscle. J Cell Biol. 1982;95(2 Pt 1):403-13. Epub 1982/11/01. PubMed PMID: 6890560; PubMed Central PMCID: PMCPMC2112980.
51. Draeger A, Amos WB, Ikebe M, Small JV. The cytoskeletal and contractile apparatus of smooth muscle: contraction bands and segmentation of the contractile elements. J Cell Biol. 1990;111(6 Pt 1):2463-73. Epub 1990/12/01. PubMed PMID: 2277068; PubMed Central PMCID: PMCPMC2116423.
52. Lazarides E, Granger BL. Fluorescent localization of membrane sites in glycerinated chicken skeletal muscle fibers and the relationship of these sites to the protein composition of the Z disc. Proc Natl Acad Sci U S A. 1978;75(8):3683-7. Epub 1978/08/01. PubMed PMID: 358193; PubMed Central PMCID: PMCPMC392850.
53. Draeger A, Wray S, Babiychuk EB. Domain architecture of the smooth-muscle plasma membrane: regulation by annexins. Biochem J. 2005;387(Pt 2):309-14. Epub 2004/11/13. doi: 10.1042/BJ20041363. PubMed PMID: 15537390; PubMed Central PMCID: PMCPMC1134958.
54. Eddinger TJ, Schiebout JD, Swartz DR. Adherens junction-associated protein distribution differs in smooth muscle tissue and acutely isolated cells. Am J Physiol Gastrointest Liver Physiol. 2007;292(2):G684-97. Epub 2006/10/21. doi: 10.1152/ajpgi.00277.2006. PubMed PMID: 17053160.

55. North AJ, Galazkiewicz B, Byers TJ, Glenney JR, Jr., Small JV. Complementary distributions of vinculin and dystrophin define two distinct sarcolemma domains in smooth muscle. J Cell Biol. 1993;120(5):1159-67. Epub 1993/03/01. PubMed PMID: 8436588; PubMed Central PMCID: PMCPMC2119721.

56. Lo SH. Tensin. Int J Biochem Cell Biol. 2004;36(1):31-4. Epub 2003/11/01. PubMed PMID: 14592531.

57. Horton ER, Byron A, Askari JA, Ng DHJ, Millon-Fremillon A, Robertson J, et al. Definition of a consensus integrin adhesome and its dynamics during adhesion complex assembly and disassembly. Nat Cell Biol. 2015;17(12):1577-87. Epub 2015/10/20. doi: 10.1038/ncb3257. PubMed PMID: 26479319; PubMed Central PMCID: PMCPMC4663675.

58. Ochodnicky P, Cruz CD, Yoshimura N, Cruz F. Neurotrophins as regulators of urinary bladder function. Nat Rev Urol. 2012;9(11):628-37. Epub 2012/10/10. doi: 10.1038/nrurol.2012.178. PubMed PMID: 23045265.

59. Drake MJ, Kanai A, Bijos DA, Ikeda Y, Zabbarova I, Vahabi B, et al. The potential role of unregulated autonomous bladder micromotions in urinary storage and voiding dysfunction; overactive bladder and detrusor underactivity. BJU Int. 2017;119(1):22-9. Epub 2016/07/23. doi: 10.1111/bju.13598. PubMed PMID: 27444952; PubMed Central PMCID: PMCPMC5177525.

60. Chew DJ, Zhu L, Delivopoulos E, Minev IR, Musick KM, Mosse CA, et al. A microchannel neuroprosthesis for bladder control after spinal cord injury in rat. Sci Transl Med. 2013;5(210):210ra155. Epub 2013/11/08. doi: 10.1126/scitranslmed.3007186. PubMed PMID: 24197736.

61. Yuan Z, Tang Z, He C, Tang W. Diabetic cystopathy: A review. J Diabetes. 2015;7(4):442-7. Epub 2015/01/27. doi: 10.1111/1753-0407.12272. PubMed PMID: 25619174.

62. Persson K, Alm P, Uvelius B, Andersson KE. Nitrergic and cholinergic innervation of the rat lower urinary tract after pelvic ganglionectomy. Am J Physiol. 1998;274(2 Pt 2):R389-97. Epub 1998/03/05. PubMed PMID: 9486296.

63. Berggren T, Uvelius B. Acute effects of unilateral pelvic ganglionectomy on urinary bladder function *in vivo* in the male rat. Scand J Urol Nephrol. 1996;30(3):179-84. Epub 1996/06/01. PubMed PMID: 8837248.

64. Berggren T, Uvelius B, Arner A. Denervation and outlet obstruction induce a net synthesis of contractile and cytoskeletal proteins in the urinary bladder of the male rat. Urol Res. 1996;24(3):135-40. Epub 1996/01/01. PubMed PMID: 8839480.

65. Uvelius B, Gabella G. The distribution of intramural nerves in urinary bladder after partial denervation in the female rat. Urol Res. 1998;26(5):291-7. Epub 1998/12/05. PubMed PMID: 9840337.

66. Lindsay RM, Wiegand SJ, Altar CA, DiStefano PS. Neurotrophic factors: from molecule to man. Trends Neurosci. 1994;17(5):182-90. Epub 1994/05/01. PubMed PMID: 7520198.

67. Ellis-Behnke RG, Liang YX, You SW, Tay DK, Zhang S, So KF, et al. Nano neuro knitting: peptide nanofiber scaffold for brain repair and axon regeneration with functional return of vision. Proc Natl Acad Sci U S A. 2006;103(13):5054-9. Epub

2006/03/22. doi: 10.1073/pnas.0600559103. PubMed PMID: 16549776; PubMed Central PMCID: PMCPMC1405623.

68. McDonald JW, Liu XZ, Qu Y, Liu S, Mickey SK, Turetsky D, et al. Transplanted embryonic stem cells survive, differentiate and promote recovery in injured rat spinal cord. Nat Med. 1999;5(12):1410-2. Epub 1999/12/02. doi: 10.1038/70986. PubMed PMID: 10581084.
69. Silver J, Miller JH. Regeneration beyond the glial scar. Nat Rev Neurosci. 2004;5(2):146-56. Epub 2004/01/22. doi: 10.1038/nrn1326. PubMed PMID: 14735117.
70. Purves D, Snider WD, Voyvodic JT. Trophic regulation of nerve cell morphology and innervation in the autonomic nervous system. Nature. 1988;336(6195):123-8. Epub 1988/11/10. doi: 10.1038/336123a0. PubMed PMID: 3054564.
71. Gunn-Moore FJ, Tavare JM. Progress toward understanding the molecular mechanisms of neurotrophic factor signalling. Cell Signal. 1998;10(3):151-7. Epub 1998/06/02. PubMed PMID: 9607137.
72. Kawakami T, Wakabayashi Y, Isono T, Aimi Y, Okada Y. Expression of neurotrophin messenger RNAs during rat urinary bladder development. Neurosci Lett. 2002;329(1):77-80. Epub 2002/08/06. PubMed PMID: 12161267.
73. Lin G, Shindel AW, Fandel TM, Bella AJ, Lin CS, Lue TF. Neurotrophic effects of brain-derived neurotrophic factor and vascular endothelial growth factor in major pelvic ganglia of young and aged rats. BJU Int. 2010;105(1):114-20. Epub 2009/06/06. doi: 10.1111/j.1464-410X.2009.08647.x. PubMed PMID: 19493269; PubMed Central PMCID: PMCPMC3001390.
74. Stewart AL, Anderson RB, Kobayashi K, Young HM. Effects of NGF, NT-3 and GDNF family members on neurite outgrowth and migration from pelvic ganglia from embryonic and newborn mice. BMC Dev Biol. 2008;8:73. Epub 2008/07/29. doi: 10.1186/1471-213X-8-73. PubMed PMID: 18657279; PubMed Central PMCID: PMCPMC2515305.
75. Vizzard MA, Wu KH, Jewett IT. Developmental expression of urinary bladder neurotrophic factor mRNA and protein in the neonatal rat. Brain Res Dev Brain Res. 2000;119(2):217-24. Epub 2000/02/17. PubMed PMID: 10675771.
76. Cruz CD. Neurotrophins in bladder function: what do we know and where do we go from here? Neurourol Urodyn. 2014;33(1):39-45. Epub 2013/06/19. doi: 10.1002/nau.22438. PubMed PMID: 23775873.
77. Daneshgari F, Liu G, Birder L, Hanna-Mitchell AT, Chacko S. Diabetic bladder dysfunction: current translational knowledge. J Urol. 2009;182(6 Suppl):S18-26. Epub 2009/10/23. doi: 10.1016/j.juro.2009.08.070. PubMed PMID: 19846137; PubMed Central PMCID: PMCPMC4684267.
78. Vizzard MA. Changes in urinary bladder neurotrophic factor mRNA and NGF protein following urinary bladder dysfunction. Exp Neurol. 2000;161(1):273-84. Epub 2000/02/23. doi: 10.1006/exnr.1999.7254. PubMed PMID: 10683293.
79. Tusher VG, Tibshirani R, Chu G. Significance analysis of microarrays applied to the ionizing radiation response. Proc Natl Acad Sci U S A. 2001;98(9):5116-21. Epub

2001/04/20. doi: 10.1073/pnas.091062498. PubMed PMID: 11309499; PubMed Central PMCID: PMCPMC33173.

80. Ekman M, Bhattachariya A, Dahan D, Uvelius B, Albinsson S, Sward K. Mir-29 repression in bladder outlet obstruction contributes to matrix remodeling and altered stiffness. PLoS One. 2013;8(12):e82308. Epub 2013/12/18. doi: 10.1371/journal.pone.0082308. PubMed PMID: 24340017; PubMed Central PMCID: PMCPMC3858279.
81. Ekman M, Uvelius B, Albinsson S, Sward K. HIF-mediated metabolic switching in bladder outlet obstruction mitigates the relaxing effect of mitochondrial inhibition. Lab Invest. 2014;94(5):557-68. Epub 2014/03/05. doi: 10.1038/labinvest.2014.48. PubMed PMID: 24589856.
82. Krawczyk KK, Ekman M, Rippe C, Grossi M, Nilsson BO, Albinsson S, et al. Assessing the contribution of thrombospondin-4 induction and ATF6alpha activation to endoplasmic reticulum expansion and phenotypic modulation in bladder outlet obstruction. Sci Rep. 2016;6:32449. Epub 2016/09/02. doi: 10.1038/srep32449. PubMed PMID: 27581066; PubMed Central PMCID: PMCPMC5007532.
83. Sadegh MK, Ekman M, Krawczyk K, Svensson D, Goransson O, Dahan D, et al. Detrusor induction of miR-132/212 following bladder outlet obstruction: association with MeCP2 repression and cell viability. PLoS One. 2015;10(1):e0116784. Epub 2015/01/27. doi: 10.1371/journal.pone.0116784. PubMed PMID: 25617893; PubMed Central PMCID: PMCPMC4305303.
84. Zeng J, Ekman M, Jiang C, Uvelius B, Sward K. Non-uniform changes in membrane receptors in the rat urinary bladder following outlet obstruction. Eur J Pharmacol. 2015;762:82-8. Epub 2015/05/26. doi: 10.1016/j.ejphar.2015.05.037. PubMed PMID: 26004535.
85. Gheinani AH, Kiss B, Moltzahn F, Keller I, Bruggmann R, Rehrauer H, et al. Characterization of miRNA-regulated networks, hubs of signaling, and biomarkers in obstruction-induced bladder dysfunction. JCI Insight. 2017;2(2):e89560. Epub 2017/02/01. doi: 10.1172/jci.insight.89560. PubMed PMID: 28138557; PubMed Central PMCID: PMCPMC5256140.
86. Stuart JM, Segal E, Koller D, Kim SK. A gene-coexpression network for global discovery of conserved genetic modules. Science. 2003;302(5643):249-55. Epub 2003/08/23. doi: 10.1126/science.1087447. PubMed PMID: 12934013.
87. Roy S, Bhattacharyya DK, Kalita JK. Reconstruction of gene co-expression network from microarray data using local expression patterns. BMC Bioinformatics. 2014;15 Suppl 7:S10. Epub 2014/08/01. doi: 10.1186/1471-2105-15-S7-S10. PubMed PMID: 25079873; PubMed Central PMCID: PMCPMC4110735.
88. Consortium GT. The Genotype-Tissue Expression (GTEx) project. Nat Genet. 2013;45(6):580-5. Epub 2013/05/30. doi: 10.1038/ng.2653. PubMed PMID: 23715323; PubMed Central PMCID: PMCPMC4010069.
89. Consortium GT, Laboratory DA, Coordinating Center -Analysis Working G, Statistical Methods groups-Analysis Working G, Enhancing Gg, Fund NIHC, et al. Genetic effects on gene expression across human tissues. Nature.

2017;550(7675):204-13. Epub 2017/10/13. doi: 10.1038/nature24277. PubMed PMID: 29022597; PubMed Central PMCID: PMCPMC5776756.

90. Nelander S, Mostad P, Lindahl P. Prediction of cell type-specific gene modules: identification and initial characterization of a core set of smooth muscle-specific genes. Genome Res. 2003;13(8):1838-54. Epub 2003/07/19. doi: 10.1101/gr.1197303. PubMed PMID: 12869577; PubMed Central PMCID: PMCPMC403775.
91. Rippe C, Zhu B, Krawczyk KK, Bavel EV, Albinsson S, Sjolund J, et al. Hypertension reduces soluble guanylyl cyclase expression in the mouse aorta via the Notch signaling pathway. Sci Rep. 2017;7(1):1334. Epub 2017/05/04. doi: 10.1038/s41598-017-01392-1. PubMed PMID: 28465505; PubMed Central PMCID: PMCPMC5430981.
92. Robinson MD, Oshlack A. A scaling normalization method for differential expression analysis of RNA-seq data. Genome Biol. 2010;11(3):R25. Epub 2010/03/04. doi: 10.1186/gb-2010-11-3-r25. PubMed PMID: 20196867; PubMed Central PMCID: PMCPMC2864565.
93. Dean CB, Nielsen JD. Generalized linear mixed models: a review and some extensions. Lifetime Data Anal. 2007;13(4):497-512. Epub 2007/11/15. doi: 10.1007/s10985-007-9065-x. PubMed PMID: 18000755.
94. Schaack J. Induction and inhibition of innate inflammatory responses by adenovirus early region proteins. Viral Immunol. 2005;18(1):79-88. Epub 2005/04/02. doi: 10.1089/vim.2005.18.79. PubMed PMID: 15802954.
95. Thacker EE, Nakayama M, Smith BF, Bird RC, Muminova Z, Strong TV, et al. A genetically engineered adenovirus vector targeted to CD40 mediates transduction of canine dendritic cells and promotes antigen-specific immune responses *in vivo.* Vaccine. 2009;27(50):7116-24. Epub 2009/09/30. doi: 10.1016/j.vaccine.2009.09.055. PubMed PMID: 19786146; PubMed Central PMCID: PMCPMC2784276.
96. Zhong L, Granelli-Piperno A, Choi Y, Steinman RM. Recombinant adenovirus is an efficient and non-perturbing genetic vector for human dendritic cells. Eur J Immunol. 1999;29(3):964-72. Epub 1999/03/26. doi: 10.1002/(SICI)1521-4141(199903)29:03<964::AID-IMMU964>3.0.CO;2-P. PubMed PMID: 10092101.
97. Noureddini SC, Curiel DT. Genetic targeting strategies for adenovirus. Mol Pharm. 2005;2(5):341-7. Epub 2005/10/04. doi: 10.1021/mp050045c. PubMed PMID: 16196486.
98. Ilan Y, Droguett G, Chowdhury NR, Li Y, Sengupta K, Thummala NR, et al. Insertion of the adenoviral E3 region into a recombinant viral vector prevents antiviral humoral and cellular immune responses and permits long-term gene expression. Proc Natl Acad Sci U S A. 1997;94(6):2587-92. Epub 1997/03/18. PubMed PMID: 9122239; PubMed Central PMCID: PMCPMC20132.
99. Small JC, Kurupati RK, Zhou X, Bian A, Chi E, Li Y, et al. Construction and characterization of E1- and E3-deleted adenovirus vectors expressing two antigens from two separate expression cassettes. Hum Gene Ther. 2014;25(4):328-38. Epub

2013/12/26. doi: 10.1089/hum.2013.216. PubMed PMID: 24367921; PubMed Central PMCID: PMCPMC3996997.

100. Chahal JS, Qi J, Flint SJ. The human adenovirus type 5 E1B 55 kDa protein obstructs inhibition of viral replication by type I interferon in normal human cells. PLoS Pathog. 2012;8(8):e1002853. Epub 2012/08/23. doi: 10.1371/journal.ppat.1002853. PubMed PMID: 22912576; PubMed Central PMCID: PMCPMC3415460.
101. Schaack J, Bennett ML, Colbert JD, Torres AV, Clayton GH, Ornelles D, et al. E1A and E1B proteins inhibit inflammation induced by adenovirus. Proc Natl Acad Sci U S A. 2004;101(9):3124-9. Epub 2004/02/21. doi: 10.1073/pnas.0303709101. PubMed PMID: 14976240; PubMed Central PMCID: PMCPMC365754.
102. Paddison PJ, Caudy AA, Bernstein E, Hannon GJ, Conklin DS. Short hairpin RNAs (shRNAs) induce sequence-specific silencing in mammalian cells. Genes Dev. 2002;16(8):948-58. Epub 2002/04/18. doi: 10.1101/gad.981002. PubMed PMID: 11959843; PubMed Central PMCID: PMCPMC152352.
103. Brummelkamp TR, Bernards R, Agami R. A system for stable expression of short interfering RNAs in mammalian cells. Science. 2002;296(5567):550-3. Epub 2002/03/23. doi: 10.1126/science.1068999. PubMed PMID: 11910072.
104. Ahlquist P. RNA-dependent RNA polymerases, viruses, and RNA silencing. Science. 2002;296(5571):1270-3. Epub 2002/05/23. doi: 10.1126/science.1069132. PubMed PMID: 12016304.
105. Bernstein E, Caudy AA, Hammond SM, Hannon GJ. Role for a bidentate ribonuclease in the initiation step of RNA interference. Nature. 2001;409(6818):363-6. Epub 2001/02/24. doi: 10.1038/35053110. PubMed PMID: 11201747.
106. Hidaka C, Milano E, Leopold PL, Bergelson JM, Hackett NR, Finberg RW, et al. CAR-dependent and CAR-independent pathways of adenovirus vector-mediated gene transfer and expression in human fibroblasts. J Clin Invest. 1999;103(4):579-87. Epub 1999/02/18. doi: 10.1172/JCI5309. PubMed PMID: 10021467; PubMed Central PMCID: PMCPMC408101.
107. Richardson C, Brennan P, Powell M, Prince S, Chen YH, Spiller OB, et al. Susceptibility of B lymphocytes to adenovirus type 5 infection is dependent upon both coxsackie-adenovirus receptor and alphavbeta5 integrin expression. J Gen Virol. 2005;86(Pt 6):1669-79. Epub 2005/05/26. doi: 10.1099/vir.0.80806-0. PubMed PMID: 15914844.
108. Parker AL, White KM, Lavery CA, Custers J, Waddington SN, Baker AH. Pseudotyping the adenovirus serotype 5 capsid with both the fibre and penton of serotype 35 enhances vascular smooth muscle cell transduction. Gene Ther. 2013;20(12):1158-64. Epub 2013/09/06. doi: 10.1038/gt.2013.44. PubMed PMID: 24005577; PubMed Central PMCID: PMCPMC3853367.
109. Seiradake E, Henaff D, Wodrich H, Billet O, Perreau M, Hippert C, et al. The cell adhesion molecule "CAR" and sialic acid on human erythrocytes influence adenovirus *in vivo* biodistribution. PLoS Pathog. 2009;5(1):e1000277. Epub 2009/01/03. doi: 10.1371/journal.ppat.1000277. PubMed PMID: 19119424; PubMed Central PMCID: PMCPMC2607015.

110. Cashman SM, Morris DJ, Kumar-Singh R. Adenovirus type 5 pseudotyped with adenovirus type 37 fiber uses sialic acid as a cellular receptor. Virology. 2004;324(1):129-39. Epub 2004/06/09. doi: 10.1016/j.virol.2004.04.001. PubMed PMID: 15183060.

111. Carthew RW, Sontheimer EJ. Origins and Mechanisms of miRNAs and siRNAs. Cell. 2009;136(4):642-55. Epub 2009/02/26. doi: 10.1016/j.cell.2009.01.035. PubMed PMID: 19239886; PubMed Central PMCID: PMCPMC2675692.

112. Petrocca F, Lieberman J. Promise and challenge of RNA interference-based therapy for cancer. J Clin Oncol. 2011;29(6):747-54. Epub 2010/11/17. doi: 10.1200/JCO.2009.27.6287. PubMed PMID: 21079135.

113. Berridge MV, Herst PM, Tan AS. Tetrazolium dyes as tools in cell biology: new insights into their cellular reduction. Biotechnol Annu Rev. 2005;11:127-52. Epub 2005/10/12. doi: 10.1016/S1387-2656(05)11004-7. PubMed PMID: 16216776.

114. Freeman WM, Walker SJ, Vrana KE. Quantitative RT-PCR: pitfalls and potential. Biotechniques. 1999;26(1):112-22, 24-5. Epub 1999/01/23. PubMed PMID: 9894600.

115. Radonic A, Thulke S, Mackay IM, Landt O, Siegert W, Nitsche A. Guideline to reference gene selection for quantitative real-time PCR. Biochem Biophys Res Commun. 2004;313(4):856-62. Epub 2004/01/07. PubMed PMID: 14706621.

116. Livak KJ, Schmittgen TD. Analysis of relative gene expression data using real-time quantitative PCR and the 2(-Delta Delta C(T)) Method. Methods. 2001;25(4):402-8. Epub 2002/02/16. doi: 10.1006/meth.2001.1262. PubMed PMID: 11846609.

117. Schmittgen TD, Zakrajsek BA, Mills AG, Gorn V, Singer MJ, Reed MW. Quantitative reverse transcription-polymerase chain reaction to study mRNA decay: comparison of endpoint and real-time methods. Anal Biochem. 2000;285(2):194-204. Epub 2000/10/06. doi: 10.1006/abio.2000.4753. PubMed PMID: 11017702.

118. Wong ML, Medrano JF. Real-time PCR for mRNA quantitation. Biotechniques. 2005;39(1):75-85. Epub 2005/08/03. doi: 10.2144/05391RV01. PubMed PMID: 16060372.

119. Sharkey FH, Banat IM, Marchant R. Detection and quantification of gene expression in environmental bacteriology. Appl Environ Microbiol. 2004;70(7):3795-806. Epub 2004/07/09. doi: 10.1128/AEM.70.7.3795-3806.2004. PubMed PMID: 15240248; PubMed Central PMCID: PMCPMC444812.

120. Bustin SA, Benes V, Garson JA, Hellemans J, Huggett J, Kubista M, et al. The MIQE guidelines: minimum information for publication of quantitative real-time PCR experiments. Clin Chem. 2009;55(4):611-22. Epub 2009/02/28. doi: 10.1373/clinchem.2008.112797. PubMed PMID: 19246619.

121. Bass JJ, Wilkinson DJ, Rankin D, Phillips BE, Szewczyk NJ, Smith K, et al. An overview of technical considerations for Western blotting applications to physiological research. Scand J Med Sci Sports. 2017;27(1):4-25. Epub 2016/06/07. doi: 10.1111/sms.12702. PubMed PMID: 27263489; PubMed Central PMCID: PMCPMC5138151.

122. Anfinsen CB. Principles that govern the folding of protein chains. Science. 1973;181(4096):223-30. Epub 1973/07/20. PubMed PMID: 4124164.

123. Krieg RC, Dong Y, Schwamborn K, Knuechel R. Protein quantification and its tolerance for different interfering reagents using the BCA-method with regard to 2D SDS PAGE. J Biochem Biophys Methods. 2005;65(1):13-9. Epub 2005/10/18. doi: 10.1016/j.jbbm.2005.08.005. PubMed PMID: 16226314.

124. Yamamoto S, Nishimura O, Misaki K, Nishita M, Minami Y, Yonemura S, et al. Cthrc1 selectively activates the planar cell polarity pathway of Wnt signaling by stabilizing the Wnt-receptor complex. Dev Cell. 2008;15(1):23-36. Epub 2008/07/09. doi: 10.1016/j.devcel.2008.05.007. PubMed PMID: 18606138.

125. Sennepin AD, Charpentier S, Normand T, Sarre C, Legrand A, Mollet LM. Multiple reprobing of Western blots after inactivation of peroxidase activity by its substrate, hydrogen peroxide. Anal Biochem. 2009;393(1):129-31. Epub 2009/06/16. doi: 10.1016/j.ab.2009.06.004. PubMed PMID: 19523435.

126. Friedman RC, Farh KK, Burge CB, Bartel DP. Most mammalian mRNAs are conserved targets of microRNAs. Genome Res. 2009;19(1):92-105. Epub 2008/10/29. doi: 10.1101/gr.082701.108. PubMed PMID: 18955434; PubMed Central PMCID: PMCPMC2612969.

127. Farazi TA, Spitzer JI, Morozov P, Tuschl T. miRNAs in human cancer. J Pathol. 2011;223(2):102-15. Epub 2010/12/03. doi: 10.1002/path.2806. PubMed PMID: 21125669; PubMed Central PMCID: PMCPMC3069496.

128. Feldman AT, Wolfe D. Tissue processing and hematoxylin and eosin staining. Methods Mol Biol. 2014;1180:31-43. Epub 2014/07/13. doi: 10.1007/978-1-4939-1050-2_3. PubMed PMID: 25015141.

129. Girard BM, Galli JR, Vizzard MA, Parsons RL. Galanin expression in the mouse major pelvic ganglia during explant culture and following cavernous nerve transection. J Mol Neurosci. 2012;48(3):713-20. Epub 2012/05/16. doi: 10.1007/s12031-012-9810-9. PubMed PMID: 22585545.

130. Mii S, Duong J, Tome Y, Uchugonova A, Liu F, Amoh Y, et al. The role of hair follicle nestin-expressing stem cells during whisker sensory-nerve growth in long-term 3D culture. J Cell Biochem. 2013;114(7):1674-84. Epub 2013/02/28. doi: 10.1002/jcb.24509. PubMed PMID: 23444061.

131. Matsui H, Musicki B, Sopko NA, Liu X, Hurley PJ, Burnett AL, et al. Early-stage Type 2 Diabetes Mellitus Impairs Erectile Function and Neurite Outgrowth From the Major Pelvic Ganglion and Downregulates the Gene Expression of Neurotrophic Factors. Urology. 2017;99:287 e1- e7. Epub 2016/10/30. doi: 10.1016/j.urology.2016.08.045. PubMed PMID: 27639791; PubMed Central PMCID: PMCPMC5384100.

132. Lin G, Chen KC, Hsieh PS, Yeh CH, Lue TF, Lin CS. Neurotrophic effects of vascular endothelial growth factor and neurotrophins on cultured major pelvic ganglia. BJU Int. 2003;92(6):631-5. Epub 2003/09/27. PubMed PMID: 14511050.

133. Stepkowski TM, Meczynska-Wielgosz S, Kruszewski M. mitoLUHMES: An Engineered Neuronal Cell Line for the Analysis of the Motility of Mitochondria. Cell Mol Neurobiol. 2017;37(6):1055-66. Epub 2016/11/11. doi: 10.1007/s10571-016-0438-0. PubMed PMID: 27832395; PubMed Central PMCID: PMCPMC5494036.

134. Hacker C, Lucocq JM. Analysis of specificity in immunoelectron microscopy. Methods Mol Biol. 2014;1117:315-23. Epub 2013/12/21. doi: 10.1007/978-1-62703-776-1_14. PubMed PMID: 24357369.

135. Lehman W, Morgan KG. Structure and dynamics of the actin-based smooth muscle contractile and cytoskeletal apparatus. J Muscle Res Cell Motil. 2012;33(6):461-9. Epub 2012/02/09. doi: 10.1007/s10974-012-9283-z. PubMed PMID: 22311558; PubMed Central PMCID: PMCPMC3394904.

136. Milligan RA, Whittaker M, Safer D. Molecular structure of F-actin and location of surface binding sites. Nature. 1990;348(6298):217-21. Epub 1990/11/15. doi: 10.1038/348217a0. PubMed PMID: 2234090.

137. Jia L, Wang R, Tang DD. Abl regulates smooth muscle cell proliferation by modulating actin dynamics and ERK1/2 activation. Am J Physiol Cell Physiol. 2012;302(7):C1026-34. Epub 2012/02/04. doi: 10.1152/ajpcell.00373.2011. PubMed PMID: 22301057; PubMed Central PMCID: PMCPMC3330739.

138. Peter B, Nador J, Juhasz K, Dobos A, Korosi L, Szekacs I, et al. Incubator proof miniaturized Holomonitor to in situ monitor cancer cells exposed to green tea polyphenol and preosteoblast cells adhering on nanostructured titanate surfaces: validity of the measured parameters and their corrections. J Biomed Opt. 2015;20(6):067002. Epub 2015/06/10. doi: 10.1117/1.JBO.20.6.067002. PubMed PMID: 26057033.

139. Huang J, Guo P, Moses MA. A Time-lapse, Label-free, Quantitative Phase Imaging Study of Dormant and Active Human Cancer Cells. J Vis Exp. 2018;(132). Epub 2018/03/20. doi: 10.3791/57035. PubMed PMID: 29553530.

140. Kovacs AF, Lang O, Turiak L, Acs A, Kohidai L, Fekete N, et al. The impact of circulating preeclampsia-associated extracellular vesicles on the migratory activity and phenotype of THP-1 monocytic cells. Sci Rep. 2018;8(1):5426. Epub 2018/04/05. doi: 10.1038/s41598-018-23706-7. PubMed PMID: 29615814; PubMed Central PMCID: PMCPMC5882809.

141. Ilina O, Friedl P. Mechanisms of collective cell migration at a glance. J Cell Sci. 2009;122(Pt 18):3203-8. Epub 2009/09/04. doi: 10.1242/jcs.036525. PubMed PMID: 19726629.

142. Friedl P, Gilmour D. Collective cell migration in morphogenesis, regeneration and cancer. Nat Rev Mol Cell Biol. 2009;10(7):445-57. Epub 2009/06/24. doi: 10.1038/nrm2720. PubMed PMID: 19546857.

143. Friedl P, Wolf K. Plasticity of cell migration: a multiscale tuning model. J Cell Biol. 2010;188(1):11-9. Epub 2009/12/03. doi: 10.1083/jcb.200909003. PubMed PMID: 19951899; PubMed Central PMCID: PMCPMC2812848.

144. Vedula SR, Ravasio A, Lim CT, Ladoux B. Collective cell migration: a mechanistic perspective. Physiology (Bethesda). 2013;28(6):370-9. Epub 2013/11/05. doi: 10.1152/physiol.00033.2013. PubMed PMID: 24186932.

145. Rorth P. Collective cell migration. Annu Rev Cell Dev Biol. 2009;25:407-29. Epub 2009/07/07. doi: 10.1146/annurev.cellbio.042308.113231. PubMed PMID: 19575657.

146. Rorth P. Fellow travellers: emergent properties of collective cell migration. EMBO Rep. 2012;13(11):984-91. Epub 2012/10/13. doi: 10.1038/embor.2012.149. PubMed PMID: 23059978; PubMed Central PMCID: PMCPMC3492716.

147. Grada A, Otero-Vinas M, Prieto-Castrillo F, Obagi Z, Falanga V. Research Techniques Made Simple: Analysis of Collective Cell Migration Using the Wound Healing Assay. J Invest Dermatol. 2017;137(2):e11-e6. Epub 2017/01/24. doi: 10.1016/j.jid.2016.11.020. PubMed PMID: 28110712.

148. Jonkman JE, Cathcart JA, Xu F, Bartolini ME, Amon JE, Stevens KM, et al. An introduction to the wound healing assay using live-cell microscopy. Cell Adh Migr. 2014;8(5):440-51. Epub 2014/12/09. doi: 10.4161/cam.36224. PubMed PMID: 25482647; PubMed Central PMCID: PMCPMC5154238.

149. Boopathi E, Gomes CM, Goldfarb R, John M, Srinivasan VG, Alanzi J, et al. Transcriptional repression of Caveolin-1 (CAV1) gene expression by GATA-6 in bladder smooth muscle hypertrophy in mice and human beings. Am J Pathol. 2011;178(5):2236-51. Epub 2011/04/26. doi: 10.1016/j.ajpath.2011.01.038. PubMed PMID: 21514437; PubMed Central PMCID: PMCPMC3081182.

150. Clowes MM, Lynch CM, Miller AD, Miller DG, Osborne WR, Clowes AW. Long-term biological response of injured rat carotid artery seeded with smooth muscle cells expressing retrovirally introduced human genes. J Clin Invest. 1994;93(2):644-51. Epub 1994/02/01. doi: 10.1172/JCI117016. PubMed PMID: 8113400; PubMed Central PMCID: PMCPMC293889.

151. Brem G, Wanke R, Wolf E, Buchmuller T, Muller M, Brenig B, et al. Multiple consequences of human growth hormone expression in transgenic mice. Mol Biol Med. 1989;6(6):531-47. Epub 1989/12/01. PubMed PMID: 2634813.

152. Barrow KM, Perez-Campo FM, Ward CM. Use of the cytomegalovirus promoter for transient and stable transgene expression in mouse embryonic stem cells. Methods Mol Biol. 2006;329:283-94. Epub 2006/07/19. doi: 10.1385/1-59745-037-5:283. PubMed PMID: 16845998.

153. Odom DT, Dowell RD, Jacobsen ES, Gordon W, Danford TW, MacIsaac KD, et al. Tissue-specific transcriptional regulation has diverged significantly between human and mouse. Nat Genet. 2007;39(6):730-2. Epub 2007/05/29. doi: 10.1038/ng2047. PubMed PMID: 17529977; PubMed Central PMCID: PMCPMC3797512.

154. Wilson MD, Barbosa-Morais NL, Schmidt D, Conboy CM, Vanes L, Tybulewicz VL, et al. Species-specific transcription in mice carrying human chromosome 21. Science. 2008;322(5900):434-8. Epub 2008/09/13. doi: 10.1126/science.1160930. PubMed PMID: 18787134; PubMed Central PMCID: PMCPMC3717767.

155. Gilad Y, Oshlack A, Smyth GK, Speed TP, White KP. Expression profiling in primates reveals a rapid evolution of human transcription factors. Nature. 2006;440(7081):242-5. Epub 2006/03/10. doi: 10.1038/nature04559. PubMed PMID: 16525476.

156. Khaitovich P, Hellmann I, Enard W, Nowick K, Leinweber M, Franz H, et al. Parallel patterns of evolution in the genomes and transcriptomes of humans and chimpanzees. Science. 2005;309(5742):1850-4. Epub 2005/09/06. doi: 10.1126/science.1108296. PubMed PMID: 16141373.

157. Wittkopp PJ, Haerum BK, Clark AG. Regulatory changes underlying expression differences within and between Drosophila species. Nat Genet. 2008;40(3):346-50. Epub 2008/02/19. doi: 10.1038/ng.77. PubMed PMID: 18278046.

158. Park CC, Ahn S, Bloom JS, Lin A, Wang RT, Wu T, et al. Fine mapping of regulatory loci for mammalian gene expression using radiation hybrids. Nat Genet. 2008;40(4):421-9. Epub 2008/03/26. doi: 10.1038/ng.113. PubMed PMID: 18362883; PubMed Central PMCID: PMCPMC3014048.

159. Gilad Y, Rifkin SA, Pritchard JK. Revealing the architecture of gene regulation: the promise of eQTL studies. Trends Genet. 2008;24(8):408-15. Epub 2008/07/04. doi: 10.1016/j.tig.2008.06.001. PubMed PMID: 18597885; PubMed Central PMCID: PMCPMC2583071.

160. Schwanhausser B, Busse D, Li N, Dittmar G, Schuchhardt J, Wolf J, et al. Global quantification of mammalian gene expression control. Nature. 2011;473(7347):337-42. Epub 2011/05/20. doi: 10.1038/nature10098. PubMed PMID: 21593866.

161. Lo HP, Hall TE, Parton RG. Mechanoprotection by skeletal muscle caveolae. Bioarchitecture. 2016;6(1):22-7. Epub 2016/01/14. doi: 10.1080/19490992.2015.1131891. PubMed PMID: 26760312; PubMed Central PMCID: PMCPMC4914031.

162. Sinha B, Koster D, Ruez R, Gonnord P, Bastiani M, Abankwa D, et al. Cells respond to mechanical stress by rapid disassembly of caveolae. Cell. 2011;144(3):402-13. Epub 2011/02/08. doi: 10.1016/j.cell.2010.12.031. PubMed PMID: 21295700; PubMed Central PMCID: PMCPMC3042189.

163. Zeng J, Pan C, Jiang C, Lindstrom S. Cause of residual urine in bladder outlet obstruction: an experimental study in the rat. J Urol. 2012;188(3):1027-32. Epub 2012/07/24. doi: 10.1016/j.juro.2012.04.101. PubMed PMID: 22819110.

164. Shah M, Patel K, Fried VA, Sehgal PB. Interactions of STAT3 with caveolin-1 and heat shock protein 90 in plasma membrane raft and cytosolic complexes. Preservation of cytokine signaling during fever. J Biol Chem. 2002;277(47):45662-9. Epub 2002/09/18. doi: 10.1074/jbc.M205935200. PubMed PMID: 12235142.

165. Hassel D, Dahme T, Erdmann J, Meder B, Huge A, Stoll M, et al. Nexilin mutations destabilize cardiac Z-disks and lead to dilated cardiomyopathy. Nat Med. 2009;15(11):1281-8. Epub 2009/11/03. doi: 10.1038/nm.2037. PubMed PMID: 19881492.

166. Dupont S, Morsut L, Aragona M, Enzo E, Giulitti S, Cordenonsi M, et al. Role of YAP/TAZ in mechanotransduction. Nature. 2011;474(7350):179-83. Epub 2011/06/10. doi: 10.1038/nature10137. PubMed PMID: 21654799.

167. Speight P, Kofler M, Szaszi K, Kapus A. Context-dependent switch in chemo/mechanotransduction via multilevel crosstalk among cytoskeleton-regulated MRTF and TAZ and TGFbeta-regulated Smad3. Nat Commun. 2016;7:11642. Epub 2016/05/18. doi: 10.1038/ncomms11642. PubMed PMID: 27189435; PubMed Central PMCID: PMCPMC4873981.

168. Pyagay P, Heroult M, Wang Q, Lehnert W, Belden J, Liaw L, et al. Collagen triple helix repeat containing 1, a novel secreted protein in injured and diseased arteries, inhibits collagen expression and promotes cell migration. Circ Res. 2005;96(2):261-

8. Epub 2004/12/25. doi: 10.1161/01.RES.0000154262.07264.12. PubMed PMID: 15618538.

169. Shakirova Y, Sward K, Uvelius B, Ekman M. Biochemical and functional correlates of an increased membrane density of caveolae in hypertrophic rat urinary bladder. Eur J Pharmacol. 2010;649(1-3):362-8. Epub 2010/09/28. doi: 10.1016/j.ejphar.2010.09.050. PubMed PMID: 20868660.

170. Aitken KJ, Bagli DJ. The bladder extracellular matrix. Part I: architecture, development and disease. Nat Rev Urol. 2009;6(11):596-611. Epub 2009/11/06. doi: 10.1038/nrurol.2009.201. PubMed PMID: 19890339.

Printed by Media-Tryck, Lund 2018 NORDIC SWAN ECOLABEL 3041 0903

Transcriptional control mechanisms in the wall of the urinary bladder

Normal bladder function depends on the main tissues in the bladder (e.g. smooth muscle), the extracellular matrix, the nerve innervation, and central nervous control. Most of these domains of bladder structure and function have been touched upon in the present thesis, and novel insights have been gained. Progress is therefore slowly made towards understanding of this large, complicated, and mysterious system. The work also suggests strategies for recovering bladder function disrupted by pathological conditions such as bladder outlet obstruction and bladder denervation.

Section of Cell and Tissue Biology
Department of Experimental Medical Science

Lund University, Faculty of Medicine
Doctoral Dissertation Series 2018:104
ISBN 978-91-7619-672-4
ISSN 1652-8220

LUND UNIVERSITY